INTERACTION OF THE NON STEROIDAL ANTI-INFLAMMATORY DRUG CELECOXIB WITH PURE AND CHOLESTEROL-CONTAINING MODEL MEMBRANES

A THESIS SUBMITTED TO
THE GRADUATE SCHOOL OF NATURAL AND APPLIED SCIENCES
OF
MIDDLE EAST TECHNICAL UNIVERSITY

BY

ASLI SADE

IN PARTIAL FULFILLMENT OF THE REQUIREMENTS
FOR
THE DEGREE OF MASTER OF SCIENCE
IN
BIOLOGY

JULY 2009

Approval of the thesis:

INTERACTION OF THE NON STEROIDAL ANTI-INFLAMMATORY DRUG CELECOXIB WITH PURE AND CHOLESTEROL-CONTAINING MODEL MEMBRANES

submitted by **ASLI SADE** in partial fulfillment of the requirements for the degree of **Master of Science in Biology Department, Middle East Technical University** by,

Prof. Dr. Canan Özgen _____
Dean, Graduate School of **Natural and Applied Sciences**

Prof. Dr. Zeki Kaya _____
Head of Department, **Biology**

Assist. Prof. Dr. Sreeparna Banerjee _____
Supervisor, **Biology Dept., METU**

Prof. Dr. Feride Severcan _____
Co-Supervisor, **Biology Dept., METU**

Examining Committee Members:

Prof. Dr. Mesude İşcan _____
Biology Dept., METU

Assist. Prof. Dr. Sreeparna Banerjee _____
Biology Dept., METU

Assist. Prof. Dr. Elif Erson _____
Biology Dept., METU

Prof. Dr. Nadide Kazancı _____
Physics Dept., Ege University

Assist. Prof. Dr. Neslihan Toyran Al-Otaibi _____
Physiology Dept., Faculty of Medicine,
Başkent University

Date: 06/07/09

I hereby declare that all information in this document has been obtained and presented in accordance with academic rules and ethical conduct. I also declare that, as required by these rules and conduct, I have fully cited and referenced all material and results that are not original to this work.

Name, Last name: Aslı Sade

Signature :

ABSTRACT

INTERACTION OF THE NON STEROIDAL ANTI-INFLAMMATORY DRUG CELECOXIB WITH PURE AND CHOLESTEROL-CONTAINING MODEL MEMBRANES

Sade, Aslı

M.Sc., Department of Biology

Supervisor : Assist. Prof.Dr. Sreeparna Banerjee

Co-Supervisor: Prof. Dr. Feride Severcan

July 2009, 94 Pages

The interactions of the non steroidal anti-inflammatory drug celecoxib with pure and cholesterol containing distearoyl phosphatidylcholine multilamellar vesicles were studied using Fourier transform infrared spectroscopy, differential scanning calorimetry and turbidity technique at 440 nm.

The results reveal that celecoxib exerts opposing effects on membrane order in a concentration dependent manner while cholesterol disorders and orders the membrane in the gel and liquid crystalline phase, respectively. Ternary mixtures of DSPC/Cholesterol/celecoxib behave similar to cholesterol with a small effect of celecoxib. While celecoxib decreases fluidity of the DSPC membranes, cholesterol shows an opposite effect, and in ternary mixtures, a dominant effect of cholesterol is observed. Celecoxib induces opposite effects on the hydration status of the carbonyl groups in the binary system whereas; cholesterol induces hydrogen bonding around

this group. An evidence of phase separation has also been observed for all three systems (DSPC/celecoxib, DSPC/Chol, and DSPC/Chol/celecoxib). In addition, a possible location of celecoxib in the interfacial region of the membrane has been proposed. Finally, penetration of celecoxib into the hydrophobic core of the ternary system at high cholesterol concentrations and formation of a new phase has also been suggested.

Thus, depending on the concentration used, celecoxib induces significant changes in the biophysical properties of membranes that may aid in understanding its mechanism of action. Furthermore, highly complex interactions take place in ternary membrane systems and further investigations are needed to explore them in detail.

Key words: celecoxib, DSC, DSPC, FTIR, MLV

ÖZ

BİR NON STEROİDAL ANTI-İNFLAMATUVAR İLAÇ OLAN SELEKOKSOBİN KOLESTEROL İÇEREN VE İÇERMEYEN MODEL MEMBRANLARLA ETKİLEŞİMİ

Sade, Aslı
Yüksek Lisans, Biyoloji Bölümü
Tez Yöneticisi : Y. Doç. Dr. Sreeparna Banerjee
Ortak Tez Yöneticisi: Prof. Dr. Feride Severcan

Temmuz 2009, 94 sayfa

Bir non steroid anti-inflamatuvar ilaç olan selekoksibin kolesterol içeren ve içermeyen distearoyl fosfokolin çok katmanlı lipozomlarla etkileşimi Fourier transform infrared spektroskopisi, diferansiyel taramalı kalorimetri ve 440 nm'de türbidite teknikleri ile incelenmiştir.

Sonuçlara göre, selekoksib membran düzenliliği üzerinde konsantrasyona bağlı olarak, zıt etki gösterirken, kolesterol membranları jel fazda daha düzensiz, sıvıkristal fazda düzenli hale getirmiştir. DSPC/Cholesterol/celecoxib ile oluşturulan üçlü sistem ise kolesterole benzer özellikler göstermiştir. Selekoksib membran akışkanlığını azaltırken, kolesterol zıt etki göstermiş ve üçlü sistemde kolesterolün baskın etkisi gözlenmiştir. Selekoksib, kafa gruplarına yakın gliserol iskeletinin hidrasyon seviyeleri üzerinde zıt etki göstermiş, kolesterol ise bu grublarda hidrojen bağlarını artırmıştır. Bunlara ek olarak, her üç sistem için faz ayrımı gözlenmiştir.

Ayrıca selekoksibin interfasyal bölgedeki muhtemel lokalizasyonu önerilmiştir. Son olarak, üçlü sistemde selekoksibin yüksek kolesterol konsantrasyonu sebebiyle, membranların hidrofobik bölgelerine yerleştiğine dair bir model öne sürülmüştür.

Sonuç olarak, selekoksib, membranların biyofiziksel özellikleri üzerinde, konsantrasyona bağlı olarak anlamlı değişimlere neden olmaktadır ve bu etkiler, ilacın etki mekanizmasını anlamada yarar sağlayacaktır. Ayrıca, üçlü membran sistemlerinde karmaşık etkileşimler görülmektadir ve bunları daha detaylı anlamak için daha fazla araştırma gerekmektedir.

Anahtar kelimeler: selekoksib, DSC, DSPC, FTIR, MLV.

To My Family

ACKNOWLEDGEMENTS

I express my sincere gratitude to my supervisor Assist. Prof. Dr. Sreeparna Banerjee for her valuable guidance, encouragement and understanding throughout the research.

I would like to thank my co-supervisor Prof. Dr. Feride Severcan for her valuable guidance, comments and discussions.

I would like to thank Sevgi Görgülü, Özlem Bozkurt and Nihal Özek for their helpful comments, discussions and support throughout the study.

My special gratitudes go to my parents and my sister for their encouragement, support and patience.

Finally, I would like to thank my lab mates for their sincere friendship, support and comments throughout the study.

The study was funded by the Scientific Research Council of Middle East Technical University Project no: 2007-(R)-08-11-02 and BAP-07.02.2009.04.

TABLE OF CONTENTS

ABSTRACT iv

ÖZ vi

ACKNOWLEDGEMENTS ix

TABLE OF CONTENTS x

CHAPTERS

1 INTRODUCTION 1

1.1 Cyclooxygenases and Inflammation 1

1.2 Nonsteroidal Anti-inflammatory Drugs and Celecoxib 3

1.2.1 COX-2 Independent Mechanisms of Celecoxib Action 5

1.2.2 Interaction of Celecoxib with Membranes 6

1.3 Basic Theory of Biological Membranes 7

1.3.1 Molecular Motions in Membranes 8

1.3.2 Structural Isomerizations in Membranes 9

1.3.3 Thermotropic Phase Transitions in Membranes 10

1.3.4 Liposomes as Model Membranes 13

1.4 Structure and Function of Cholesterol 15

1.5 Electromagnetic Radiation and Optical Spectroscopy 22

1.5.1 Infrared Spectroscopy 24

1.5.2 Fourier Transform Infrared Spectroscopy (FTIR) 25

1.5.3 Infrared Spectroscopy in Membrane Research 26

1.5.4 Turbidity Technique at 440 nm 28

1.6 Differential Scanning Calorimetry (DSC) 28

1.7 Scope and Aim of This Study 30

2 MATERIALS AND METHODS 32

2.1 Reagents 32
2.2 Phosphate Buffered Saline Preparation 32
2.3 Preparation of Drug and Lipid Stock Solutions 32
2.4 Preparation of Multilamellar Vesicles 33
2.5 Sample preparation for FTIR measurements 33
2.5.1 Infrared Spectral Regions Used in This Study 34
2.5.2 Spectral Analysis 37
2.6 Turbidity Measurements 40
2.7 Sample Preparation for DSC measurements 41
2.7.1 Thermogram Analyses 41
2.8 Statistical Analyses 43
3 RESULTS 44
3.1 DSC Studies 44
3.1.1 Liposomes Containing Celecoxib 44
3.1.2 Liposomes Containing Cholesterol 46
3.1.3 Liposomes containing cholesterol and celecoxib 48
3.2 FTIR Studies 51
3.2.1 Interactions of Celecoxib with DSPC Membranes 51
3.2.2 Interactions of Cholesterol wlth DSPC Membranes 63
3.2.3 Interactions of Celecoxib-Cholesterol-DSPC Membranes 67
3.3 Turbidity Studies 73
4 DISCUSSION 75
5 CONCLUSIONS 84
REFERENCES 86

LIST OF TABLES

TABLES

Table 3.1 The pretransition temperature (Tp), the main phase transition temperature (Tm) and transition enthalpy changes for different concentrations of celecoxib..... 46

Table 3.2 The main phase transition temperature (Tm) and transition enthalpy changes for different concentrations of cholesterol. 48

Table 3.3 The main phase transition temperature (Tm) and transition enthalpy changes for different concentrations of cholesterol, in the presence of 6 mol% celecoxib. 49

LIST OF FIGURES

FIGURES

Figure 1.1 The arachidonic acid cascade (Vane et al., 1998). 2

Figure 1.2 Chemical structure of celecoxib. 4

Figure 1.3 Structure of phosphatidylcholine (figure taken from meyerbio1b. wikispaces.com/%E2%80%A2Lipids). 8

Figure 1.4 Molecular motions in membranes. (a) rotational motion, (b) lateral diffusion, (c) flip-flop (Jain, 1979a)..... 9

Figure 1.5 Trans-gauche isomerizations in acyl chains of phospholipids 10

Figure 1.6 Different phases of phospholipids (left) and the structure of DSPC (right) (Stuart, 1997). 13

Figure 1.7 Structure of a liposome (Left) Types of liposomes (Right) (www.scf-online.com/.../galenik_25_d_dr.htm)..... 14

Figure 1.8 Structure of cholesterol.. 15

Figure 1.9 Localization of cholesterol in the phospholipid bilayer (Chen and Tripp, 2008). 16

Figure 1.10 Phase diagram for DSPC–cholesterol binary bilayer membrane. 18

Figure 1.11 Schematic illustration for various types of regular distribution of cholesterol in binary bilayer membranes. 20

Figure 1.12 Typical energy-level diagram showing the ground state and the first excited state.. 23

Figure 1.13 The schematic representation of some of the molecular vibrations in a linear (A) and a non-linear (B) triatomic molecule. (+) and (-) represent out of plane movements (Arrondo et al., 1993). 25

Figure 1.14 Basic components of an FTIR spectrometer. 26

Figure 2.1 The main infrared bands in the FTIR spectrum of DSPC liposomes 36

Figure 2.2 FTIR spectrum of DSPC liposomes before (upper spectrum) and after (lower spectrum) buffer subtraction. 37

Figure 2.3 FTIR spectra of DSPC liposomes containing 24 mol% celecoxib (straight line) and pure celecoxib (dashed line). Inset shows PO_2^- region. 39

Figure 2.4 FTIR spectra of DSPC liposomes containing 2:1 mol ratio of cholesterol (straight line) and pure cholesterol (dashed line). Inset shows the C-H region. 40

Figure 2.5 DSC thermogram of DSPC liposomes. The small peak shows pretransition, the sharp peak shows main phase transition. The peak maximums and transition enthalpy are indicated in the figure. 42

Figure 3.1 DSC thermograms of DSPC MLVs in the absence and presence of different concentrations of celecoxib. The pre- and main phase transition temperatures are given for pure DSPC MLVs. 45

Figure 3.2 DSC thermograms of DSPC MLVs in the absence and presence of different concentrations of cholesterol. 47

Figure 3.3 DSC thermograms of DSPC MLVs containing 6 mol% celecoxib with different concentrations of cholesterol. 50

Figure 3.4 Representative FTIR spectra of DSPC MLVs in the presence of 0, 6 and 24 mol% celecoxib at 40 °C. 52

Figure 3.5 Variation in the frequency of the CH_2 antisymmetric stretching modes of DSPC MLVs as a function of (**A)** temperature at varying concentrations of celecoxib and (**B)** celecoxib concentration at 40 and 60 °C. 54

Figure 3.6 Variation in the frequency of the CH_2 symmetric stretching modes of DSPC MLVs as a function of (**A)** temperature at varying concentrations of celecoxib and (**B)** celecoxib concentration at 40 and 60 °C. 55

Figure 3.7 Variation in the bandwidth of the CH_2 antisymmetric stretching modes of DSPC MLVs as a function of (**A)** temperature at varying concentrations of celecoxib and (**B)** celecoxib concentration at 40 and 60 °C. 57

Figure 3.8 Variation in the bandwidth of the CH_2 symmetric stretching modes of DSPC MLVs as a function of (**A)** temperature at varying concentrations of celecoxib and (**B)** celecoxib concentration at 40 and 60 °C. 58

Figure 3.9 Variation in the frequency of the C=O stretching mode of DSPC MLVs as a function of **(A)** temperature at varying concentrations of celecoxib and **(B)** celecoxib concentration at 40 and 60 °C. 60

Figure 3.10 Variation in the frequency of the PO_2^- antisymmetric double stretching mode of DSPC MLVs as a function of **(A)** temperature at varying concentrations of celecoxib and **(B)** celecoxib concentration at 40 and 60 °C. 62

Figure 3.11 Variation in the frequency of the CH_2 antisymmetric stretching modes of DSPC MLVs as a function of cholesterol concentration at 35 and 65 °C. 64

Figure 3.12 Variation in the bandwidth of the CH_2 antisymmetric stretching modes of DSPC MLVs as a function of cholesterol concentration at 35 and 65 °C. 65

Figure 3.13 Variation in the frequency of the C=O stretching modes of DSPC MLVs as a function of cholesterol concentration at 35 and 65 °C. 66

Figure 3.14 Variation in the frequency of the PO_2^- antisymmetric double stretching modes of DSPC MLVs as a function of cholesterol concentration at 35 and 65 °C. 66

Figure 3.15 Average frequency changes in the CH_2 antisymmetric stretching mode of DSPC MLVs as a function of cholesterol concentration, in the presence and absence of 6 mol% celecoxib at 30 and 65 °C. 68

Figure 3.16 Average bandwidth changes in the CH_2 antisymmetric stretching mode of DSPC MLVs as a function of cholesterol concentration, in the presence and absence of 6 mol% celecoxib at 30 and 65 °C. 69

Figure 3.17 Average frequency changes in the C=O stretching mode of DSPC MLVs as a function of cholesterol concentration, in the presence and absence of 6 mol% celecoxib at 30 **(A)** and 65 °C **(B)**..... 71

Figure 3.18 Average bandwidth changes in the PO_2^- antisymmetric double stretching mode of DSPC MLVs as a function of cholesterol concentration, in the presence and absence of 6 mol% celecoxib at 30 and 65 °C.. 73

Figure 3.19 Temperature dependence of the absorbance at 440 nm for DSPC MLVs in the presence of different celecoxib concentrations. 74

CHAPTER 1

INTRODUCTION

In this study, the interactions of the non steroidal anti-inflammatory drug celecoxib with pure and cholesterol-containing 1,2-Distearoyl-sn-Glycero-3-Phosphocholine (DSPC) multilamellar vesicles (MLVs) were investigated at molecular level, using Fourier transform infrared spectroscopy, differential scanning calorimetry and turbidity technique at 440 nm.

This chapter summarizes the available literature on biological and model membranes, cholesterol and celecoxib, all of which has directed us to conduct this study. The basic principles of Fourier transform infrared spectroscopy, turbidity technique at 440 nm and differential scanning calorimetry are also included in this chapter.

1.1 Cyclooxygenases and Inflammation

Cyclooxygenases (COX), also called prostaglandin H synthases (PGHS), are enzymes localized at the nuclear or endoplasmic reticulum membrane of eukaryotic cells. These are the key enzymes of the eicosanoid cascade which can convert arachidonic acid (AA), a fatty acid distributed throughout the lipid bilayer, to prostaglandins (PGs) (Fig 1.1). Once cleaved by phospholipase enzymes, arachidonic acid is converted to PGH_2 by a two step mechanism. PGH_2 is the root prostaglandin from which other prostaglandin isomers are produced by downstream synthases. These isomers, including thromboxane and PGD_2, PGJ_2, PGE_2 and PGI_2, are involved in various physiological processes, such as inflammation, fever, algesia,

angiogenesis, platelet aggregation, ovulation, renal function, vasoconstriction and vasodilation (Funk, 2001).

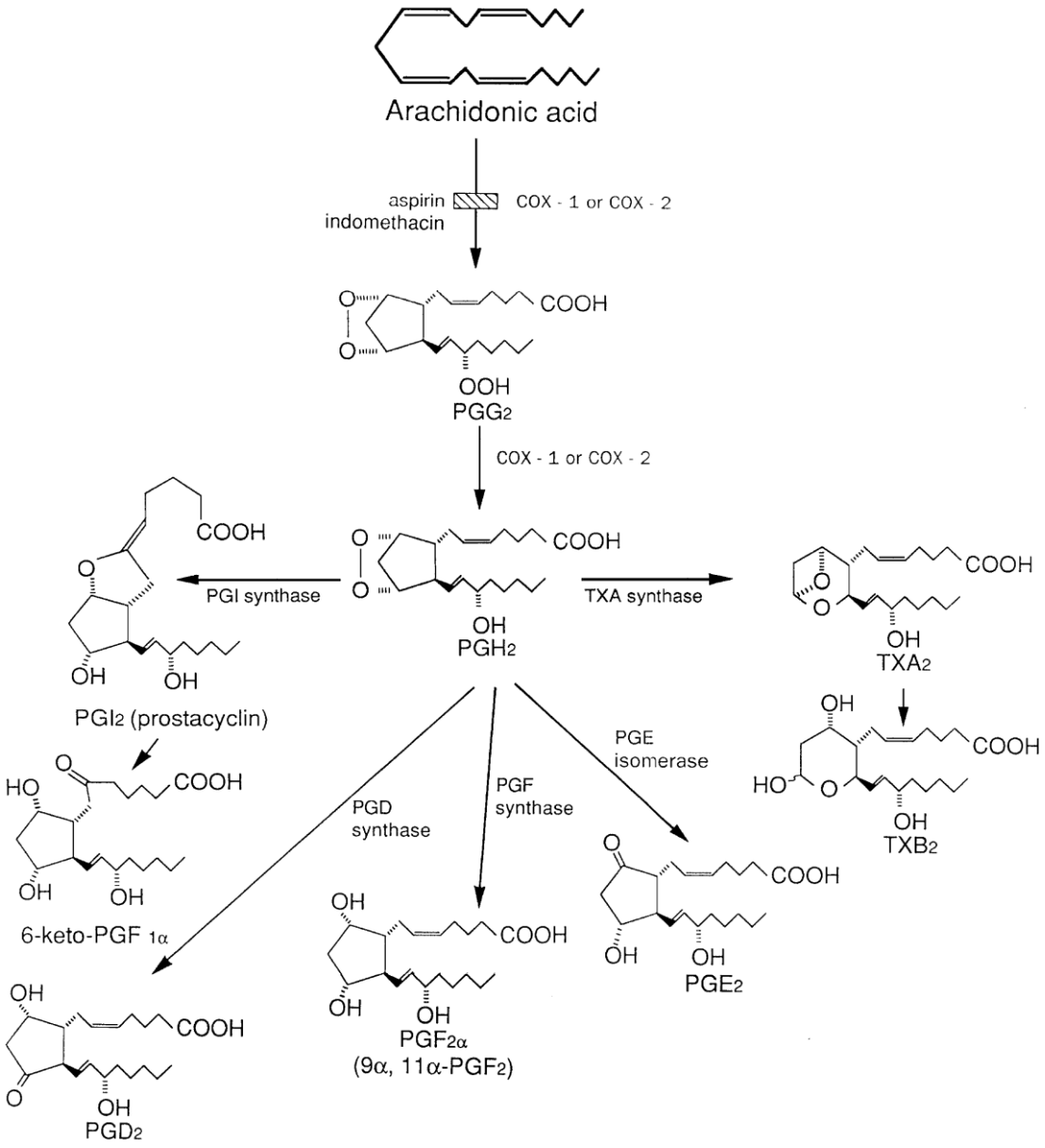

Fig. 1.1 The arachidonic acid cascade (Vane et al., 1998).

Cyclooxygenases have two isoforms, COX-1 and COX-2, which have different expression patterns in the tissues. COX-1 is expressed constitutively in most tissues and is responsible for a basal level of prostaglandin synthesis required for 'housekeeping' functions in the body such as gastrointestinal cytoprotection, renal functions and vascular homeostasis. COX-2 on the other hand, is not constitutively expressed in most tissues with the exception of kidney and brain (Funk, 2001). This isoform can be induced by a number of stimuli, such as bacterial lipopolysaccharide (LPS), interleukin-1 and 2, and tumor necrosis factor (TNF)-α, all of which are related to inflammation (Funk, 2001).The induction of COX-2 by inflammatory mediators led investigators to label this enzyme as pathological (Vane et al., 1998), since chronic inflammation is known to result in several diseases, especially cancer (Mantovani et al., 2008).

1.2 Nonsteroidal Anti-inflammatory Drugs and Celecoxib

Nonsteroidal anti-inflammatory drugs (NSAIDs), such as aspirin, ibuprofen and indomethacin, are widely prescribed in inflammatory diseases like osteoarthritis and rheumatoid arthritis, in order to relieve pain and other symptoms of inflammation. In 1971, Vane et al. showed that NSAIDs block prostaglandin synthesis by binding to both isoforms of COX and inhibiting conversion of AA to PGG_2 (Vane, 1971). Classical NSAIDs, except aspirin, reversibly affect COX activity by competing with the substrate AA for the active site of the enzyme. Aspirin inhibition is due to a covalent and irreversible modification of the active site by acetylation of Ser529. Because prostaglandins participate in a number of homeostatic functions, it is not surprising that chronic inhibition of COX leads to some undesirable side effects. These include gastrointestinal ulceration, perforation and bleeding. Therefore, it is widely accepted that the anti-inflammatory activity of NSAIDs results from COX-2 inhibition and the undesirable side effects are primarily due to COX-1 inhibition (Vane et al., 1998).

This phenomenon led to the hypothesis that selective inhibition of COX-2 might retain the anti-inflammatory function of NSAIDs without affecting the important activity of COX-1. Based on this hypothesis, a new class of selective NSAIDs was developed (FitzGerald, 2003). Celecoxib (Fig 1.2) is a diaryl substituted pyrazole class of compound with the chemical designation (4-[5-(4-methylphenyl)-3-(trifluoromethyl)-1H-pyrazol-1-yl] benzenesulfonamide. This new generation of selective NSAID has been indicated to relieve the symptoms of osteoarthritis and rheumatoid arthritis with reduced gastrointestinal side effects compared to classical NSAIDs (Goldenberg, 1999). The phenylsulfoneamide moiety of celecoxib binds to a pocket found in COX-2 but not COX-1. The selectivity of celecoxib for COX-2 comes from the smaller valine molecule in COX-2, giving access to this side pocket which is also the site for the binding of all other selective inhibitors. On the other hand the larger isoleucine in COX-1, blocks the access to this pocket.

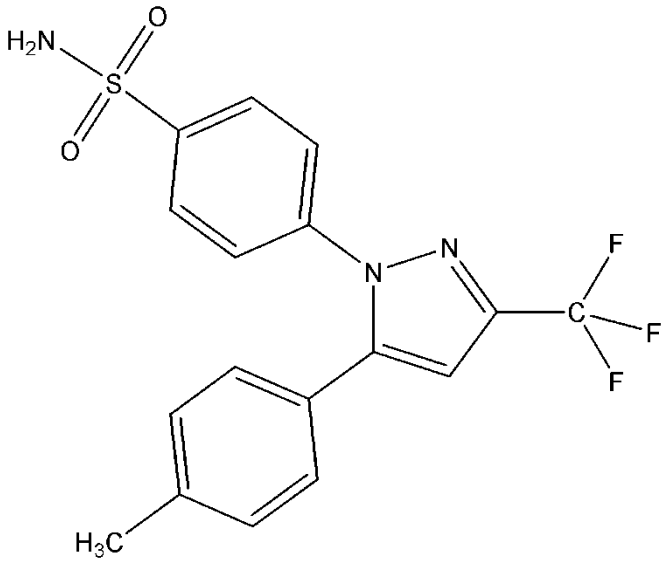

Fig. 1.2 Chemical structure of celecoxib.

However, celecoxib is not totally devoid of side effects. Besides being an inflammation induced enzyme, COX-2 is also constitutively expressed in some tissues like vascular endothelium, kidney and brain (FitzGerald, 2003). Although there are controversial findings about the side effects of celecoxib, several clinical trials have revealed an association of celecoxib usage with increased incidence of cardiovascular risks (Bertagnolli et al., 2006). The same kind of effects was also observed for other coxibs, including rofecoxib which was then withdrawn from the market. Consequently, serious questions have risen about the other coxibs which are currently on the market. Some recent studies, revealed that COX-2, and not COX-1, was the predominant source of prostacyclin, which is responsible for the inhibition of platelet aggregation and induction of vasodilation, in the vascular endothelium (Belton et al., 2000; McAdam et al., 1999). On the other hand, COX-1 is associated with the production of thromboxane A_2 (TXA_2), a potent inducer of vasoconstriction and platelet aggregation (Dogne et al., 2004). Therefore, the cardiovascular risks associated with the selective inhibition of COX-2 are mostly because of the shift of thromboxane/prostacyclin ratio towards thromboxane, in the vascular endothelium.

1.2.1 COX-2 Independent Mechanisms of Celecoxib Action

Epidemiological studies have revealed that celecoxib usage is associated with a chemopreventive activity in breast (Harris et al., 2006), lung (Harris et al., 2007) and colorectal carcinogenesis (Arber et al., 2006; Bertagnolli et al., 2006). This is an expected finding since COX-2 expression is indicative of inflammation which in turn is accepted as predisposition to cancer (Coussens and Werb, 2002). Increased COX-2 expression is involved in the development of cancer by inhibiting apoptosis (Nzeako et al., 2001), enhancing metastasis (Li et al., 2002) and inducing cell division (Chinery et al., 1999). Currently celecoxib is the only NSAID that has been approved by the FDA for supplementary treatment of patients with familial adenomatous polyposis. However, the mechanisms underlying the anti-carcinogenic nature of celecoxib are not completely understood. In addition to its COX-2 inhibitory activity,

several cancer related pathways are known to be affected by celecoxib independently of its inhibitory effect on COX-2 (Grosch et al., 2006). Celecoxib has been shown to induce cell cycle arrest, apoptosis and to inhibit angiogenesis and metastasis by influencing either the expression or the activity of related proteins. Some direct targets of celecoxib such as protein kinase B or phosphoinositide-dependent kinase 1 has been proposed. In addition, celecoxib was found to inhibit the activity of some membrane bound proteins such as Ca^{2+} ATPase, however the action mechanism is not clear (Grosch et al., 2006).

Celecoxib has also been shown to have an uncharacterized role in Alzheimer's disease. On the other hand some COX independent mechanisms, such as membrane dynamics and structure, have also been suggested for its activity (Gamerdinger et al., 2007). It was proposed that celecoxib induces formation of amyloid-β peptides by ordering the cellular membranes and thus changing the activity of membrane bound proteins, especially β- and γ-secretase.

1.2.2 Interaction of Celecoxib with Membranes

It is not clear whether celecoxib exerts its function through a direct interaction with membrane bound enzymes or its interaction with cellular membranes alters the activity of these enzymes. Studies on the interaction of celecoxib with membranes at molecular level are very limited. Using small angle X-ray diffraction, Walter et al. (Walter et al., 2004) showed that celecoxib is localized at the interfacial region of 1-palmitoyl-2-oleoyl-sn-glycero-3-phosphocholine (POPC) - cholesterol membranes, at a 1:10 drug : phospholipid mole ratio (9.1 mol% drug). In other studies, fluorescence anisotropy technique revealed that celecoxib decreases membrane fluidity in a mouse neuroblastoma cell line N2a (Gamerdinger et al., 2007) and Tomisato et al. (Tomisato et al., 2004) reported that celecoxib causes a decrease in membrane fluidity in egg phosphatidylcholine model membranes using fluorescence polarization.

1.3 Basic Theory of Biological Membranes

Biomembranes define and separate functional compartments within the cell, as well as separating the cell from its environment. All biological membranes are composed essentially of lipids and proteins some of which contain short chains of carbohydrates (Hauser and Poupart, 2004). Membrane lipids are amphipathic; one part of the molecule is hydrophobic and the other is hydrophilic. The hydrophobic interactions with each other and the hydrophilic interactions with water direct their packing into lipid bilayers. Membranes are mainly composed of three kinds of lipids; glycerophospholipids, cholesterol and sphingolipids. Glycerophospholipids possess a glycerol backbone to which two fatty acids are attached in an ester linkage to the first and second carbons (*sn* 1 and 2 positions) and a phosphate group is attached through a phosphodiester linkage to the third carbon (*sn* 3 position). The phosphate group bound to an alchohol constitutes the highly polar head group of phospholipids. Phosphatidylcholine (PC) which has choline in its head group is one of the major phospholipids found in biological membranes (Fig 1.3). The fatty acids in phosphoglycerides can be any of a wide variety, each of which is specific for a kind of organism or a tissue. In general, glycerophospholipids contain a C16 or C18 saturated fatty acid at C-1 and a C18 to C20 unsaturated fatty acid at C-2.

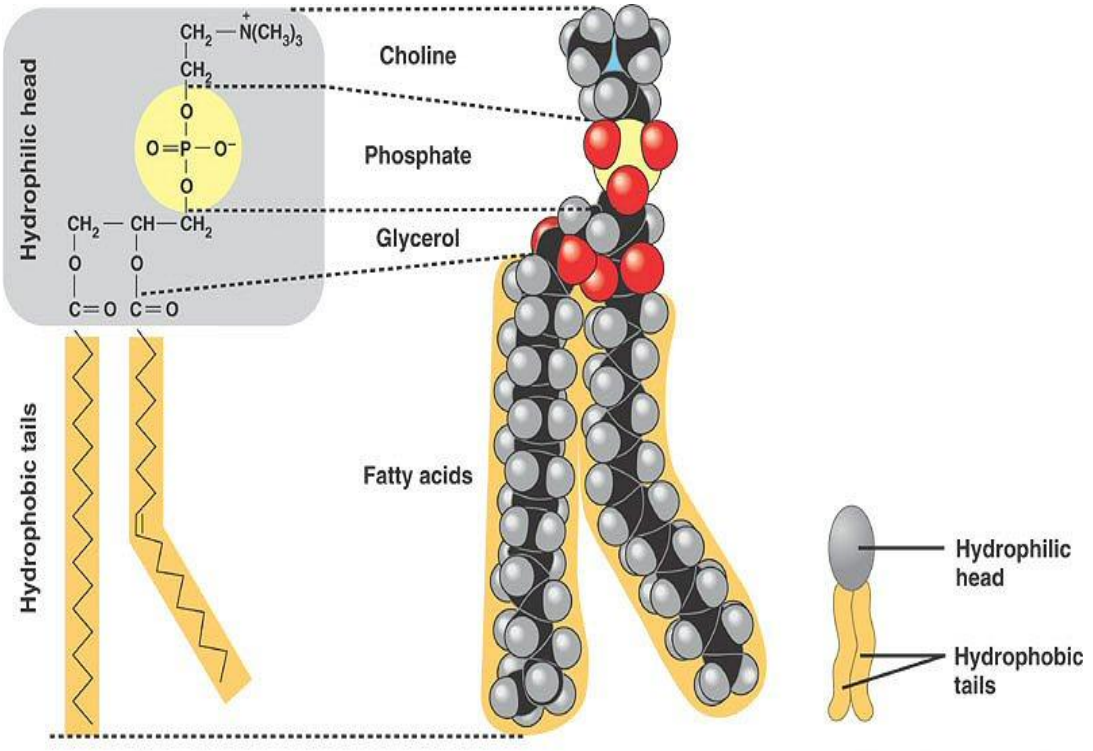

Fig. 1.3 Structure of phosphatidylcholine (figure taken from meyerbio1b.-wikispaces.com/%E2%80%A2Lipids).

1.3.1 Molecular Motions in Membranes

The types of motion of phospholipids in a membrane can be classified into intermolecular and intramolecular motions. Intermolecular motions include rotation around the long molecular axis, translational diffusion within a leaflet of the bilayer and transverse diffusion (flip-flop) between the two leaflets of the bilayer. Intramolecular motions include torsional motions around single bonds and segmental motions like rotation of the acyl chains or the head groups (Jain, 1979a). These types of motions are summarized in Fig 1.4.

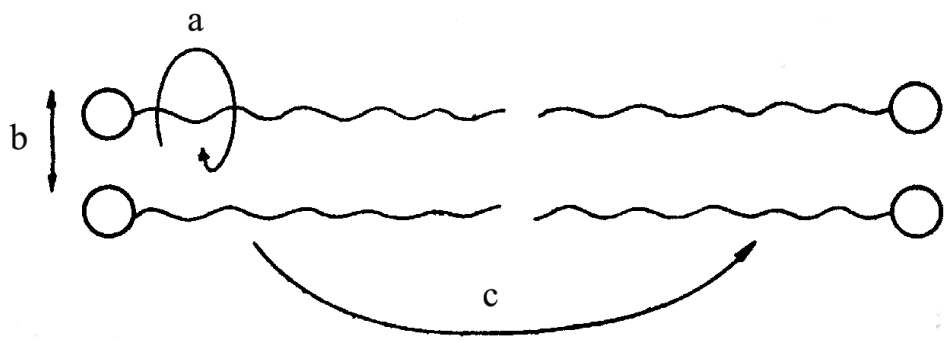

Fig. 1.4 Molecular motions in membranes. (a) rotational motion, (b) lateral diffusion, (c) flip-flop (Jain, 1979a).

Rotational motion around the long axis of a lipid molecule occurs without disruption of intermolecular interactions. Although the lipid molecule has van der Waals interactions with the neighboring lipid chains, the polar head groups are only stabilized by surrounding water molecules and to some extend by electrostatic forces with nearby polar groups. Lateral diffusion occurs due to non-specific van der Waals interactions between the components of the membrane, so that the molecules move past each other in the plane of the membrane. This type of motion can induce phase separation in the bilayer. Transverse motion is a rare process since it requires interaction of head groups with the hydrophobic core of the membrane. Membrane asymmetry is a result of this type of motion. These types of motions can account for the dynamics and fluidity of the bilayer.

1.3.2 Structural Isomerizations in Membranes

These include isomerizations between different conformations (*trans-gauche* isomerization of acyl chains). The trans-gauche isomerizations of acyl chains account for the flexibility of the chains and result from rotations around the C-C bonds. If the

rotation is 120°, it leads to transient gauche isomer (or kink) formation (Fig 1.5). The all-trans conformation allows for the closest packing of the fatty acyl chains and the presence of one or more gauche conformer would produce distortions in the shape and size of the acyl chains. Gauche conformers increase the cross-sectional area and decrease the length of the acyl chains by producing kinks in their structure (Jain, 1979a).

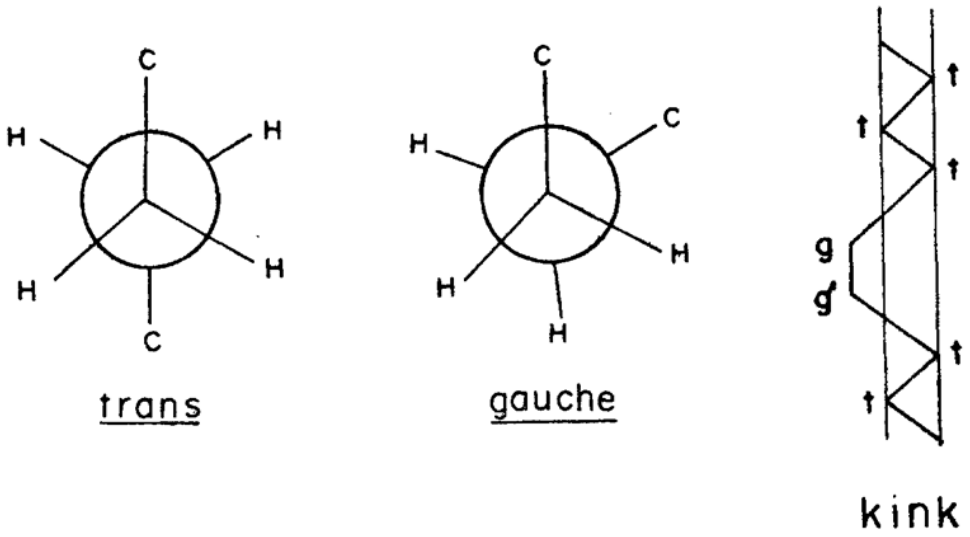

Fig. 1.5 Trans-gauche isomerizations in acyl chains of phospholipids (Jain, 1979a)

1.3.3 Thermotropic Phase Transitions in Membranes

The membrane lipids can exist in a variety of different kinds of organized structures, that is, they are highly polymorphic. The polymorphic form that predominates at particular conditions depends on the structure of the lipids, temperature, pressure, and pH. The behavior of lipid molecules in membranes is strongly influenced by temperature. Phospholipid bilayers exist in all-trans conformation at low

temperatures because this conformation has the lowest free energy. The probability of gauche conformations increases with increasing temperature. The van der Waals forces that stabilize the acyl chains in all-trans conformers require extensive overlap between neighboring chains. If a gauche conformer is introduced into a chain, the neighboring chains would also be forced to have a similar structure. Therefore if there is an external perturbation like temperature, a cooperative change in the packing of the bilayer would be induced. This is what happens in the case of gel to liquid-crystalline phase transition of membranes. The thermally induced transition of membranes from a relatively ordered, gel phase to a relatively disordered, fluid like state as a result of the cooperative melting of the fatty acyl chains is called gel to liquid-crystalline lipid phase transition (Melchior and Steim, 1976). When the membrane is undergoing phase transition, energy is absorbed by the system, without causing an increase in the temperature. This temperature is said to be the phase transition temperature (Tm).

The phase transitions of membranes can be monitored by a number of spectroscopic and calorimetric techniques. Each kind of phospholipid have a characteristic phase transition temperature, that is, transitions of pure phospholipids are sharp, symmetrical and first order processes. In addition, this temperature is affected by the degree of unsaturation and the length of the fatty acyl chains. Therefore, the transitions of biological membranes appear to be broad and asymmetric since they are composed of different kinds of lipids. In addition, since lipids undergo rapid lateral diffusion, fractional crystallization and hence lateral phase separation can be observed (Zhao et al., 2007). Mixture of two or more kinds of lipids that differ in their structure and phase transition characteristics, often exhibit lateral phase separations within the plane of the membrane.

In addition to main phase transition, there are two other transitions observed in lipid membranes, namely, subtransition and pretransition. The subtransition arises from changes in the hydration states of the head groups and the pretransition reflects

changes in the tilt angle of the acyl chains (Casal and Mantsch, 1984). Therefore the molecular organization of phospholipids in the bilayer is found in four different states; crystalline gel (L_c), lamellar gel ($L_{\beta'}$), rippled gel (P_β) and liquid crystalline (L_α) (Fig 1.6). As for the main phase transition, the temperatures for subtransition and pretransition are characteristic for each kind of phospholipid. It is known that, 1,2-Distearoyl-sn-Glycero-3-Phosphocholine (DSPC), used in this study (Fig 1.6), undergoes transitions at the temperatures shown in the below diagram (Chen et al., 1980; Mabrey and Sturtevant, 1976).

$$L_c \xrightarrow{T_s\,(21\,^\circ C)} L_\beta \xrightarrow{T_P\,(51\,^\circ C)} P_\beta \xrightarrow{T_m\,(54\,^\circ C)} L_\alpha$$

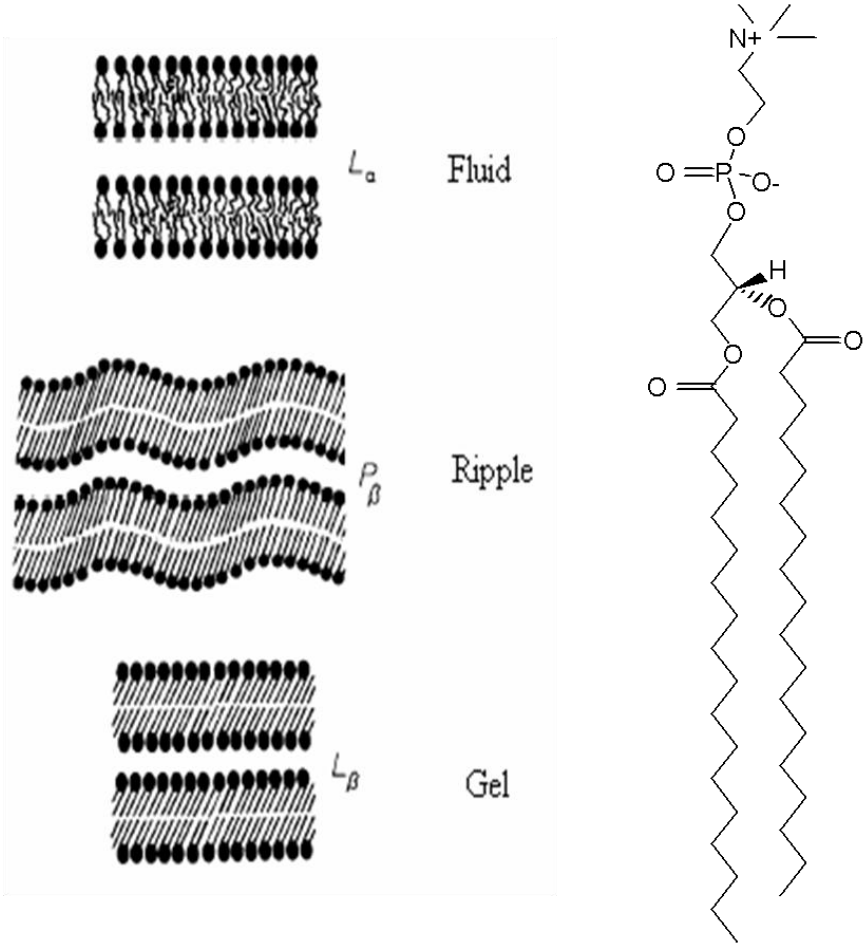

Fig. 1.6 Different phases of phospholipids (left) and the structure of DSPC (right) (Stuart, 1997).

1.3.4 Liposomes as Model Membranes

Liposomes are closed structures that can be formed after suspending dry lipid material in an aqueous solution with mechanical agitation (Bangham, 1972). Phospholipids are the most commonly used lipids; however, liposomes can also be prepared from single chain amphiphiles, lysophosphatides in the presence of equimolar cholesterol. According to the preparation method and the composition of lipids used, several kinds of liposomes can be formed (Szoka and Papahadjopoulos,

1980). Liposomes, called multilamellar vesicles (MLVs), resulting from aqueous dispersions of most phospholipids have diameters between 20-5000 nm and contain multiple layers. On sonication or extrusion, MLVs disperse into unilamellar vesicles which are categorized into two groups according their sizes. Vesicles of sizes under 100 nm are usually considered as small unilamellar vesicles (SUVs) and the larger ones are called large unilamellar vesicles (LUVs) (Szoka and Papahadjopoulos, 1980). Figure 1.7 shows the structure of a liposome and types of liposomes.

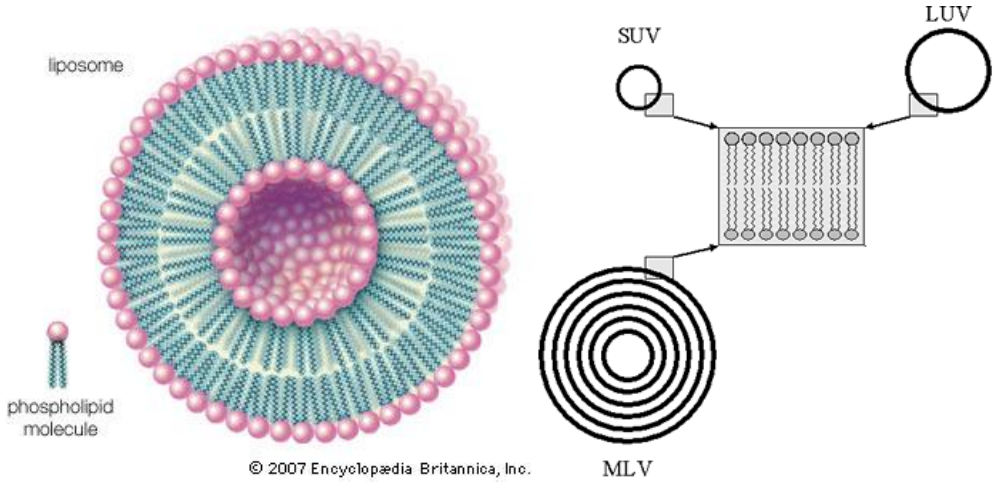

Fig. 1.7 Structure of a liposome (Left) Types of liposomes (Right) (www.scf-online.com/.../galenik_25_d_dr.htm)

The extremely complex structure and function of biological membranes necessitates the use of model membranes of much less complexity. Liposomes are used as models for cells, to characterize the properties of bilayers or as a matrix for the reconstitution of membrane functions from isolated membrane components (Jain, 1988). MLVs are the best model systems if physical properties and interactions between the molecules are of interest, however, in permeability studies unilamellar vesicles are preferred

(Bangham, 1972; Madden, 1997). This is mainly because unilamellar vesicles are more unstable and have smaller radius of curvature compared to MLVs. MLVs were proved to be useful systems in examining the physical and structural properties of phospholipids and became a favored model due to their simplicity and ease of preparation (Korkmaz and Severcan, 2005; Madden, 1997; Mannock et al., 2008). Besides being an invaluable tool as model membranes, liposomes are also used as delivery systems for drugs (Drummond et al., 1999) and DNA (Srinivasan and Burgess, 2009).

1.4 Structure and Function of Cholesterol

Cholesterol is the major sterol present in mammalian cell membranes. Usually a cholesterol:phospholipid ratio of 1:1 is favored in most biological membranes but 2:1 ratio is also observed under some circumstances. This ratio changes from 0.11 to 0.33 in plasma membranes and subcellular membranes (Demel and Dekruyff, 1976). The structure of cholesterol is shown in Figure 1.8.

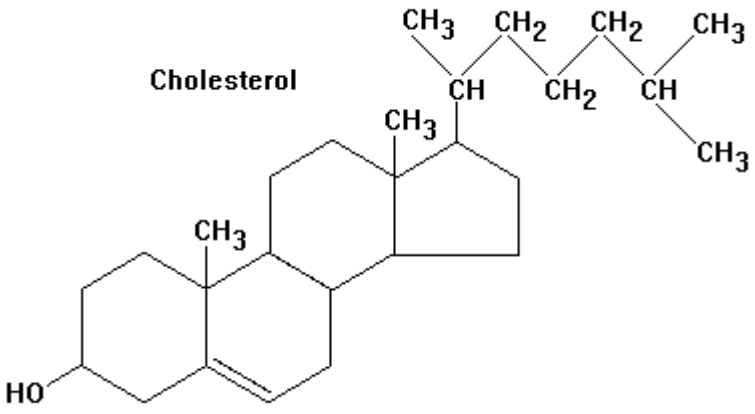

Fig. 1.8 Structure of cholesterol.

The cholesterol molecule consists of a steroid ring system, referred to as planar sterol nuclei, a hydroxyl group at C3 and a hydrophobic tail at C17. Although most of the molecule is hydrophobic, the hydroxyl group gives cholesterol an amphipathic character. This property determines the orientation of cholesterol in the bilayer. The polar hydroxyl group faces the aqueous solvent and the hydrophobic steroid rings are oriented parallel to the fatty acyl chains of phospholipids, which is shown in Fig 1.9. ^{31}P NMR (Yeagle et al., 1975), X-ray diffraction (McIntosh, 1978) and infrared (Mannock et al., 2008) studies have excluded the possibility of an interaction between cholesterol the head groups of phospholipids. It is widely accepted that the –OH group of cholesterol should be located close to the ester carbonyl group, and H-bonding between these moieties have been proposed by several investigators (Arsov and Quaroni, 2007; Yeagle et al., 1975).

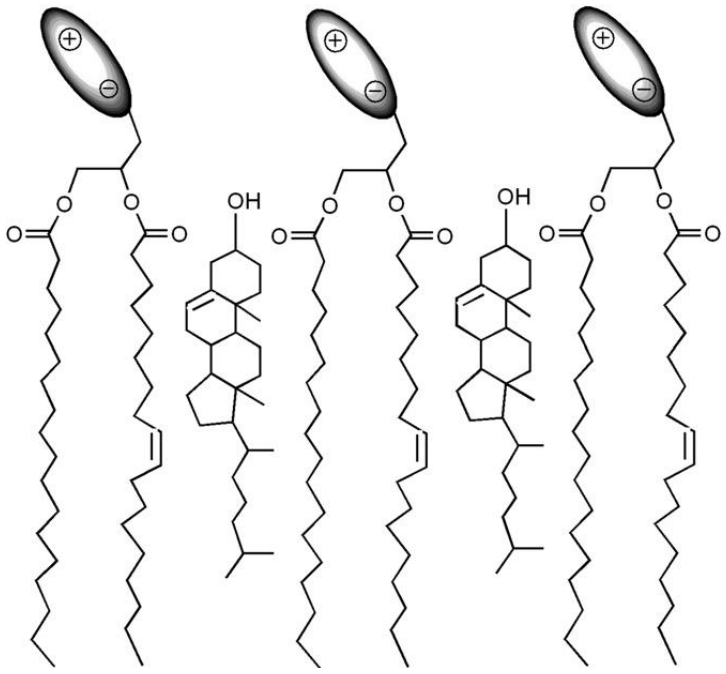

Fig. 1.9 Localization of cholesterol in the phospholipid bilayer (Chen and Tripp, 2008).

Since cholesterol is the most abundant sterol in biological membranes, it is believed that it is a primary modulator of the characteristics of bilayers. The effect of cholesterol on the phase behavior, structure, permeability and dynamics of model and biological membranes has been investigated extensively, using a wide range of physical techniques. One of the best known effects of cholesterol is on the phase transition properties of phospholipid bilayers. Cholesterol decreases the T_m, enthalpy and the cooperativity of the L_β/L_α phase transition in a concentration dependent manner, eliminating it totally at 50 mol%. It also eliminates the pretransition at a concentration around 6 mol% (McMullen et al., 1993). Cholesterol exerts opposite effects on the acyl chain conformation below and over the T_m of phospholipids. It disorders and orders the membrane in the gel phase and liquid crystalline phases respectively. This property of cholesterol results in a differential effect on permeability and condensation of the membrane. With cholesterol incorporation, the permeability of the membrane increases and decreases in the gel phase and liquid crystalline phase, respectively (Demel and Dekruyff, 1976; Yeagle, 1985). It is believed that diffusion of small molecules through a membrane is aided by gauche conformations that form kinks, resulting in transient voids between the chains of phospholipids (Yeagle, 1985). Since cholesterol suppresses the formation of gauche conformers in the liquid crystalline phase, the permeability is decreased in this phase and vice versa in the gel phase. Cholesterol also has a condensing effect on the membrane in the liquid crystalline phase (Hung et al., 2007; Levine and Wilkins, 1971). This effect is described as the reduction in the average cross-sectional area of phospholipids and again results from the decrease in the number of gauche conformers.

All of these observations have led the investigators to conclude that, cholesterol converts the L_α and L_β of the lipid membranes to a state intermediate between them, called the liquid ordered (L_o) phase (Vist and Davis, 1990). Several investigators have constructed temperature/composition phase diagrams for cholesterol/phospholipid binary mixtures, of which the most cited is the one

constructed by Vist and Davis (Vist and Davis, 1990). The authors used DSC and ^{2}H-NMR to determine the phase properties and phase boundaries of DPPC/Chol binary mixtures. Recently two groups have constructed a phase diagram for DSPC/Chol mixtures (Liu and Conboy, 2009; Tamai et al., 2008). The phase diagram from Tamai et al. (Tamai et al., 2008) and modified for simplicity, is shown in Fig 1.10.

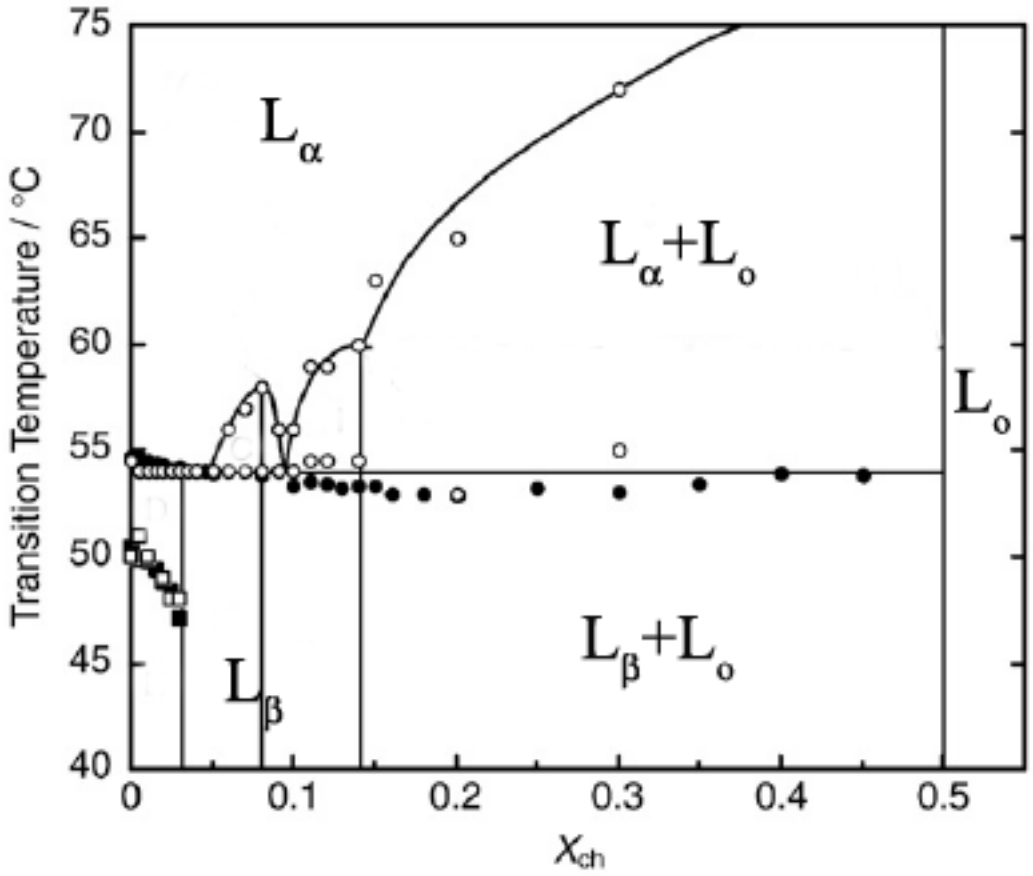

Fig. 1.10 Phase diagram for DSPC–cholesterol binary bilayer membrane. X_{ch} is defined as $m_{ch}/(m_{DSPC}+m_{ch})$, where m_{ch} and m_{DSPC} represent the molalities of cholesterol and DSPC in the sample solution, respectively. Open and closed symbols mean the data from fluorescence and DSC measurements, respectively.

This diagram shows that, between X_{ch} = 0.15 and 0.50, and below the main transition temperature, L_o phase coexists with the L_β phase. L_β phase at temperatures higher than the transition temperature, L_o phase coexists with L_α phase. However, at cholesterol concentrations higher than 0.5, only L_o phase exists at all temperatures. The segments separated by vertical lines in the figure are assigned to new phases formed by the interaction of cholesterol with some phospholipid molecules at different stoichiometric ratios. The authors suggest that cholesterol is distributed in a regular pattern in the bilayer membrane which is favored energetically. This type of organization of cholesterol was previously proposed by Somerharju et al. (Somerharju et al., 1999) and called the supperlatice model. This model suggests that different phopholipid classes tend to adopt regular, rather than random distributions. Since the head groups of PCs occupy a larger crossectional area than their acyl chains, a repulsive force occurs between them and the glycerol backbone gains a tilted configuration in order to overcome this effect. When a molecule with a smaller hydrophilic group like cholesterol is incorparated into this system, the packing frustrations are relieved because of complementary structures of the two species. The tilt angle of the backbone decreases and the head groups are hydrated by water molecules (Chen and Tripp, 2008; Demel and Dekruyff, 1976). This is energetically the most favored organization and maximal effect is obtained when the two species gain a regular, superlattice like distribution. According to this model there are only a limited number of allowed, critical concentrations for each component and a superlattice is in dynamic equilibrium with randomly arranged domains, as well as with superlattices with a different composition. On the basis of the superlattice model, Tamai et al. (Tamai et al., 2008) constructed some illustrations showing the possible distributions of DSPC/Cho mixtures at different stoichiometric ratios (Fig. 1.11).

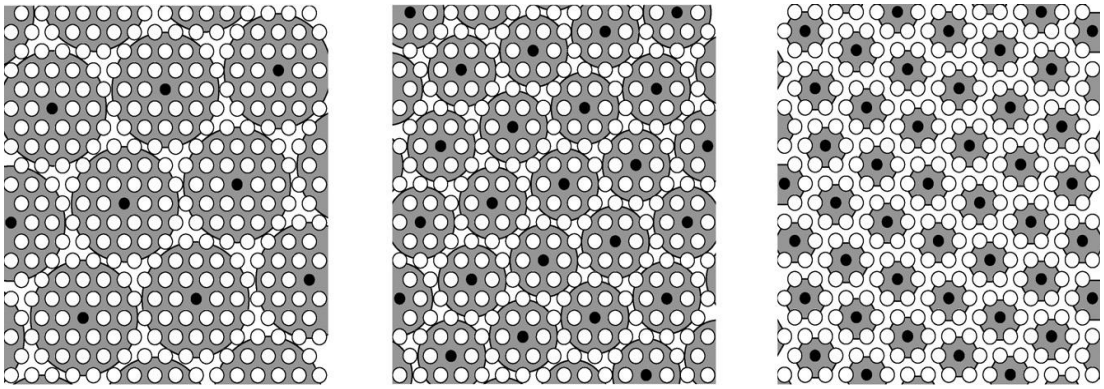

Fig. 1.11 Schematic illustration for various types of regular distribution of cholesterol in binary bilayer membranes. Closed and open circle represent a cholesterol and a DSPC molecule, respectively. A fundamental unit is indicated as a dark shaded area around a cholesterol molecule in each panel: (a) Unit (1:30) includes 30 phospholipid molecules (Xch=0.032), (b) Unit (1:12) 12 molecules (Xch=0.077), (c) Unit (1:6) 6 molecules (Xch=0.143). (Tamai et al., 2008)

The superlattice distribution was also proposed to determine the composition of the lipid rafts. The lipid raft hypothesis states that, biological membranes contain laterally segregated domains called lipid rafts (Edidin, 2003; London, 2005). They were originally thought as long-lived domains of relatively large size, which are depleted in phospholipids but rich in sphingolipids and lipid-anchored proteins. These rafts were suggested to exist in a L_o state, in contrast, the non-raft regions exist in a L_α state. These differences were suggested to cause the differential segregation of proteins throughout the membrane. Although the presence of such domains has been accepted as a fact, the composition, function and structure of the lipid rafts is still under debate.

Another effect of cholesterol that has showed controversial results is on membrane fluidity. In a number of studies, cholesterol was suggested to affect the fluidity of the membranes in a way similar to its effect on membrane order; increasing fluidity in

the gel and decreasing it in the liquid crystalline phase (Demel and Dekruyff, 1976; Kutchai et al., 1983). However, other studies revealed that cholesterol either increases the fluidity in all phases or has no effect on the dynamics of the membranes (Ghosh, 1988; Lindblom et al., 1981; Vanginkel et al., 1989). These discrepancies result mainly from the misuse of the terms order, microviscosity and fluidity.

Cholesterol has also been reported to have an effect on the bilayer thickness. In an early study, McIntosh et al. (McIntosh, 1978) compared the effects of cholesterol on various PCs changing in the acyl chain length from 12C to 18C, using X-ray diffraction technique. This study revealed that, cholesterol increases the bilayer thickness of 12 and 16C PC bilayers, while decreasing it in 18C PC and that this may result from the relative hydrophobic lengths of cholesterol and DSPC. The DSPC molecule should produce kinks near its methyl ends in order to fill the space caused by the shorter cholesterol molecule. In later studies by McMullen et al. (McMullen et al., 1993), some other differences on the effect of cholesterol were observed when 18C and longer PCs were considered and was explained by the hydrophobic mismatch theory. This theory is based on the fact that, the hydrophobic thickness of PC bilayers decreases by approximately one-third at the gel to liquid-crystalline phase transition due to the introduction of gauche conformers. Therefore, incorporation of an amphiphilic molecule, can affect the stabilities of the gel and liquid-crystalline phases according to the degree of mismatch between the effective hydrophobic length of the amphiphile and the phospholipid hydrocarbon chains. The least effect should be seen when the effective length of the molecule equals the mean hydrophobic length of the acyl chains. The effective length of the cholesterol molecule is ~17.5 Å which close to the thickness of 17C PC bilayer and the hydrophobic length of DSPC ~22.4 Å. Thus the differing effects of cholesterol on longer chain PCs can be explained using this theory.

1.5 Electromagnetic Radiation and Optical Spectroscopy

When electromagnetic radiation encounters matter, it can be scattered (its direction of propogation changes), absorbed (its energy is transferred to the molecule) or emitted (energy is released by the molecule). The probability of the occurrence of each process is a property of the particular molecule encountered. If the energy of the light is absorbed, the molecule is said to be excited. A molecule or part of a molecule that can be excited by absorption is called a chromophore. An excited molecule can possess any one of a set of discrete amounts (quanta) of energy described by the laws of quantum mechanics. These amounts are called the energy levels of the molecule. A typical energy-level diagram describing these energy levels is presented in Fig. 1.12. The major energy levels are determined by the possible spatial distributions of the electrons and are called electronic energy levels; on these are superimposed vibrational levels, which indicate the various modes of vibration of various covalent bonds of the molecule. The lowest electronic level is called the ground state and all others are excited states. The absorption of energy is most probable only if the amount absorbed corresponds to the difference between energy levels. A change between energy levels is called a transition. Mechanically, a transition between electronic energy levels represents the energy required to move an electron from one orbit to another (Freifelder, 1982).

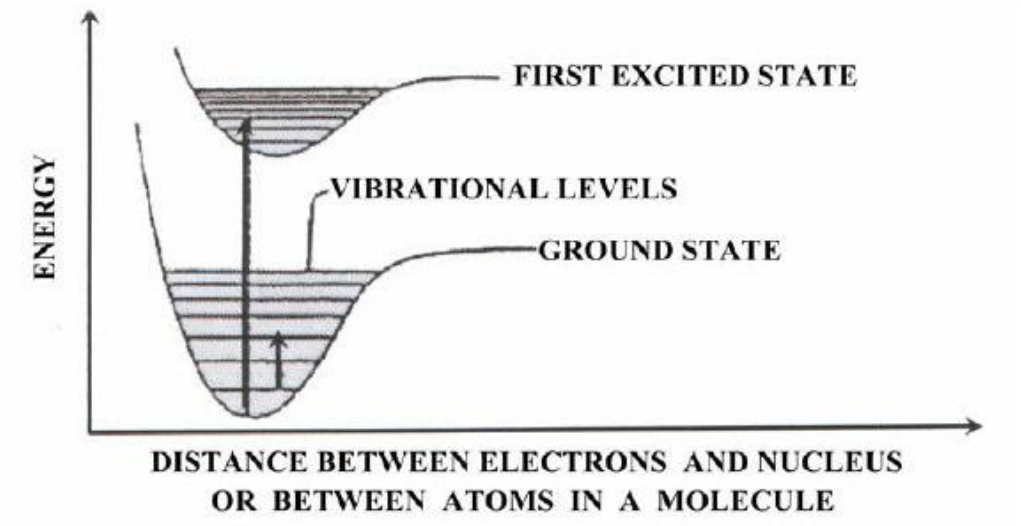

Fig. 1.12 Typical energy-level diagram showing the ground state and the first excited state. Vibrational levels are shown as thin horizontal lines. A possible electronic transition between the ground state and the fourth vibrational level of the first excited state is indicated by the long arrow. A vibrational transition within the ground state is indicated by the short arrow (Freifelder, 1982).

The total energy of a molecule is given by the sum of energies of every different motion that the molecule has. Then, the formula of total energy is:

$$E_{\text{total}} = E_{\text{transition}} + E_{\text{rotation}} + E_{\text{vibraion}} + E_{\text{electronic}} + E_{\text{electron spin orientation}} + E_{\text{nuclear spin orientation}} \quad (1.3)$$

Each *E* in the equation represents the appropriate energy as indicated by its subscript. In a solution, a molecule can translate, rotate and vibrate. The energies associated with each of these are quantized (Campbell, 1984). E_{rotation}, $E_{\text{vibration}}$ and $E_{\text{electronic}}$ are associated with the microwave, infrared and ultraviolet-visible region of the electromagnetic spectrum, respectively (Campbell, 1984).

Spectroscopy is defined as the study of the interaction of electromagnetic radiation with matter. It involves irradiation of a sample with some form of electromagnetic radiation, measurement of the scattering, absorption, or emission in terms of some measured parameters, and the interpretation of these measured parameters to give useful information.

1.5.1 Infrared Spectroscopy

Transitions between vibrational levels of the ground state of a molecule result from the absorption of light in the infrared (IR) region, between 10^3 and 10^5 nm. Infrared region is divided into three sub regions: the far infrared (400-0 cm^{-1}), the mid-infrared (4000-400 cm^{-1}) and the near infrared (14285-4000 cm^{-1}). Most infrared applications employ the mid-infrared region (Stuart, 1997). A molecule absorbs infrared radiation when the vibration of the atoms in the molecule produces an oscillating electric field with the same frequency as that of the incident IR light (Freifelder, 1982). For a molecule to show infrared absorptions the electric dipole moment of the molecule must change during the vibration. This is the selection rule for infrared spectroscopy. A dipole occurs when there is charge separation across a bond and this dipole changes when the bond stretches or bends. These two kinds of vibrations are used to describe molecular motions in infrared spectroscopy (Fig. 1. 13). A stretch is a movement along the line between the atoms so that the interatomic distance is either increasing or decreasing. A bend can occur in the plane of the molecule or out of plane and results in a change in the bond angle (Stuart, 1997).

An infrared spectrum is obtained by passing infrared radiation through a sample and determining what fraction of the incident radiation is absorbed at a particular energy. As a result, a highly complex absorption spectrum, which is the plot of absorption as a function of wavenumber (ν) expressed in terms of cm^{-1}, is produced. Therefore, infrared spectra are generated by the characteristic motions (bond stretching, bond bending, and more complex motions) of various functional groups (e.g., methyl,

carbonyl, phosphate, etc.). The value of infrared analysis comes from the fact that the modes of vibration of each group are very sensitive to changes in chemical structure, conformation, and environment which is not reflected by ultraviolet and visible light spectroscopy (Freifelder, 1982).

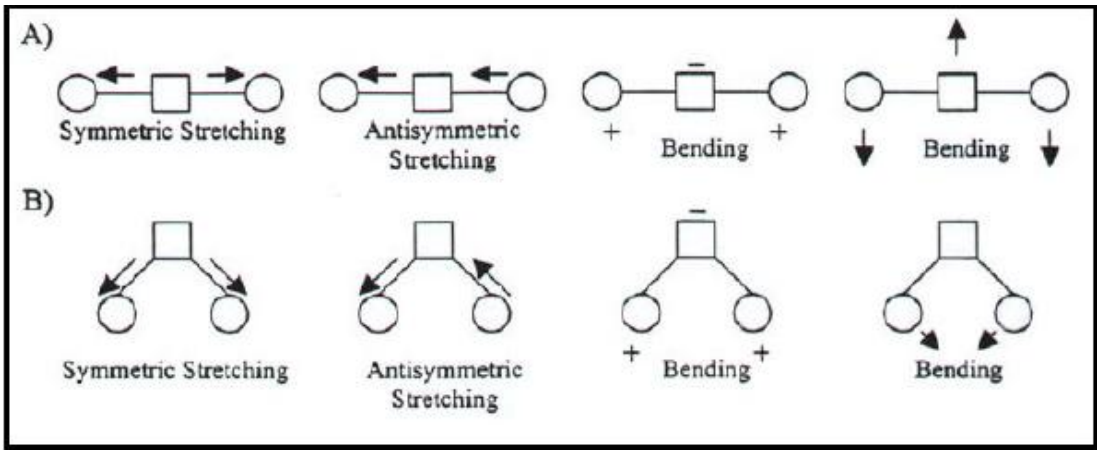

Fig. 1.13 The schematic representation of some of the molecular vibrations in a linear (A) and a non-linear (B) triatomic molecule. (+) and (-) represent out of plane movements (Arrondo et al., 1993).

1.5.2 Fourier Transform Infrared Spectroscopy (FTIR)

Fourier-transform infrared (FTIR) spectroscopy is based on the idea of the interference of radiation between two beams to yield an interferogram, which is a signal produced as a function of the change of pathlength between the two beams (Stuart, 1997). The basic components of an FTIR spectrometer are shown schematically in Fig.1.14.

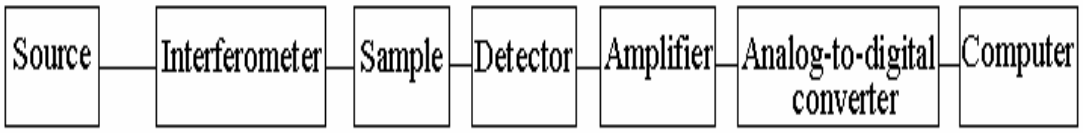

Fig. 1.14 Basic components of an FTIR spectrometer.

The radiation emerging from the source is passed through an interferometer, to the sample before reaching a detector. The beam then passes through the sample which absorbs all the wavelengths characteristic of its spectrum. The detector reports variation in energy versus time for all wavelengths, at the same time. For rapid-scanning interferometers liquid nitrogen cooled mercury cadmium telluride (MCT) detectors are used. For slower scanning types of interferometer, pyroelectric detectors (e.g. a deuterated triglycine sulfate (DTGS) detector element) can be used. This multiplexing of the infrared signals and the high optical throughput of the interferometer, result in higher signal-to-noise values for interferometric infrared spectrometers compared to dispersive instruments. After amplification of the signal, in which high-frequency contributions have been eliminated by a filter, the data are converted to digital form by an analog-to-digital converter and transferred to the computer for Fourier-transformation. Rather than recording the spectrum as energy versus time, a mathematical function called a Fourier transform allows us to convert an intensity versus time spectrum into an intensity versus frequency spectrum.

1.5.3 Infrared Spectroscopy in Membrane Research

One of the useful aspects of FTIR spectroscopy is the fact that any group or bond in a molecule gives rise to characteristic band(s) in the infrared spectra. Thus, these characteristic spectral features can simply be assigned to the particular groups or bonds in the corresponding molecules. This approach in vibrational spectroscopy is referred to as group frequencies (Stuart, 1997). The information available from an

FTIR spectrum are reflected from the form of band shapes, peak heights, half widths, frequency shifts and integrated intensity of the vibrational bands (Chapman and Hayward, 1985). Band frequency is determined by the nature of the atoms in a chemical bond, their conformation and immediate environment in the molecule, whereas bandwidth is related to the rates of motion of the molecule. Thus IR spectra provide information both on the chemical structure of the molecule under investigation and on its conformation and dynamics.

Infrared spectroscopy can provide valuable structural information about lipids, which are important molecular components of membranes. The infrared spectra of phospholipids can be divided into the spectral regions that originate from the molecular vibrations of the hydrocarbon tail, the interface region and the head group (Casal et al., 1980; Casal and Mantsch, 1984; Chapman and Hayward, 1985; Severcan et al., 2005). The hydrocarbon tail gives rises to acyl chain modes which are the most intense vibrations in the infrared spectra of lipid systems. These C-H stretching vibrations give rise to bands in the 3100 to 2800 cm^{-1} region. The most useful infrared bands for probing the glycerol-acyl chain interface of ester lipids are the ester carbonyl stretching modes (C=O stretretching) which give rise to strong infrared bands in the spectral region 1750-1700 cm^{-1}. Vibrational modes of the moieties found in the headgroup of membrane lipids give rise to a number of characteristic infrared bands. In phospholipids, infrared bands characteristic for the head groups of phospholipids originate from the vibrations of the phosphate moiety. There are two strong bands around 1230 and 1085 cm^{-1} due to the P=O doublebond stretching (PO_2^- antisymmetric and symmetric stretch, respectively).

One of the best studied physical properties of membrane lipids is their thermotropic phase behavour. As mentioned before, the gel to liquid crystalline phase transition results in remarkable structural rearrangements of phospholipids. Temperature studies of the infrared spectra of phospholipids provide a sensitive means of studying such thermally induced transitions in lipids (Casal et al., 1980). In addition, FTIR

spectroscopy is well suited for the study of the interactions of membrane lipids with a variety of small molecules such as drugs, environmental chemicals and organic solvents. Since these agents exert their efects not only by passing through the membrane but also by interacting with membrane proteins or with the membrane itself, investigating their mechanism of action is important in a number of disciplines (Jain, 1979a). The important course of action during the interpretation of the phase transitions and membrane interactions is to correlate the changes in the spectroscopic parameters with the changes that are known to occur in the structure of the lipids during those processes.

1.5.4 Turbidity Technique at 440 nm

Turbidity technique is a special form of light scattering. Scattering is usually detected at an angle θ to the incident wave, but it may also be detected by the reduction in the transmitted light at θ=0 which is called turbidity (Campbell, 1984). In other words, turbidity is the decrease by scattering of the transmitted light, and thus is equal to the scattering over all angles. Light scattering offers the distinct advantage that the system can be observed without significant perturbations. A standard spectrometer is often easily adapted to measure light scattering (Chong and Colbow, 1976).

Although turbidity is generally used in protein denaturation studies, it was shown that, it is also useful in studying thermotropic phase transitions of membranes, effects of additives on the size, structure, aggregation and fusion processes of lipid vesicles (Chong and Colbow, 1976; Eker et al., 1999).

1.6 Differential Scanning Calorimetry (DSC)

DSC is a thermal analysis method used to describe physical and chemical changes as function of temperature. The principle of DSC is indeed simple. The sample and a reference that does not undergo a phase transition within the temperature range of

interest are heated at identical predetermined rates. When the heating starts, the temperatures of the sample and the reference cell increase linearly and the temperature difference between them is zero. However, when the sample undergoes a thermal transition, this produces a temperature differential between the sample and the reference. The system then supplies more heat either to the sample or to the reference in order to keep the temperatures of the two cells equal. The recorded parameter in DSC measurements is thus the excess specific or differential heat as a function of temperature. If the sample does not undergo a thermal event, the output should be a straight, horizontal baseline, but if a transition occurs, the recorder pen is deflected from the baseline. The direction of the deflection depends on whether the event is endothermic (upwards) or exothermic (downwards), and the magnitude of the deflection depends on the magnitude of the differential heating rate (McElhaney, 1982).

The DSC curve is analyzed to determine the transition temperature, T_m, and the calorimetric enthalpy of transition, ΔH_{cal}. For first order phase transitions such as the bilayer gel to liquid-crystalline transition of a pure phospholipid, T_m is where the excess specific heat reaches its maximum value. The value of the calorimetric enthalpy (ΔH_{cal}) for the phase transition is determined by integrating the area under the peak (McElhaney, 1982).

The main applications of DSC include determination of the effect of composition, hydration, pH, and chemicals on the phase-transition temperatures and enthalpies of biological membranes and pharmaceuticals, thermal characterization of complex processes, such as the denaturation of proteins and specific heat measurements in the glass-transition of polymers. Differential scanning calorimetry is a classic method, but application to biological systems is a recent event. DSC is probably the single most powerful technique for the routine measurement of gel to liquid-crystalline phase transitions in lipid bilayers and biological membranes. The current high-sensitivity DSC instruments require only relatively dilute suspensions of material

permitting accurate control of the pH and ionic composition of the aqueous phase. Unlike other spectroscopic techniques, DSC does not require the introduction of foreign probe molecules into the system under study. Morover, this technique is unique in providing a direct and accurate measurement of the thermodynamic parameters of the lipid phase transition under investigation (McElhaney, 1982).

1.7 Scope and Aim of This Study

Celecoxib has been shown to influence the activity of several proteins. Although its action mechanism is not clear, these mechanisms were proposed to be independent of COX-2 (Grosch et al., 2006). Lipophilic and amphipathic compounds that penetrate into the lipid bilayer are reported as being able to modify the phase transition, fluidity and order of the membrane lipids and consequently membrane function (Knazek et al., 1981; Korkmaz and Severcan, 2005; Lucio et al., 2004; Severcan et al., 2000c). Furthermore these modulations on the membranes are proposed to influence the activity of integral membrane proteins (Maxfield and Tabas, 2005). Therefore the lipophilic nature of celecoxib makes it a potential modulator of membrane lipid structure and dynamics and understanding these interactions at molecular level will provide further understanding of its mechanism of action.

Biological membranes are composed of extremely complex structures, thus model membranes provide a highly convenient and simple method for studying drug-membrane interactions (Bangham, 1972; Engberts and Hoekstra, 1995; Kazanci and Severcan, 2007; Severcan et al., 2005). Despite its importance, studies on the interaction of celecoxib with membranes at a molecular level are very limited. Using small angle X-ray diffraction, Walter et al. (2004) showed that celecoxib is localized at the interfacial region of the lipid bilayer. In other studies, fluorescence anisotropy technique revealed that celecoxib decreases membrane fluidity in a mouse neuroblastoma cell line N2a (Gamerdinger et al., 2007) and Tomisato et al. (2004)

reported that celecoxib causes a decrease in membrane fluidity in egg phosphatidylcholine model membranes using fluorescence polarization.

Effects of cholesterol on biological and model membranes have been studied extensively (Demel and Dekruyff, 1976; Edidin, 2003; Vist and Davis, 1990; Yeagle, 1985). However much of these studies are carried out with dipalmitoyl phosphocholine membranes. Studies on the interaction of cholesterol with DSPC membranes are very limited. McMullen et al. (1993) investigated the effects of cholesterol on the phase behavior of a series of saturated PCs using DSC. Liu et al. (2009) used sum-frequency vibrational spectroscopy and Tamai et al. (2008) used fluorescence spectroscopy and DSC to investigate the effects of cholesterol on DSPC membranes.

In the present study, we aimed to further delineate the COX-2 independent effects of the highly hydrophobic drug celecoxib, particularly through the modulation of membrane physical properties. Therefore the effect of celecoxib on pure and cholesterol containing model membranes composed of a zwitterionic lipid, 1,2-Distearoyl-sn-Glycero-3-Phosphocholine (DSPC), in the form of multilamellar vesicles (MLVs) has been investigated using three different non-invasive techniques, namely Fourier transform infrared (FTIR) spectroscopy, differential scanning calorimetry (DSC) and turbidity measurements at 440 nm. These techniques have been widely used in model membrane studies (Biruss et al., 2007; Mannock et al., 2008; Severcan et al., 2005; Shaikh et al., 2002; Villalain et al., 1986) and allowed us to obtain detailed information about the interactions of celecoxib-cholesterol-DSPC membranes in two different membrane phases. We analyzed the effects of the drug on membrane dynamics as well as structural parameters such as lipid phase transition profile, membrane acyl chain order and hydration status of the head group and glycerol backbone regions, which to the best of our knowledge, has not been reported previously.

CHAPTER 2

MATERIALS AND METHODS

2.1 Reagents

DSPC and cholesterol was purchased from Avanti Polar Lipids (Alabaster, AL, USA) and stored at -20 °C. Celecoxib was purchased from Ranbaxy (Mumbai, India). All other chemicals were of analytical grade and purchased from Merck (Darmstadt, Germany).

2.2 Phosphate Buffered Saline Preparation

Phosphate buffered saline (PBS) 0.1 M, pH 7.4 was prepared by weighing 8 g sodium chloride (NaCl), 0.27 g potassium dihydrogen phosphate (KH_2PO_4), 3.58 g disodium hydrogen phosphate 12-hydrate ($Na_2HPO_4.12H_2O$) and mixing in 500 mL of distilled water. The pH of the solution was adjusted to 7.4 by adding hydrogen chloride (HCl) and the final volume was completed to 1 L by adding distilled water. The prepared PBS buffer was autoclaved and stored at room temperature.

2.3 Preparation of Drug and Lipid Stock Solutions

Celecoxib stock solution was prepared by dissolving 5 mg of celecoxib powder either in 1 mL of pure ethanol (EtOH) (for use in liposomes without cholesterol) or in 1 mL of pure chloroform (for use in liposomes containing cholesterol).
Cholesterol stock solution was prepared by dissolving 5 mg of cholesterol in 1 mL of pure chloroform.

2.4 Preparation of Multilamellar Vesicles

Pure phospholipid MLVs were prepared according to the procedures reported previously (Korkmaz and Severcan, 2005; Severcan et al., 2005). A desired amount of DSPC was dissolved in 150 µl chloroform and excess chloroform was evaporated by using a gentle stream of nitrogen. A dried lipid film was obtained by subjecting the samples to vacuum drying for 2 hours using HETO-spin vac system (HETO, Allerod, Denmark). The lipid films were then hydrated by adding PBS buffer, pH 7.4. MLVs were formed by vortexing the mixture at 70-75 °C which is above the T_m of DSPC (~55 °C) for 20 min.

To prepare celecoxib containing liposomes, the required amount of celecoxib (1, 6, 9, 12, 18, 24 mol%) from the stock solution was first added to the sample tube, excess ethanol was evaporated by using a gentle stream of nitrogen, then DSPC was added and dissolved in 150 µl chloroform. MLVs were then prepared as described above.

For cholesterol containing liposomes, desired amount of cholesterol (10:1, 5:1, 3:1, 2:1 DSPC:Cho mol ratio), celecoxib (6 mol%) and DSPC were mixed in 150 µl chloroform and excess chloroform was evaporated by using a gentle stream of nitrogen. MLV's were prepared as above.

2.5 Sample preparation for FTIR measurements

For the FTIR measurements, 5 mg DSPC was used and the lipid films were hydrated in 35 µl of PBS buffer, pH 7.4. Sample suspensions (20 µl) were placed between CaF_2 windows with a cell thickness of 12 µm. Spectra were recorded on a Perkin-Elmer Spectrum One FTIR spectrometer (Perkin-Elmer Inc., Norwalk, CT, USA) equipped with a deuterated triglycine sulfate (DTGS) detector. Interferograms were averaged for 50 scans at 2 cm^{-1} resolution.

The experiments were conducted in separate sets for different compositions of liposomes. For DSPC liposomes containing only celecoxib (DSPC/CLX), two separate experiments were designed. In the first, we examined the effect of temperature where the samples were scanned between 30 and 75 °C and incubated at each temperature for 5 min before data acquisition. The second study evaluated the effect of CLX concentration (between 6 and 24 mol%) at 40 and 60 °C, corresponding to the gel and liquid-crystalline phases of DSPC, respectively. For the experiments involving cholesterol, the samples were scanned at 30 and 65 °C, temperatures which were decided according to the DSC measurements, for correct monitoring of the gel and liquid crystalline phases. The last two sets of experiments were repeated five times, for statistical analyses. The temperature was controlled by a Graseby Specac (Kent, UK) digital temperature controller unit.

2.5.1 Infrared Spectral Regions Used in This Study

In this study, there are mainly four absorption bands taken into consideration (Fig.2.1). Two of them are the strong bands at 2920 cm^{-1} and 2850 cm^{-1} of the infrared spectrum that correspond to the CH_2 antisymmetric and CH_2 symmetric stretching modes of the acyl chains of the phospholipid membranes, respectively. The phase transition behavior and the order-disorder state of membrane systems can be studied by the frequency analyses of these bands (Korkmaz and Severcan, 2005; Severcan et al., 2005). The frequency of the CH_2 stretching bands of acyl chains depend on the average trans/gauche isomerization in the systems and shifts to higher wavenumbers correspond to an increase in the number of gauche conformers (Casal and Mantsch, 1984; Severcan, 1997; Severcan et al., 2005; Toyran and Severcan, 2003). In addition, variations in the bandwidth of these groups are sensitive to mobility of the lipids, thus give information about the dynamics of the membrane. An increase in the bandwidth is an indication of an increase in the dynamics of the membrane (Casal et al., 1980; Korkmaz and Severcan, 2005; Lopezgarcia et al., 1993; Severcan et al., 2000c; Severcan et al., 2005; Toyran and Severcan, 2003)

The third infrared band used in this study is the carbonyl absorption band at 1735 cm^{-1} arising from the stretching vibrations of ester carbonyl groups of phospholipids. This band is conformationally sensitive to the level of hydration at the membrane interface and is influenced by hydrogen bonding (Korkmaz and Severcan, 2005; Severcan et al., 2005). The more hydrated the carbonyl group, the lower the frequency.

The last absorption band is the PO_2^- antisymmetric double stretching band, located at 1220-1240 cm^{-1}. Information about the hydration state of the polar head groups of the phospholipids can be monitored by the analysis of the frequency of this band (Korkmaz and Severcan, 2005; Lopezgarcia et al., 1993; Severcan et al., 2005).

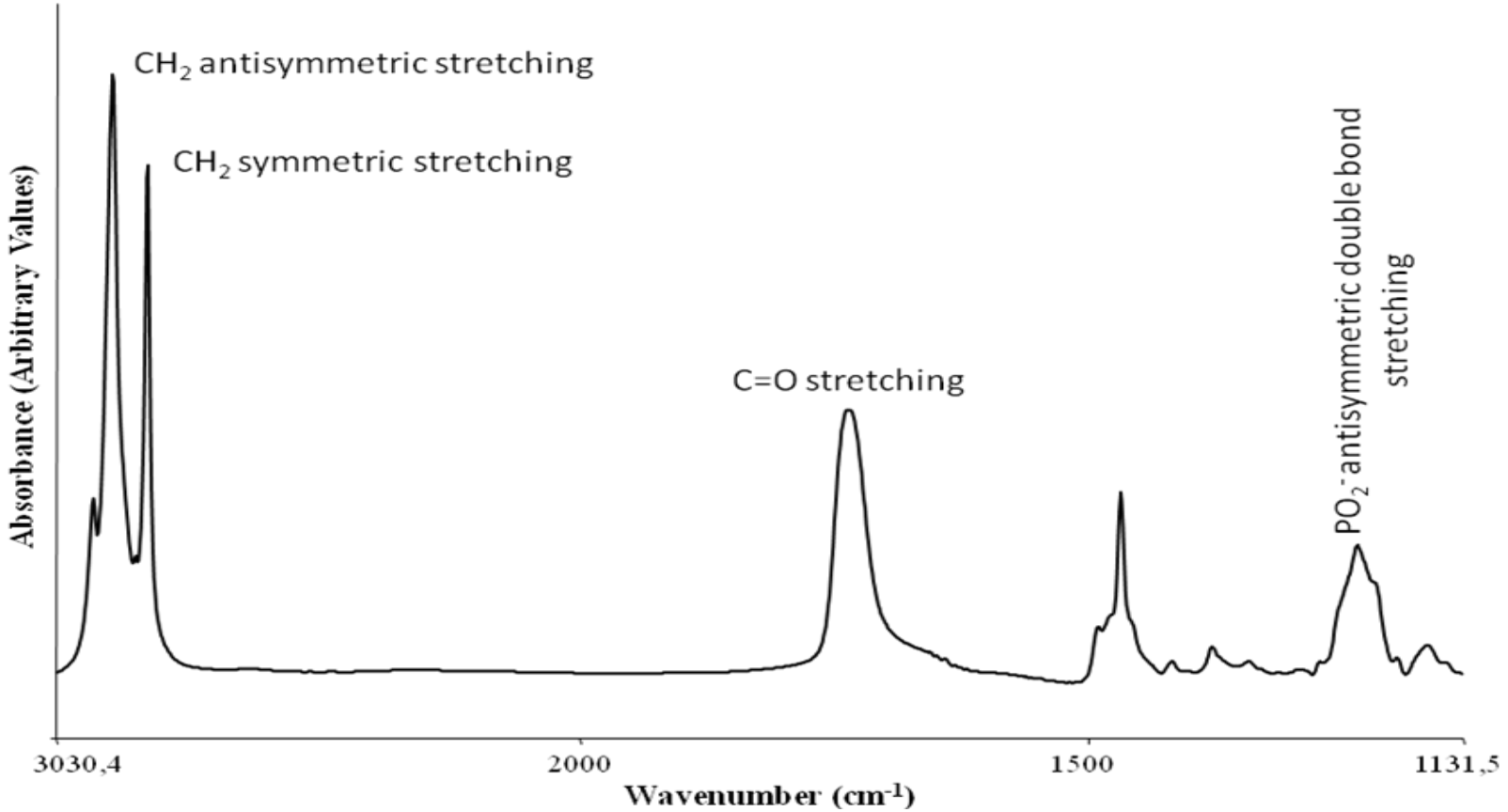

Fig. 2.1 The main infrared bands in the FTIR spectrum of DSPC liposomes

2.5.2 Spectral Analysis

The spectra were analyzed using Spectrum v5.0.1 software (Perkin-Elmer Inc., Norwalk, CT, USA). The O-H stretching bands due to water, appear in the regions of 3400-3200 cm^{-1} and 1800-1500 cm^{-1}, however, these regions overlap with the region of C-H and C=O stretching bands, respectively. Therefore, PBS buffer without celecoxib and lipids was scanned at different temperatures and it was subtracted from the spectra of liposomes at corresponding temperatures. The subtraction process was done manually by flattening the band located around 2125 cm^{-1}. Fig.2.2 shows the infrared spectrum of DSPC before and after water subtraction. Moreover, molecules in the air interfere with the spectra of samples. To prevent this interfering, spectrum of the air was recorded as a background spectrum and subtracted automatically from the spectra of samples by software programme.

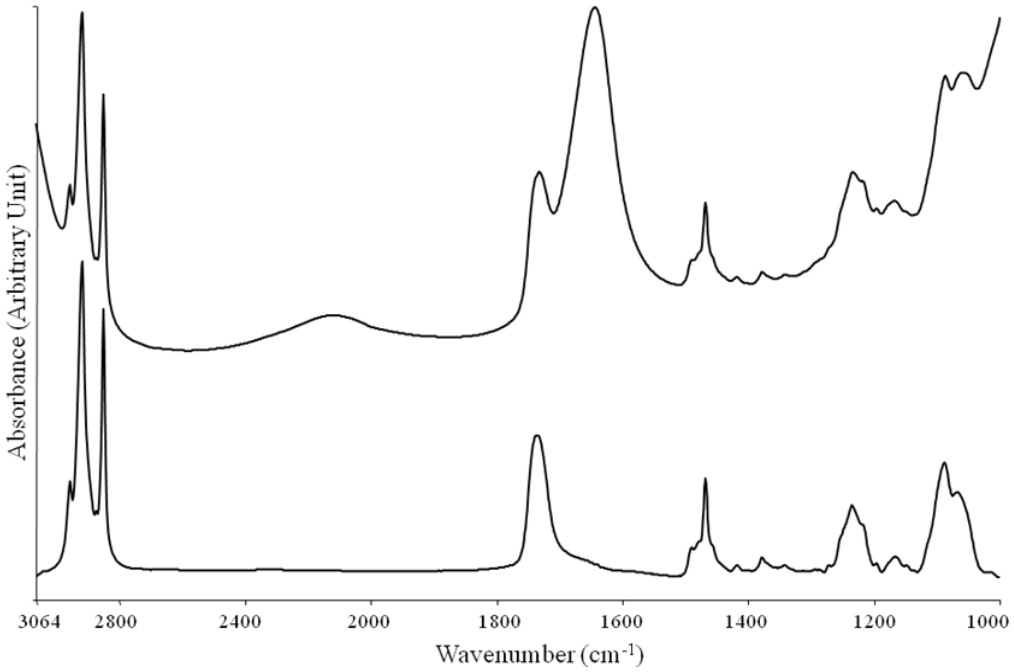

Fig. 2.2 FTIR spectrum of DSPC liposomes before (upper spectrum) and after (lower spectrum) buffer subtraction.

The additives, celecoxib in this case, usually are so small in amount with respect to the lipid that their spectra are expected as not interfering with that of the liposomes. However in this study it was seen that celecoxib, at high concentrations (12, 18 and 24 mol%), shows a significant peak at 1230 cm^{-1} which could interfere with the analysis of the PO_2^- band. This band was assigned to C-F stretching vibration of celecoxib (Gupta and Bansal, 2005). Therefore the spectrum of pure celecoxib at these concentrations was also subtracted from the corresponding celecoxib containing liposome spectra. This was done by scanning desired concentrations of pure celecoxib dissolved in DMSO at different temperatures, subtracting first the spectrum of DMSO from that of celecoxib and than using these spectra for the subtraction process of liposomes. DMSO is preferred in these processes because it has a high vaporization temperature which is advantageous in temperature dependent scannings. Fig.2.3 shows the spectrum of 24 mol% celecoxib and the spectrum of DSPC MLVs containing 24 mol% celecoxib.

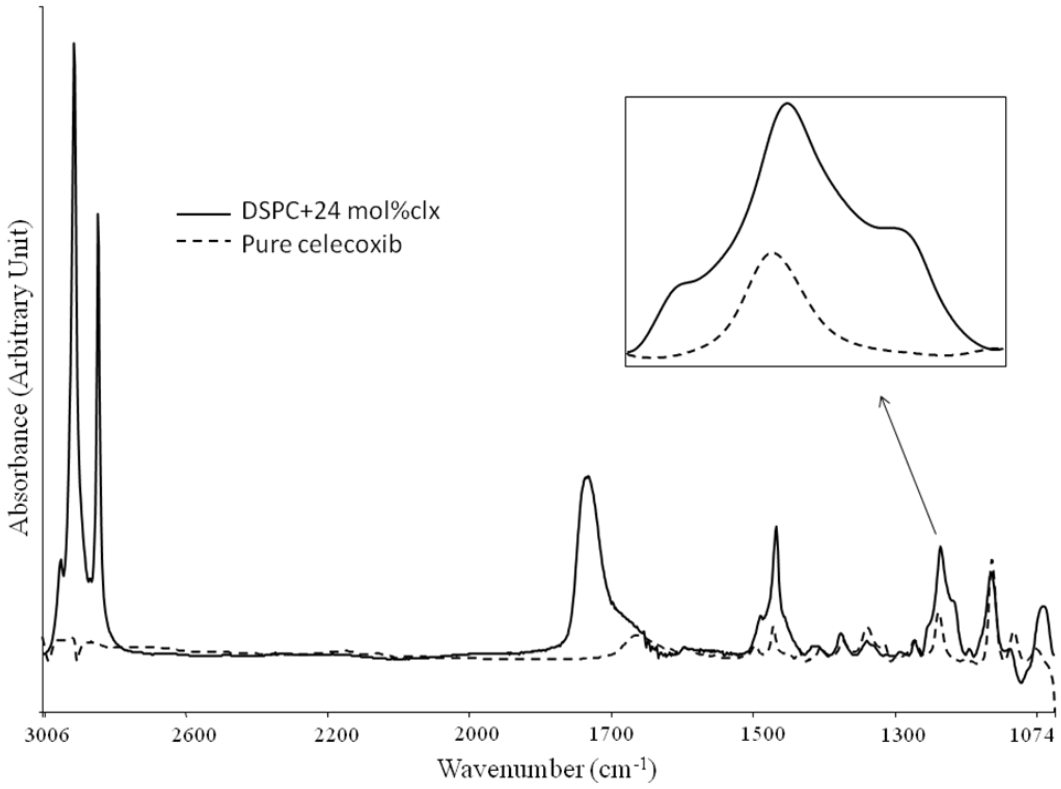

Fig. 2.3 FTIR spectra of DSPC liposomes containing 24 mol% celecoxib (straight line) and pure celecoxib (dashed line). Inset shows PO_2^- region.

The spectrum of pure cholesterol did not show any interference with none of the liposomes except for the CH_2 symmetric stretching band, shown in Fig.2.4. Therefore this band was not taken into consideration during the analysis of cholesterol containig liposomes, as has been suggested in another study (Mannock et al., 2008).

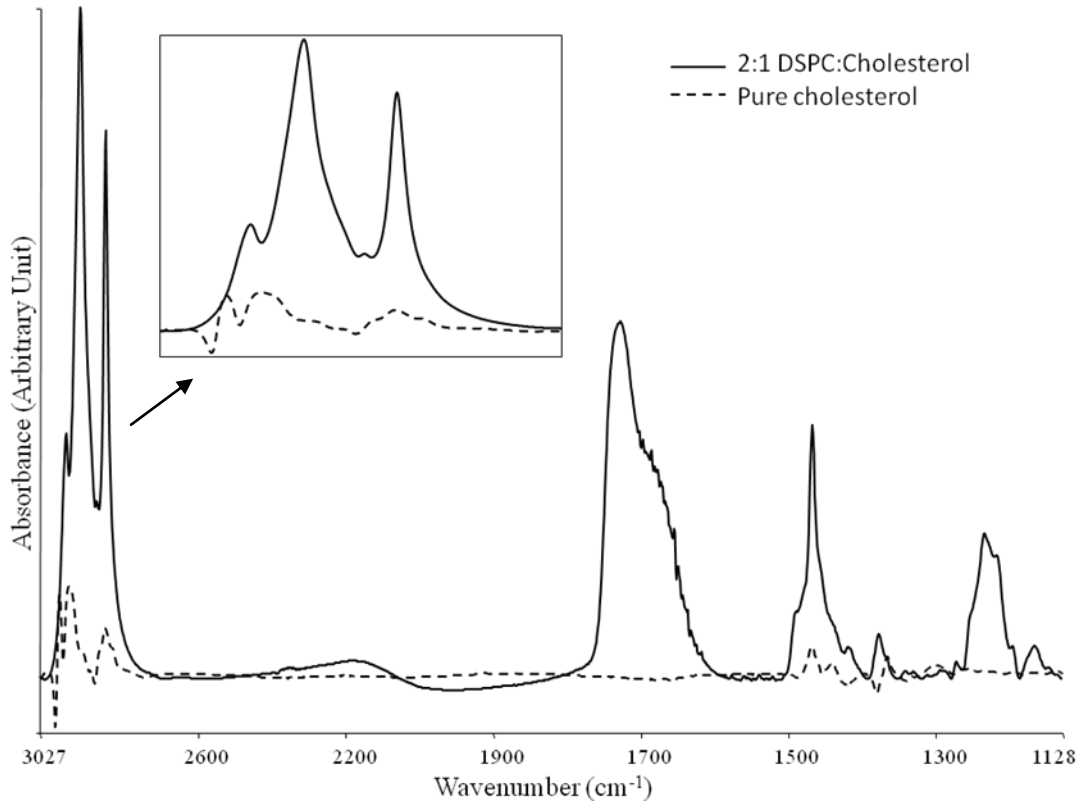

Fig. 2.4 FTIR spectra of DSPC liposomes containing 2:1 mol ratio of cholesterol (straight line) and pure cholesterol (dashed line). Inset shows the C-H region.

The band positions were measured according to the center of weight and bandwidth was measured at 0.80× peak height position. Normalization process was applied using the Perkin Elmer software only for visual demonstration of the structural changes. The purpose of the normalization is to remove differences in peak heights between the spectra acquired under different conditions. However, subtracted original spectra were used to determine spectral parameters.

2.6 Turbidity Measurements

DSPC (0.4 mg) was used to prepare thin films and the films were hydrated with 1.5 mL 0.1 M PBS, pH 7.4. Turbidity studies were carried out using a Varian-Cary 300

UV/Visible spectrophotometer (Varian Inc., Melbourne, Australia) as reported previously (Severcan et al., 2000c). Plastic clear cuvettes (LP Italiana, Milan, Italy) of 1 cm path length were used. Reference cuvettes were filled with PBS buffer to automatically account for background absorbance of the buffer. Turbidity measurements were performed at 440 nm to minimize any light scattering effect (Severcan et al., 2000b).

2.7 Sample Preparation for DSC measurements

DSPC (2 mg) was used to prepare thin films and the films were hydrated with 50 µl 0.1 M PBS, pH 7.4. The experiments were carried out in a Universal TA DSC Q 100 (TA Instruments Inc., New Castle, DE, USA). The samples were encapsulated in hermetically sealed standard aluminum DSC pans. An empty pan was used as a reference to exclude the calorimetric effect of the pan. The samples were scanned over a temperature range of 20-75°C at a heating rate of 1°C/min as reported previously (Severcan et al., 2005).

2.7.1 Thermogram Analyses

In the DSC thermograms of pure lipids, each lipid has its own transition temperature and enthalpy change. DSPC has a main phase transition temperature of ~55 °C and a transition enthalpy of 8.3 cal/g. The pretransition temperature of DSPC is ~51 °C (Mabrey and Sturtevant, 1976; McMullen and McElhaney, 1997; Tamai et al., 2008)}. On the DSC thermogram, the main phase transition of a lipid appears as a sharp peak and occurs within a very narrow temperature interval. Therefore, thermally induced phase transition occurs abruptly. Fig. 2.5 shows the DSC thermogram of DSPC liposomes. The maximum point of the peak was taken as the main phase transition temperature of the lipid. The transition enthalpies were

calculated by integrating the area under the peak, using TA Universal Analysis v4.1D programme (TA Instruments Inc., New Castle, DE, USA).

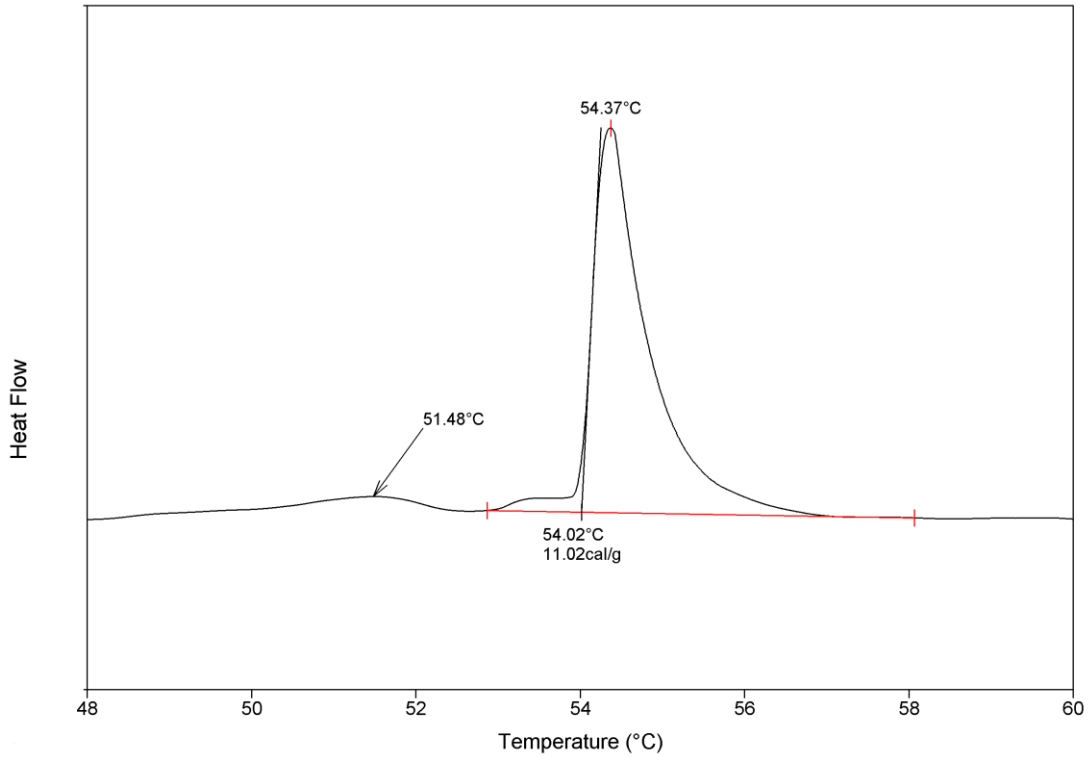

Fig. 2.5 DSC thermogram of DSPC liposomes. The small peak shows pretransition, the sharp peak shows main phase transition. The peak maximums and transition enthalpy are indicated in the figure.

Enthalpy changes reflect the changes in the packing properties of the acyl chains. An increase in ΔH_{cal} is observed with increasing chain lengths of saturated phosphatidylcholines. Since the acyl chains of longer chain PCs are more tightly packed, they resist trans to gauche isomerizations and thus more heat will be required to melt these PCs (McElhaney, 1982). The decreases in the enthalpy are also

attributed to the presence of a perturbing agent within the cooperativity region (C_1-C_8) of membranes (Zhao et al., 2007).

2.8 Statistical Analyses

Data analysis and graphing was performed using the GraphPad Prism 5 software package (La Jolla, CA, USA). Specific analysis for each experiment is indicated in the figure legends. Unless otherwise mentioned, the mean of at least five experiments was plotted together with the standard error of mean. Statistical significance was assessed using a two-tailed P value calculated with the Mann-Whitney nonparametric test. Significant difference was statistically considered at the level of $p \leq 0.05$.

CHAPTER 3

RESULTS

In this study, the lipid phase behavior in response to increasing concentrations of celecoxib and cholesterol was monitored with DSC and FTIR spectroscopy. FTIR spectroscopy was also used to determine location of the additives in the membrane. In addition it was used to investigate the changes in membrane structure and dynamics by analyzing the frequency and bandwidth of different vibrational modes which represent the acyl chains, head group and interfacial region of lipid molecules. Turbidity studies, performed at 440 nm, were used to support the FTIR results on membrane dynamics (Korkmaz and Severcan, 2005; Severcan et al., 2000c).

3.1 DSC Studies

This part of the study investigates the changes in the phase transition properties of DSPC MLVs with differing concentrations of celecoxib (1-24 mol%), cholesterol (10:1, 5:1, 3:1, 2:1 mol ratio) and phase transition properties of DSPC:Chol MLVs containing 6 mol% celecoxib.

3.1.1 Liposomes Containing Celecoxib

The effect of celecoxib on the phase transition of DSPC liposomes was determined by the DSC technique the results of which are shown in Fig. 3.1. The thermogram for pure DSPC liposomes shows two endothermic peaks corresponding to the pre- and main phase transitions occurring at 51.5 and 54.4 °C, respectively, which is in agreement with previous studies (Mabrey and Sturtevant, 1976; Tamai et al., 2008).

As seen from the figure, increasing celecoxib concentrations eliminates the pre-transition peak and lowers the main phase transition temperature. The main phase transition temperature of DSPC decreased to 51 °C at 18 mol% celecoxib. Furthermore celecoxib induces a broadening of the main phase transition peak and above 12 mol% celecoxib, the main peak is split into two signals (labeled by arrows in Fig. 7) which may be an indicator of phase separation in the DSPC liposomes.

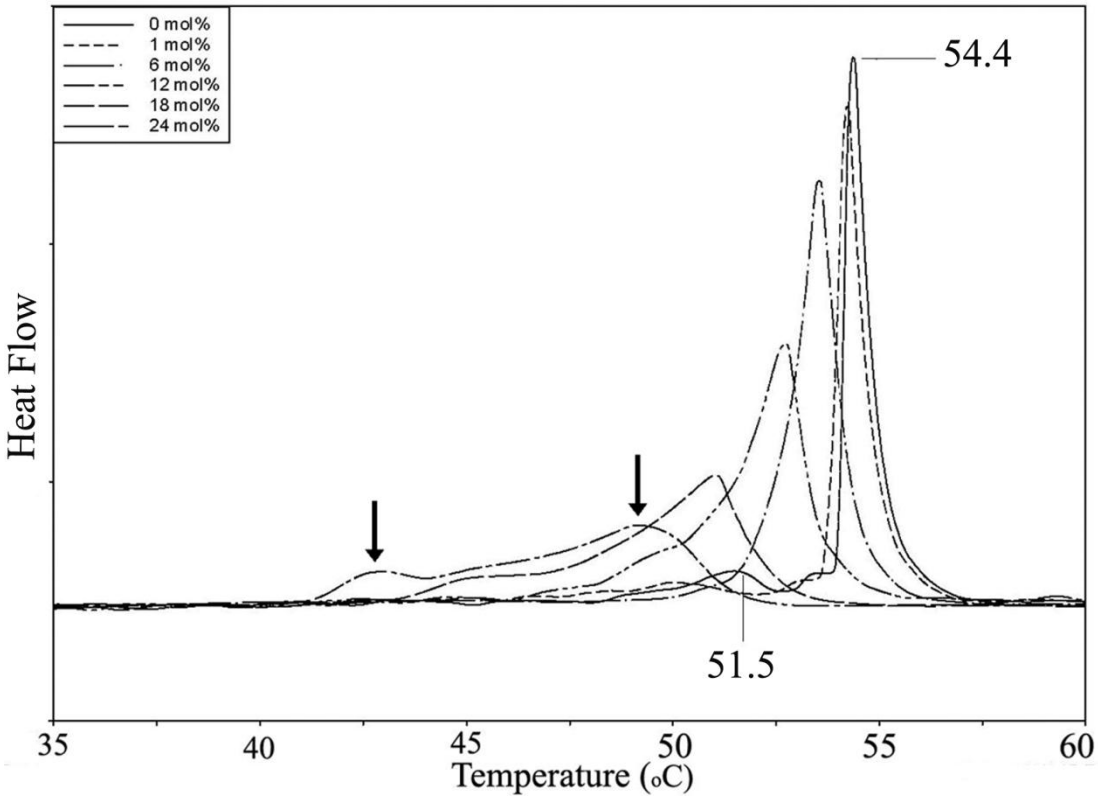

Fig. 3.1 DSC thermograms of DSPC MLVs in the absence and presence of different concentrations of celecoxib. The pre- and main phase transition temperatures are given for pure DSPC MLVs.

The pretransition, main phase transition temperatures and the enthalpy changes for different concentrations of celecoxib are given in Table 3.1. The decrease in the T_m of DSPC liposomes as a result of celecoxib incorporation is more clearly seen in this table. The pretransition temperature decreases with 1 mol% celecoxib and disappears at 6 mol% celecoxib. When the enthalpy changes are considered, an increase in ΔH_{cal} is observed for 1 and 6 mol% celecoxib, however it gradually decreases with higher concentrations of celecoxib (12, 18 and 24 mol%).

Table 3.1 The pretransition temperature (Tp), the main phase transition temperature (Tm) and transition enthalpy changes for different concentrations of celecoxib.

Celecoxib Concentration (mol%)	**T_p (˚C)**	**T_m (˚C)**	**ΔH_{cal} (cal/g)**
0	51.5	54.4	11.01
1	50.6	54.2	11.02
6	-	53.5	13.33
12	-	52.7	11.08
18	-	51.0	10.96
24	-	49.2	9.36

3.1.2 Liposomes Containing Cholesterol

The effect of different amounts of cholesterol on the phase transition of DSPC MLVs is given in Fig. 3.2. It can be seen from the figure that the pretransition is eliminated at DSPC:Chol ratio of 10:1. The main transition peak becomes smaller and

broadened with increasing amounts of cholesterol and at DSPC:Chol ratio of 2:1, it can hardly be seen. The broadening of the peak at cholesterol concentrations 10:1 and 5:1 are not symmetric, however the asymmetry is lost at cholesterol concentrations 3:1 and 5:1. The phase transition temperatures and the enthalpy changes with increasing amounts of cholesterol are given in Table 3.2. Since pretransition is lost at the lowest amount of cholesterol used in this study, T_p is not included in the table. These parameters could not be detected for DSPC:Chol 2:1. According to these data, the main phase transition temperature of DSPC MLVs first decrease at DSPC:Chol ratios of 10:1 and 5:1, then increase slightly at higher amounts of cholesterol. In contrast, ΔH_{cal} shows a continuous decrease with increasing cholesterol concentrations. All of these data are in agreement with previous studies (McMullen et al., 1993; Tamai et al., 2008).

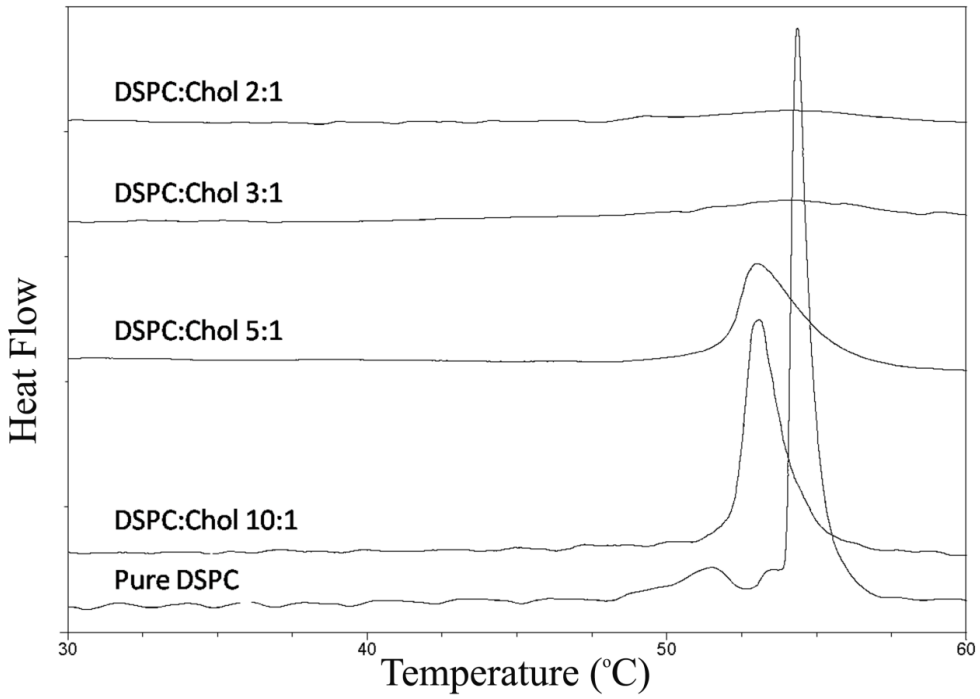

Fig. 3.2 DSC thermograms of DSPC MLVs in the absence and presence of different concentrations of cholesterol.

Table 3.2 The main phase transition temperature (Tm) and transition enthalpy changes for different concentrations of cholesterol.

DSPC:Cho (mol ratio)	T_m (˚C)	ΔH_{cal} (cal/g)
0	54.4	11.01
10:1	53.1	9.24
5:1	53.0	6.83
3:1	53.4	3.72
2:1	-	-

3.1.3 Liposomes containing cholesterol and celecoxib

DSC thermograms for DSPC MLVs containing 6 mol% celecoxib and different amounts of cholesterol are shown in Fig. 3.3A. As mentioned in the previous sections, celecoxib and cholesterol both cause broadening of the transition curve of DSPC MLVs. When both are present in the system, this effect becomes more profound and no peak is seen at DSPC:Chol ratio of 2:1. Fig 3.3B illustrates a magnified version of part A, such that only DSPC:Chol at the ratios of 10:1, 5:1, 3:1 and 2:1 with 6 mol% celecoxib are included. It is clear from this figure that the combined effect of celecoxib and cholesterol is extremely different than that of each alone. With increasing amounts of cholesterol, a new peak starts to form around 39 ˚C but the higher temperature peak continues to exist. At DSPC:Chol ratio of 2:1 both peaks are lost, and a very broad endotherm can hardly be seen.

The phase transition temperatures and the enthalpy changes in DSPC MLVs containing 6 mol% celecoxib and increasing amounts of cholesterol are given in Table 3.3. With increasing concentrations of cholesterol, the transition temperatures first decrease and then start to increase at DSPC:Chol ratio of 3:1. This behavior is

similar to that of cholesterol alone, however all T_m values are lower than the ones observed for both cholesterol and celecoxib. The enthalpy of the system decreases gradually when cholesterol concentration is increased, in the presence of 6 mol% celecoxib. This effect also resembles that of DSPC:Chol liposomes.

Table 3.3 The main phase transition temperature (Tm) and transition enthalpy changes for different concentrations of cholesterol, in the presence of 6 mol% celecoxib.

DSPC:Cho (mol ratio)	**T_m (˚C)**	**ΔH_{cal} (cal/g)**
0	53.5	15.33
10:1	51.3	6.54
5:1	50.7	4.94
3:1	52.2	4.40
2:1	-	-

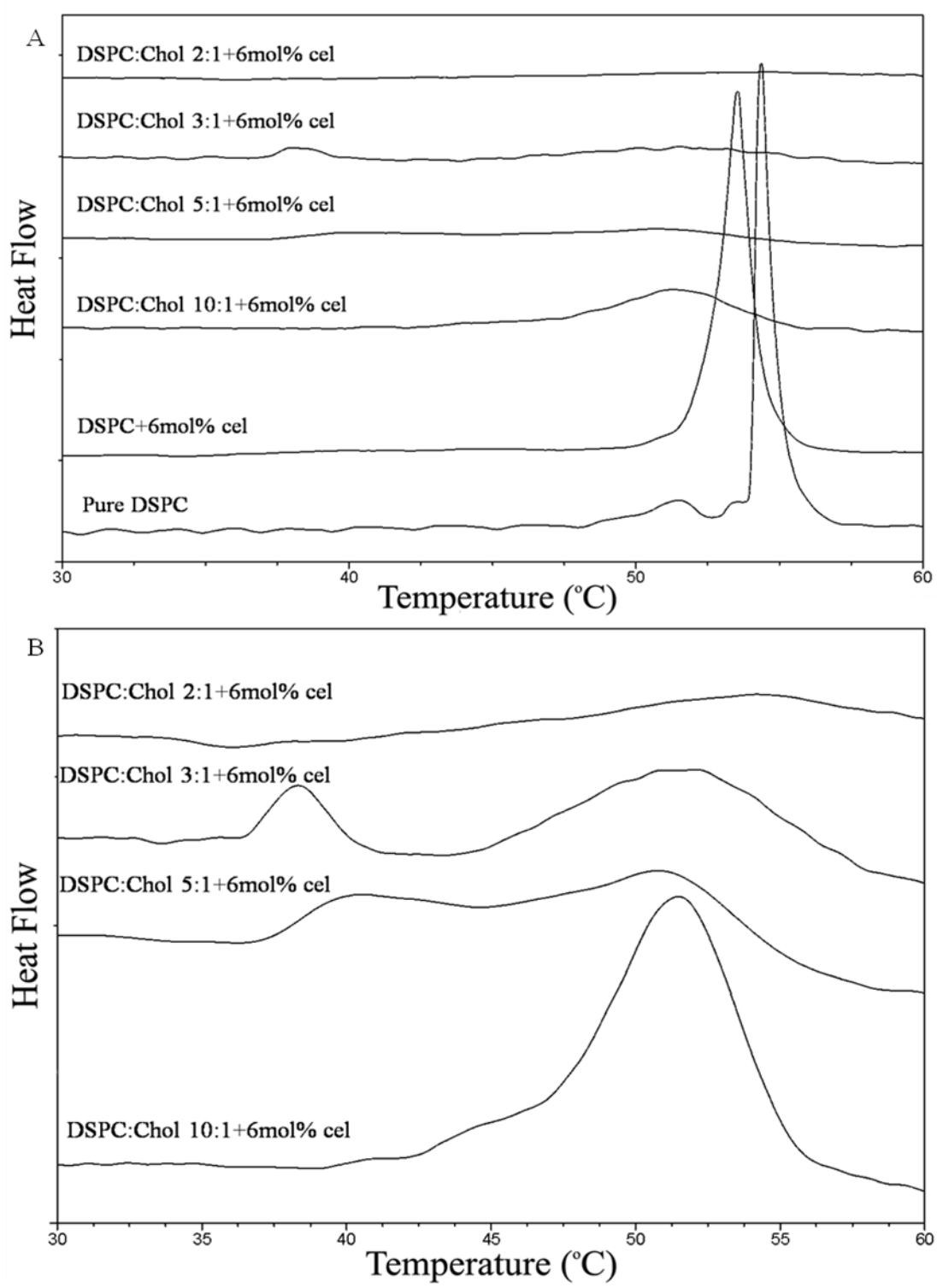

Fig. 3.3 DSC thermograms of DSPC MLVs containing 6 mol% celecoxib with different concentrations of cholesterol.

3.2 FTIR Studies

FTIR studies are divided into three parts: DSPC-celecoxib interactions, DSPC-cholesterol interactions and DSPC-cholesterol-celecoxib interactions. The C-H stretching modes at 2800-3000 cm^{-1}, the C=O stretching mode at 1735 cm^{-1} and the PO_2^- antisymmetric double bands at 1220-1240 cm^{-1} were analyzed.

3.2.1 Interactions of Celecoxib with DSPC Membranes

The infrared spectra for DSPC MLVs were first analyzed as a function of temperature (30-75°C) with different concentrations of celecoxib (1-24 mol%). These experiments were repeated three times and similar trend was obtained in each replicate. Next, in order to further delineate the significance of concentration dependent effects of celecoxib (1-24 mol%), infrared spectroscopy was additionally carried out by increasing the number of samples at each concentration, at two different temperatures, 40 and 60 °C, representing the gel and liquid crystalline phases of DSPC MLVs, respectively. Each spectrum was analyzed individually and the average of five replicates has been shown as mean ± SEM.

A representative spectrum of the DSPC MLVs at 40 °C in the presence of 0, 6 and 24 mol% celecoxib has been shown in Fig. 3.4. The spectrum was normalized according to CH_2 antisymmetric band at 2920 cm^{-1} for visual demonstration of celecoxib induced variations. It can be seen from the figure that celecoxib causes changes in the frequencies and bandwidths of the spectral bands and these changes were used to monitor several physicochemical characteristics of the DSPC liposomes.

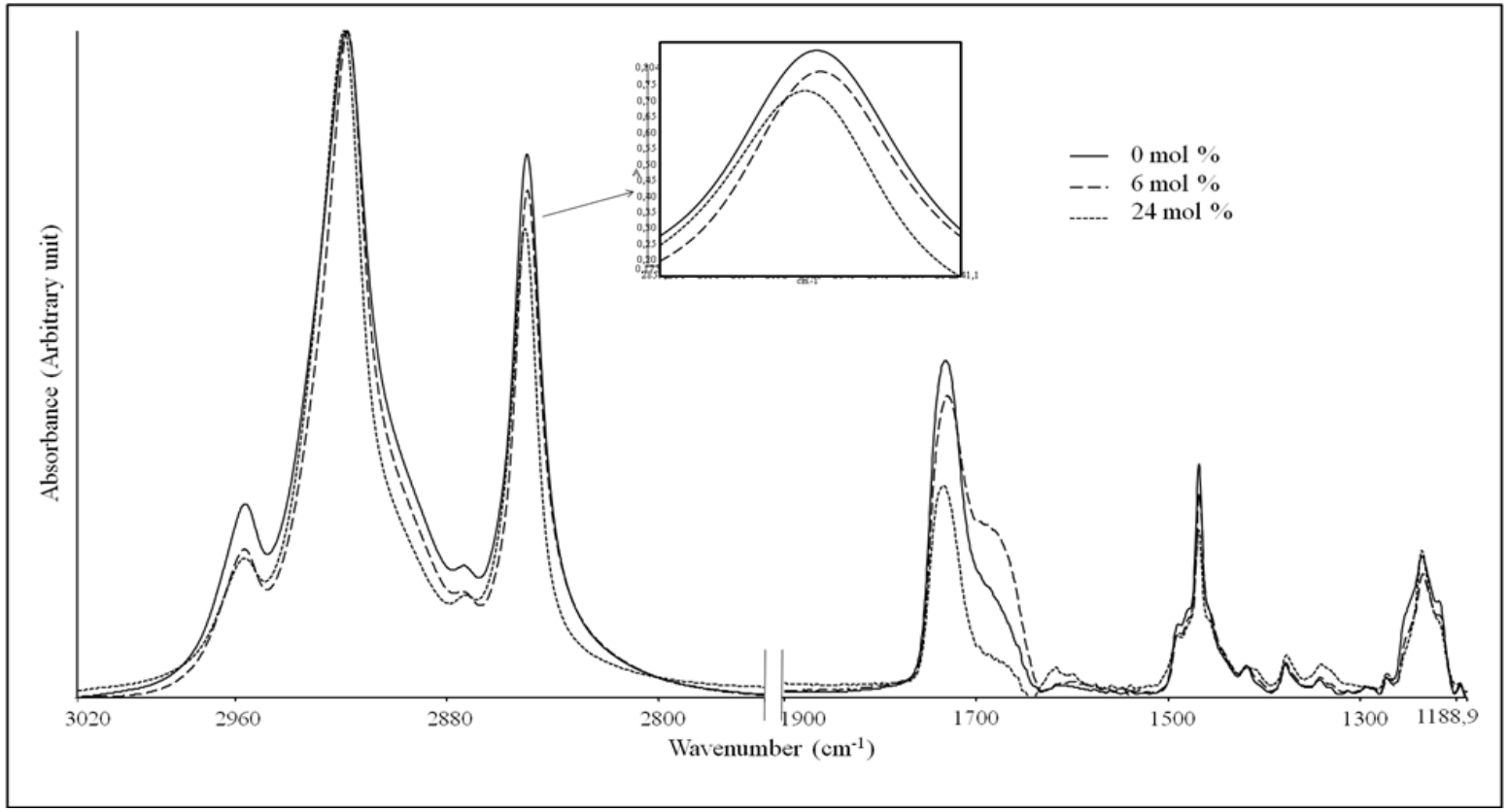

Fig. 3.4 Representative FTIR spectra of DSPC MLVs in the presence of 0, 6 and 24 mol% celecoxib at 40 °C.

The effects of celecoxib on the phase transition and order-disorder state of the membranes were studied by the analysis of the CH_2 antisymmetric and CH_2 symmetric stretching modes of the acyl chains at 2920 cm^{-1} and 2850 cm^{-1}, respectively. Fig. 3.5A displays the frequency variation of the CH_2 antisymmetric stretching band of DSPC liposomes as a function of temperature. The effect of celecoxib on phase transition temperature of DSPC membranes can be seen in this figure. The abrupt shift in the frequency of CH_2 antisymmetric stretching mode which takes place around 55 °C monitors the well known main cooperative endothermic phase transition of DSPC liposomes and has been associated with the change from all-trans to gauche conformers (Casal and Mantsch, 1984). For low concentrations of celecoxib (1 and 6 mol%) the shape of the phase transition curve is not altered and no significant shift of the phase transition temperature is observed. However higher concentrations of celecoxib (12 and 24 mol%) produce a broadening of the phase transition and shift the transition to lower temperatures. These results are in agreement with the DSC data. We observed a dual effect of celecoxib on the order parameter of DSPC liposomes. This effect is apparent in Fig. 3.5B, which shows the concentration dependence of the average frequencies of the CH_2 antisymmetric stretching mode of DSPC MLVs, at 40 and 60 °C. The incorporation of 1 and 6 mol% celecoxib into the phospholipid system slightly shifts the frequency to lower values, which indicates an increase in the number of trans conformers in both phases. This effect was significantly observed at 9 mol% celecoxib concentration. This implies a conformational ordering of the acyl chains (Severcan, 1997). In contrast, high concentrations of celecoxib (12, 18 and 24 mol%) increase the frequency both in the gel and liquid crystalline phases. A statistically significant difference was observed for 24 mol% celecoxib as can be seen in Fig. 3.5B. The observed frequency increase reflects a disordering effect of celecoxib on DSPC MLVs. Similar effects were also observed for CH_2 symmetric stretching band, shown in Fig. 3.6.

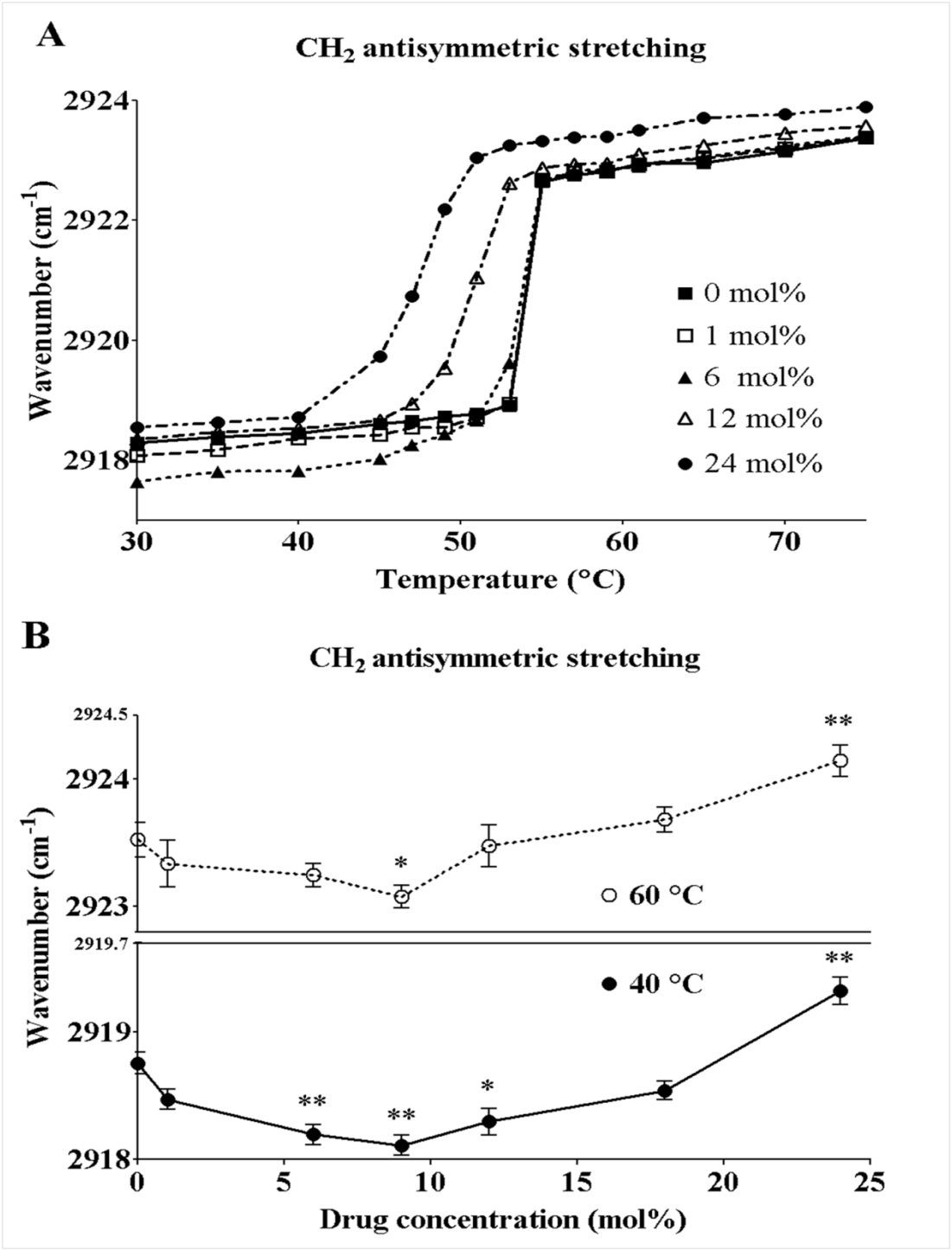

Fig. 3.5 Variation in the frequency of the CH_2 antisymmetric stretching modes of DSPC MLVs as a function of (**A)** temperature at varying concentrations of celecoxib and (**B)** celecoxib concentration at 40 and 60 °C , each point represents the mean ± SEM (n=5). *p <0.05 and **p <0.01 compared to controls (0 mol% celecoxib).

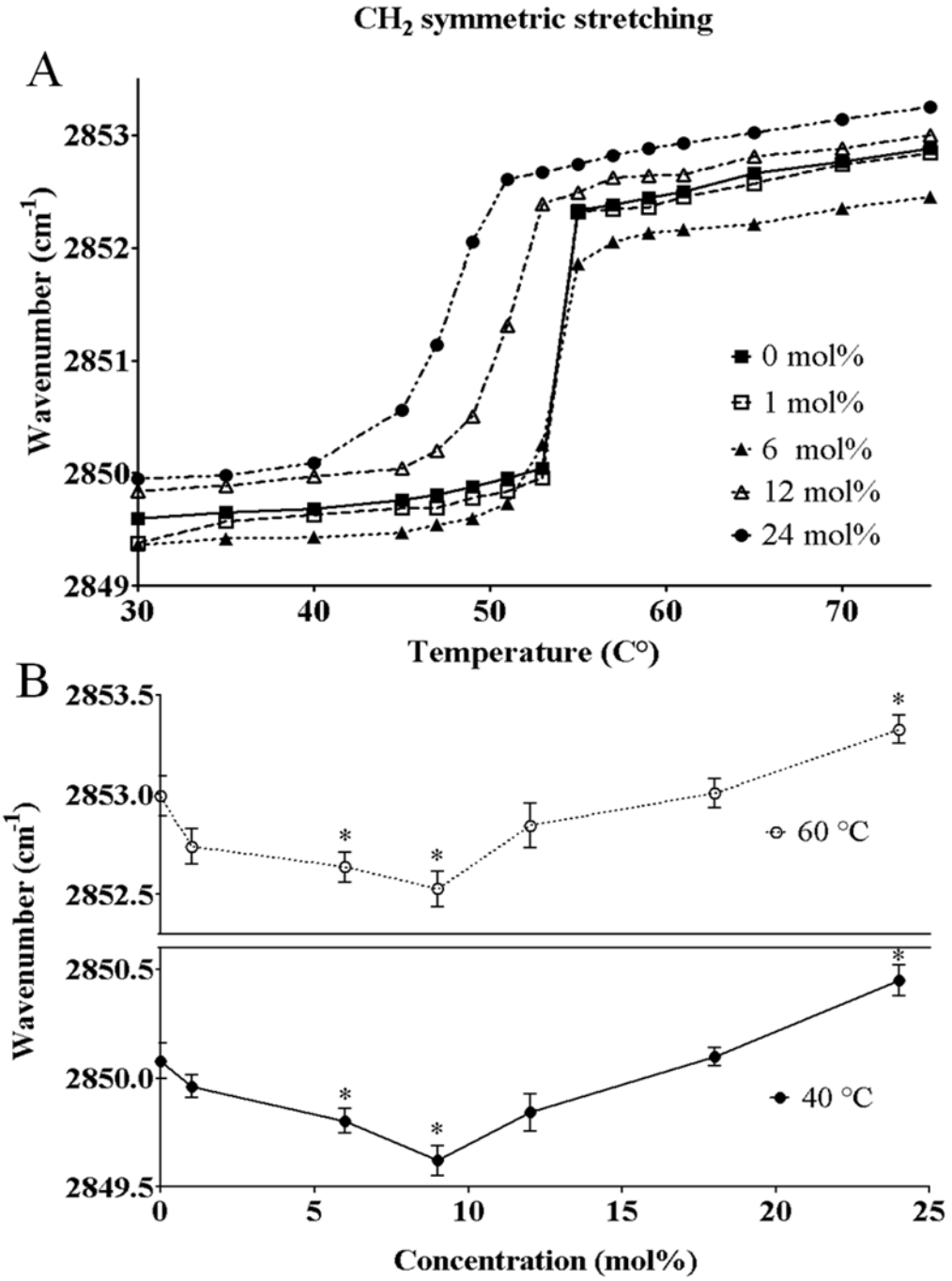

Fig. 3.6 Variation in the frequency of the CH_2 symmetric stretching modes of DSPC MLVs as a function of (**A)** temperature at varying concentrations of celecoxib and (**B)** celecoxib concentration at 40 and 60 °C, each point represents the mean ± SEM (n=5). *p <0.05 and **p <0.01 compared to controls (0 mol% celecoxib).

The bandwidth of the C-H stretching modes was analyzed for investigating the effects of celecoxib on the dynamics of the DSPC MLVs. Fig. 3.7A displays the temperature dependence of the bandwidth of the CH_2 antisymmetric stretching mode of DSPC MLVs with varying celecoxib concentrations. It is evident from the figure that the bandwidth decreases with the addition of celecoxib both in the gel and liquid crystalline phases and hence celecoxib decreases the dynamics of the membrane. This effect is more apparent in Fig. 3.7B which shows the alterations in the average bandwidth of the CH_2 antisymmetric stretching mode as a function of celecoxib concentration at 40 and 60 °C (n=5). A statistically significant difference was observed for all celecoxib concentrations higher than 9 mol%. The analysis of the CH_2 symmetric stretching band also showed similar results, shown in Fig. 3.8.

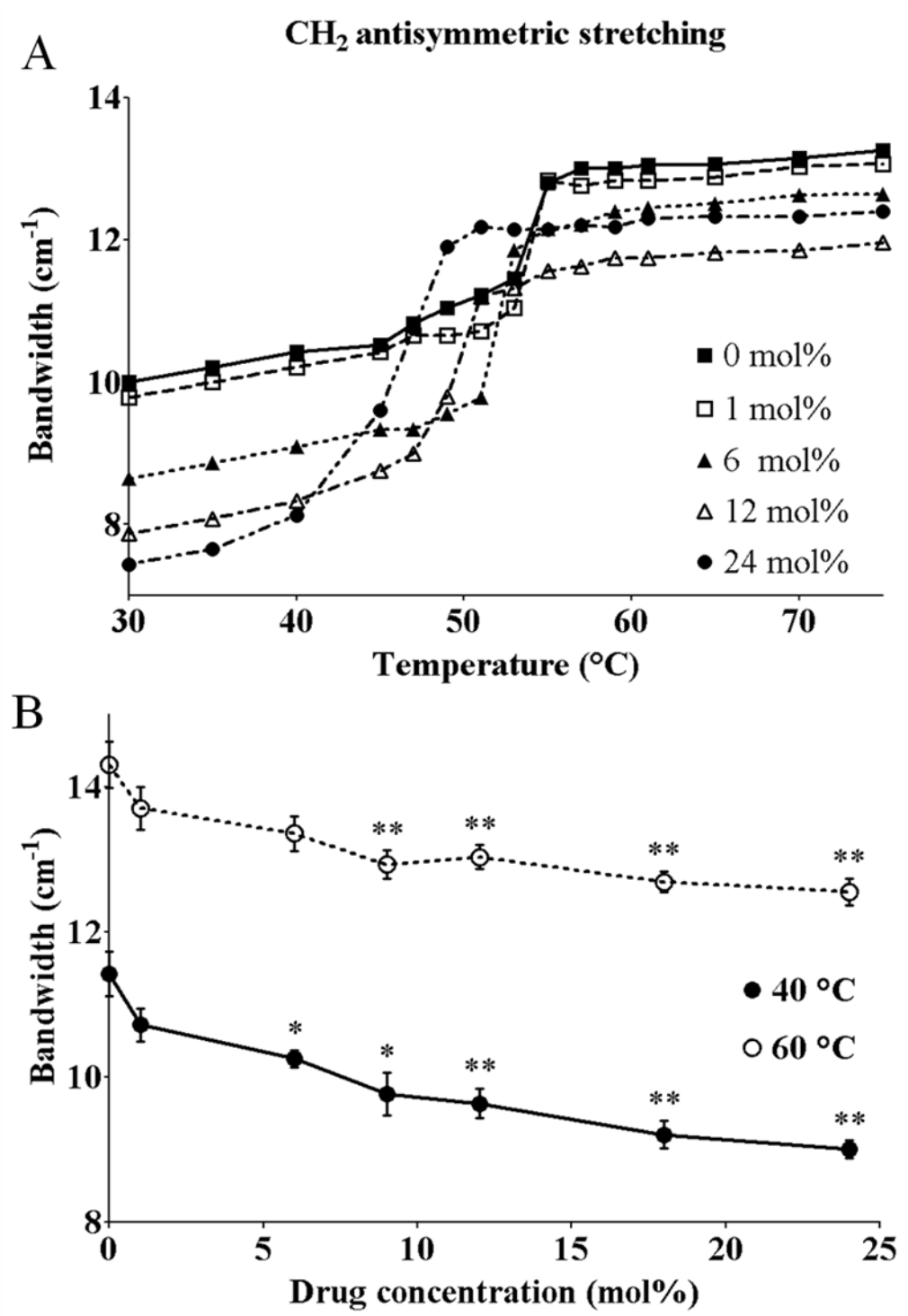

Fig. 3.7 Variation in the bandwidth of the CH_2 antisymmetric stretching modes of DSPC MLVs as a function of (**A)** temperature at varying concentrations of celecoxib and (**B)** celecoxib concentration at 40 and 60 °C , each point represents the mean ± SEM (n=5). *p <0.05 and **p <0.01 compared to controls (0 mol% celecoxib).

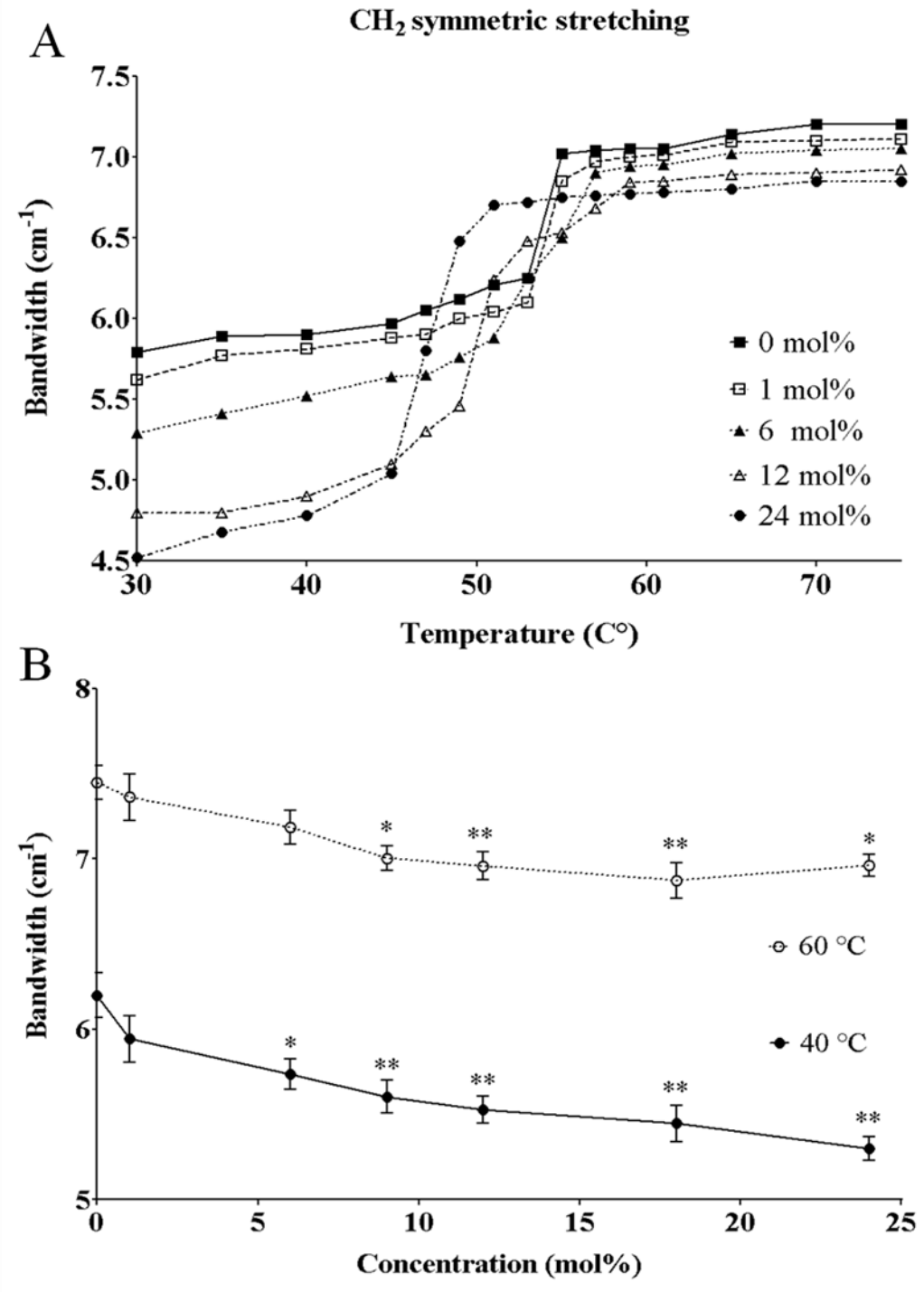

Fig. 3.8 Variation in the bandwidth of the CH_2 symmetric stretching modes of DSPC MLVs as a function of (**A)** temperature at varying concentrations of celecoxib and (**B)** celecoxib concentration at 40 and 60 °C , each point represents the mean ± SEM (n=5). *p <0.05 and **p <0.01 compared to controls (0 mol% celecoxib).

To ascertain the effect of the drug on the interfacial region near the polar head groups of the membrane, C=O stretching band at 1735 cm^{-1} was monitored. The frequency variations in the C=O stretching band of DSPC MLVs as a function of temperature and celecoxib concentration are given in Fig. 3.9A. In the liquid crystalline phase, the addition of celecoxib produces a remarkable decrease in the frequency, which indicates that celecoxib increases the hydrogen bonding around this functional group. However in the gel phase, low and high concentrations of celecoxib produce different effects on the membrane whose significance is clearly seen in Fig. 3.9B. While low concentrations of celecoxib (6 and 9 mol%) significantly decrease the frequency, at a high concentration (24 mol%) celecoxib causes a significant increase in the frequency of the C=O stretching mode. This implies that there is a decrease in the hydrogen bonding and is explained by the presence of free carbonyl groups in the system.

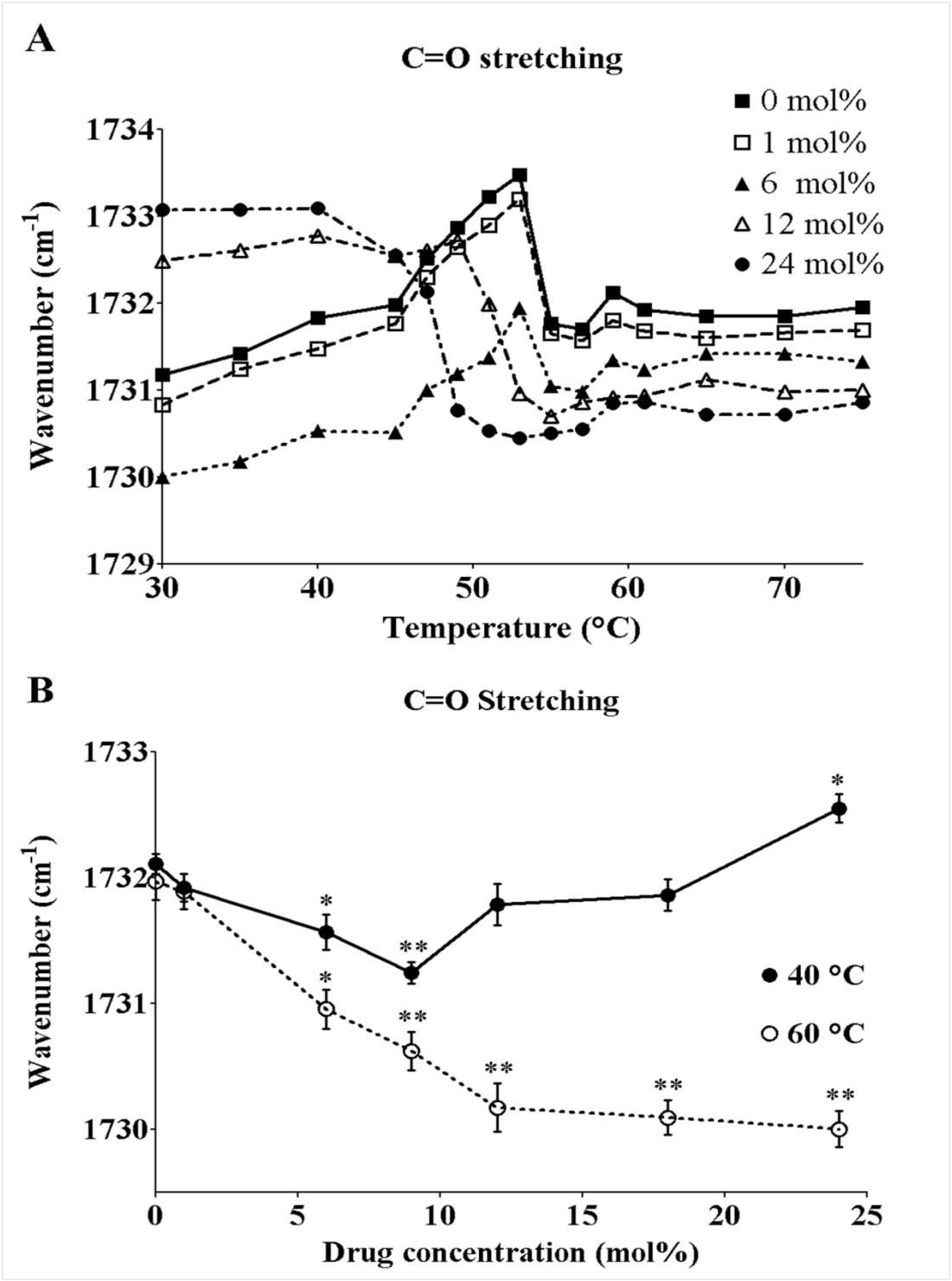

Fig. 3.9 Variation in the frequency of the C=O stretching mode of DSPC MLVs as a function of **(A)** temperature at varying concentrations of celecoxib and **(B)** celecoxib concentration at 40 and 60 °C , each point represents the mean ± SEM (n=5). *p <0.05 and **p <0.01 compared to controls (0 mol% celecoxib).

Information about the hydration state of the polar head groups of the phospholipids is monitored by the analysis of the frequency of the PO_2^- antisymmetric double stretching band located at 1220-1240 cm^{-1}. The frequency variations in PO_2^- antisymmetric double stretching band of DSPC liposomes as a function of temperature and celecoxib concentration are given in Fig. 3.10A and B, respectively. Upon celecoxib addition into the system, the frequency shifts to higher values for both gel and liquid crystalline phases, indicating an increase in dehydration of the phosphate group.

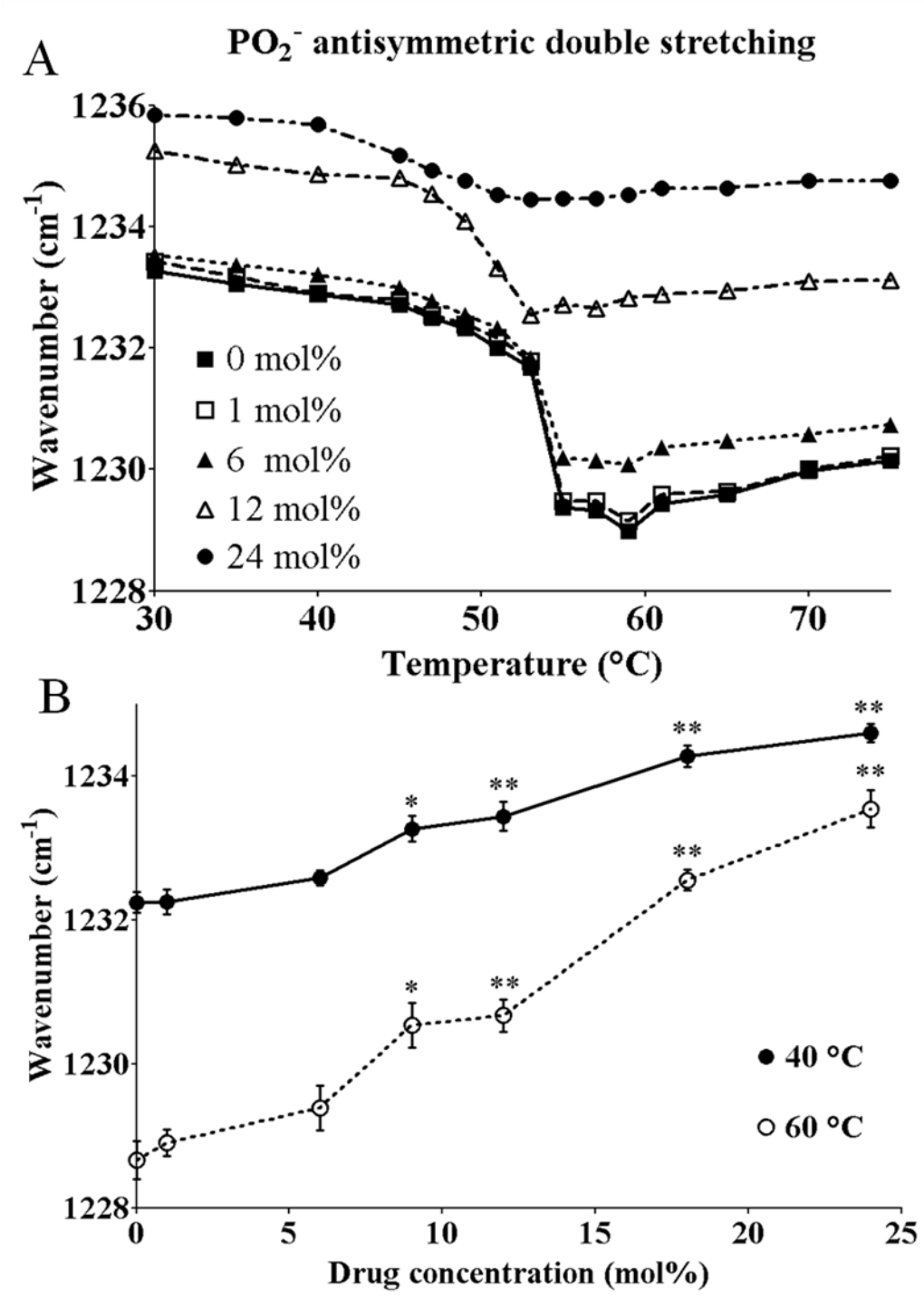

Fig. 3.10 Variation in the frequency of the PO_2^- antisymmetric double stretching mode of DSPC MLVs as a function of **(A)** temperature at varying concentrations of celecoxib and **(B)** celecoxib concentration at 40 and 60 °C , each point represents the mean ± SEM (n=5). *p <0.05 and **p <0.01 compared to controls (0 mol% celecoxib).

3.2.2 Interactions of Cholesterol wlth DSPC Membranes

Studies on the concentration dependent effects of cholesterol (DSPC:Chol 10:1, 5:1, 3:1 and 2:1 mol ratio), was carried out at two different temperatures, 30 and 65 °C for each concentration. These temperatures were chosen according to the DSC data so that they represent the gel and liquid crystalline phases of DSPC MLVs, respectively. Each spectrum was analyzed individually and the average of five replicates has been shown as mean ± SEM.

The effect of cholesterol on the order-disorder state of the acyl chains of DSPC MLVs was monitored by analyzing the CH_2 antisymmetric stretching band. As mentioned in section 2.5.2, the infrared spectrum of cholesterol interferes with the CH_2 symmetric band, thus this band was not taken into consideration in the experiments with cholesterol. Fig. 3.11 displays the average frequencies of the CH_2 antisymmetric stretching mode of DSPC MLVs, at 30 and 65 °C, as a function of cholesterol concentration (n=5). Cholesterol behaves differently in the gel and liquid crystalline phases. The frequency of the CH_2 antisymmetric stretching band shifts to higher values in the gel phase, indicating an increase in the number of gauche conformers. On the other hand, the frequency shifts to lower values in the liquid crystalline phase; thus the number of trans conformers increase in this phase. For both phases, a statistically significant difference was observed at DSPC:Chol ratios higher than 5:1.

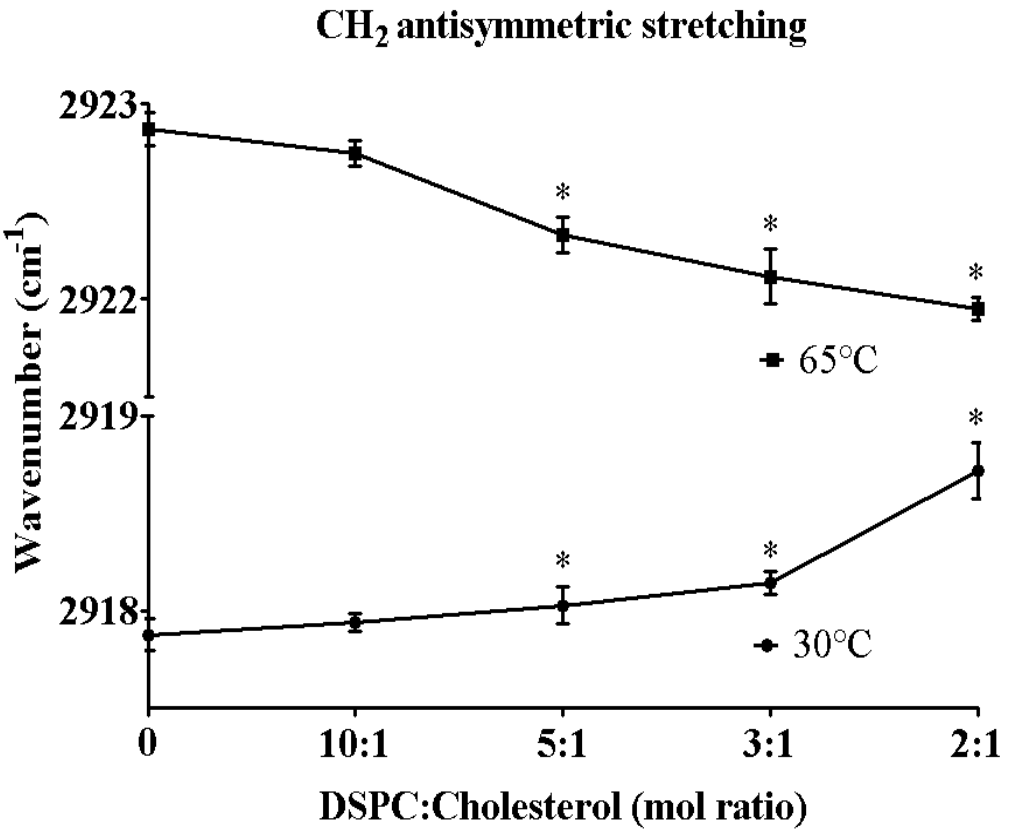

Fig. 3.11 Variation in the frequency of the CH_2 antisymmetric stretching modes of DSPC MLVs as a function of cholesterol concentration at 35 and 65 °C , each point represents the mean ± SEM (n=5). *p <0.05 and **p <0.01 compared to controls (0 cholesterol).

The bandwidth of the C-H stretching modes were analyzed for investigating the effects of cholesterol on the dynamics of the DSPC MLVs. Fig. 3.12 displays the variations in the bandwidth of the CH_2 antisymmetric stretching mode of DSPC MLVs as a function of cholesterol concentration at 35 and 60 °C (n=5). It is evident from the figure that bandwidth increases gradually with cholesterol concentration at both phases, but more profoundly in the gel phase. This indicates an increase in the dynamics of the system when cholesterol is present.

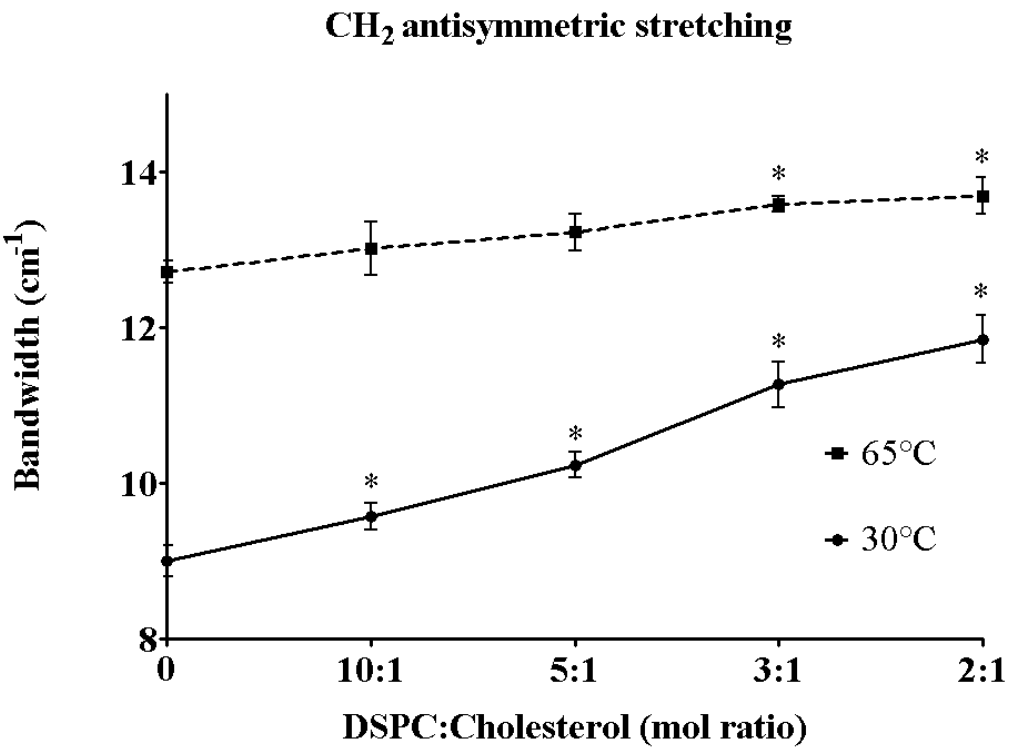

Fig. 3.12 Variation in the bandwidth of the CH_2 antisymmetric stretching modes of DSPC MLVs as a function of cholesterol concentration at 35 and 65 °C , each point represents the mean ± SEM (n=5). *p <0.05 and **p <0.01 compared to controls (0 cholesterol).

The interaction of cholesterol with the glycerol backbone and the head groups of DSPC MLVs was monitored by analyzing the C=O stertching and PO_2^- antisymmetric double stretching bands, respectively. Figures 3.13 and 3.14 illustrate the concentration dependent effects of cholesterol on the C=O stretching and PO_2^- antisymmetric double stretching band frequencies at 35 and 60 °C (n=5), respectively. Both in the gel and liquid crystalline phase, increasing amounts of cholesterol incorporation results in a shift of the frequency to lower values for each mode. This implies that, cholesterol induces H-bonding around the carbonyl ester and phosphate groups of DSPC MLVs.

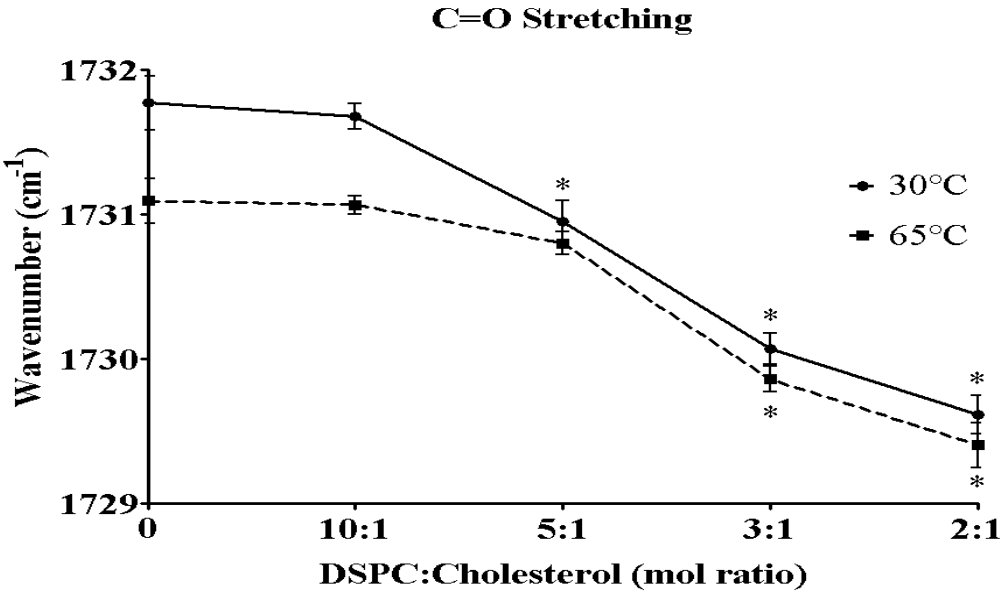

Fig. 3.13 Variation in the frequency of the C=O stretching modes of DSPC MLVs as a function of cholesterol concentration at 35 and 65 °C , each point represents the mean ± SEM (n=5). *p <0.05 and **p <0.01 compared to controls (0 cholesterol).

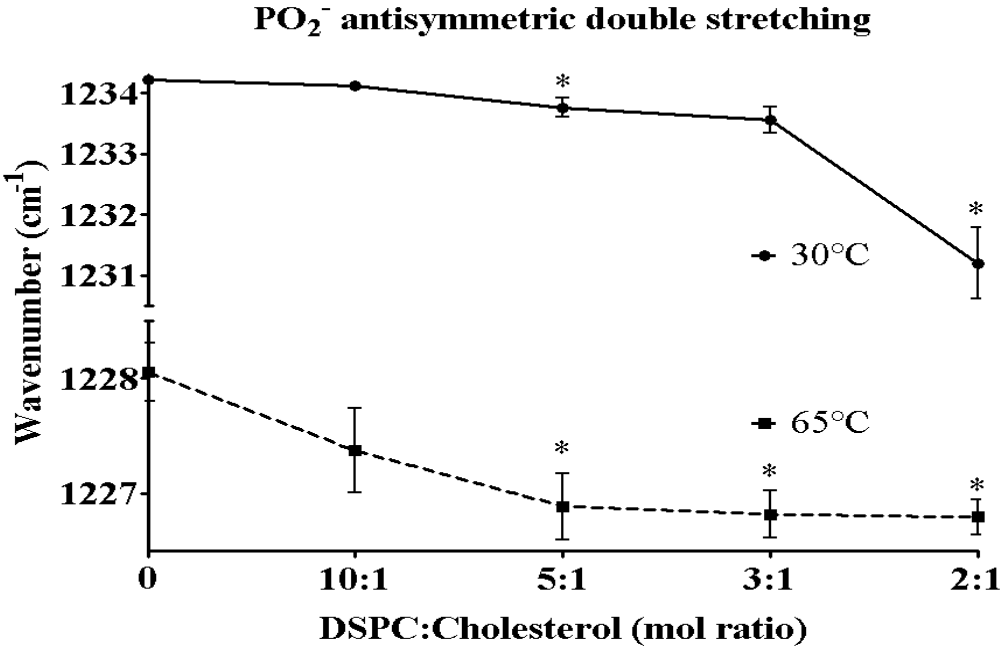

Fig. 3.14 Variation in the frequency of the PO_2^- antisymmetric double stretching modes of DSPC MLVs as a function of cholesterol concentration at 35 and 65 °C , each point represents the mean ± SEM (n=5). *p <0.05 and **p <0.01 compared to controls (0 cholesterol).

3.2.3 Interactions of Celecoxib-Cholesterol-DSPC Membranes

In this part of the study, the combined effects of cholesterol (DSPC:Chol 10:1, 5:1, 3:1 and 2:1 mol ratio) and celecoxib (6 mol%) on the structure and dynamics of DSPC MLVs were investigated at two different temperatures, 30 and 65 °C. These temperatures were chosen according to the DSC data (Fig. 3.2) so that they represent the gel and liquid crystalline phases of DSPC MLVs, respectively. Each spectrum was analyzed individually and the average of five replicates has been shown as mean ± SEM.

Fig. 3.15 shows the average frequency changes in the CH_2 antisymmetric stretching mode of DSPC MLVs for different concentrations of cholesterol, in the presence and absence of 6 mol% celecoxib at 30 and 65 °C (n=5). A horizontal line (dotted line in Fig. 3.15), corresponding to the frequency of pure DSPC MLVs for both phases, is drawn for a better comparison of the data. As shown in the previous sections and also apparent in this figure, 6 mol% celecoxib decreases but cholesterol increases the frequency of the CH_2 antisymmetric stretching mode, in the gel phase. When both are present, the frequency shifts to higher values with increasing concentrations of cholesterol (6 mol% cel at 30 °C). This effect is similar to the behavior of cholesterol when present alone. When each data point for different cholesterol amounts is examined, celecoxib seems to increase the order of the ternary mixtures at DSPC:Chol ratios of 10:1 and 5:1. However this effect is negligible. For DSPC:Chol ratios higher than 5:1, the frequency values pass over the pure DSPC line, resulting in a more disordered system. In the liquid crystalline phase, a decreasing trend of the frequencies can be observed for increasing amounts of cholesterol (the line for 6 mol% cel at 65 °C), which again is reminiscent of the effect of cholesterol itself. However, up to a DSPC:Chol ratio of 10:1, the frequency values are lower than that of cholesterol alone, which is a contribution of celecoxib. At ratios of DSPC:Chol higher than 10:1, the frequency values shift to higher values with respect to DSPC/Chol liposomes (0 mol% cel at 60 °C) , though decreasing on the whole.

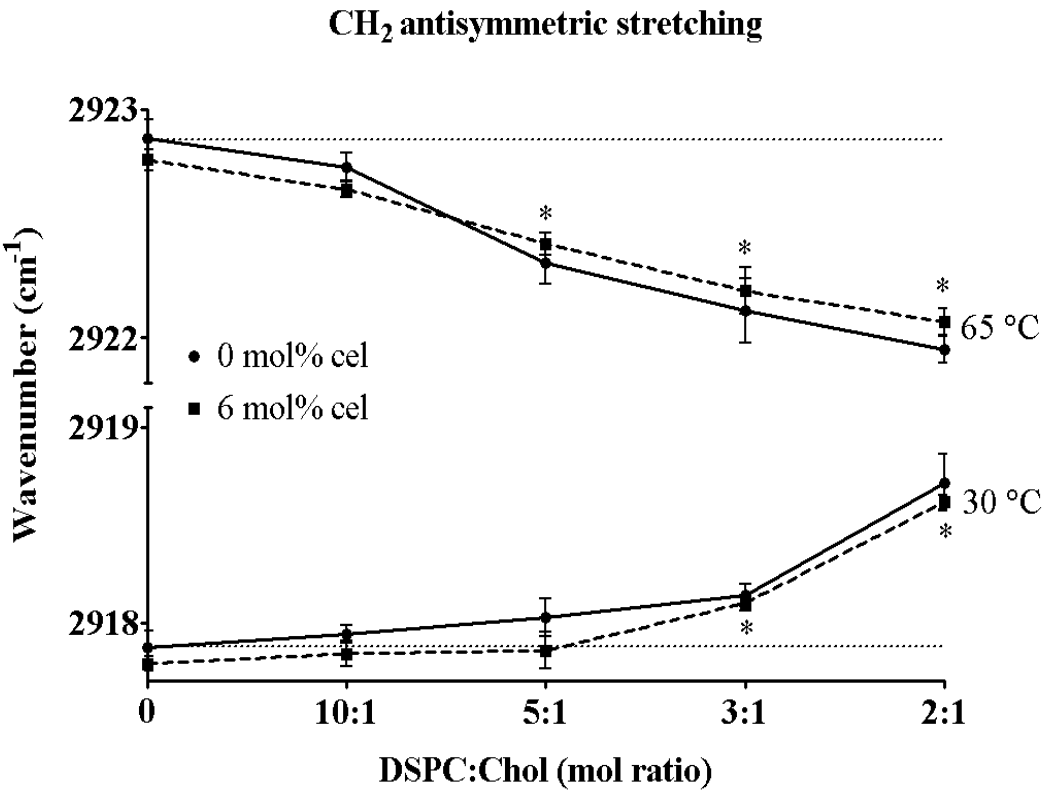

Fig. 3.15 Average frequency changes in the CH_2 antisymmetric stretching mode of DSPC MLVs as a function of cholesterol concentration, in the presence and absence of 6 mol% celecoxib at 30 and 65 °C. Each point represents the mean ± SEM (n=5). Significance is shown only for 6 mol% cel for simplicity. *p <0.05 and **p <0.01 compared to controls (0 cholesterol).

The variations in the bandwidth of DSPC MLVs for different concentrations of cholesterol, in the presence and absence of 6 mol% celecoxib at 30 and 65 °C (n=5) are given in Fig. 3.16. In the gel phase, bandwidth gradually increases for both 0 and 6 mol% celecoxib, with increasing amounts of cholesterol. Therefore, the dynamics of the system increases with cholesterol, regardless of celecoxib incorporation. However, at DSPC:Chol ratio of 10:1, there is a more profound increase with respect to 0 mol% celecoxib, when celecoxib is present. As shown in the previous sections and also seen in this figure, celecoxib causes a decrease in the dynamics of DSPC

membranes and the reverse is true for cholesterol. Therefore, the effect of celecoxib on DSPC:Chol 10:1 is opposite to its original behavior. At DSPC:Chol ratios over 5:1, the bandwidth values become lower than that of 0 mol% celecoxib. In the liquid crystalline phase, similar effects for both cholesterol and celecoxib can be seen, except that, at DSPC:Chol ratios higher than 5:1, a decreasing trend in the bandwidth, with cholesterol incorporation, is observed (6 mol% cel at 65 °C). Although the values are still higher than that of pure DSPC, the effect of celecoxib is more profound in this phase.

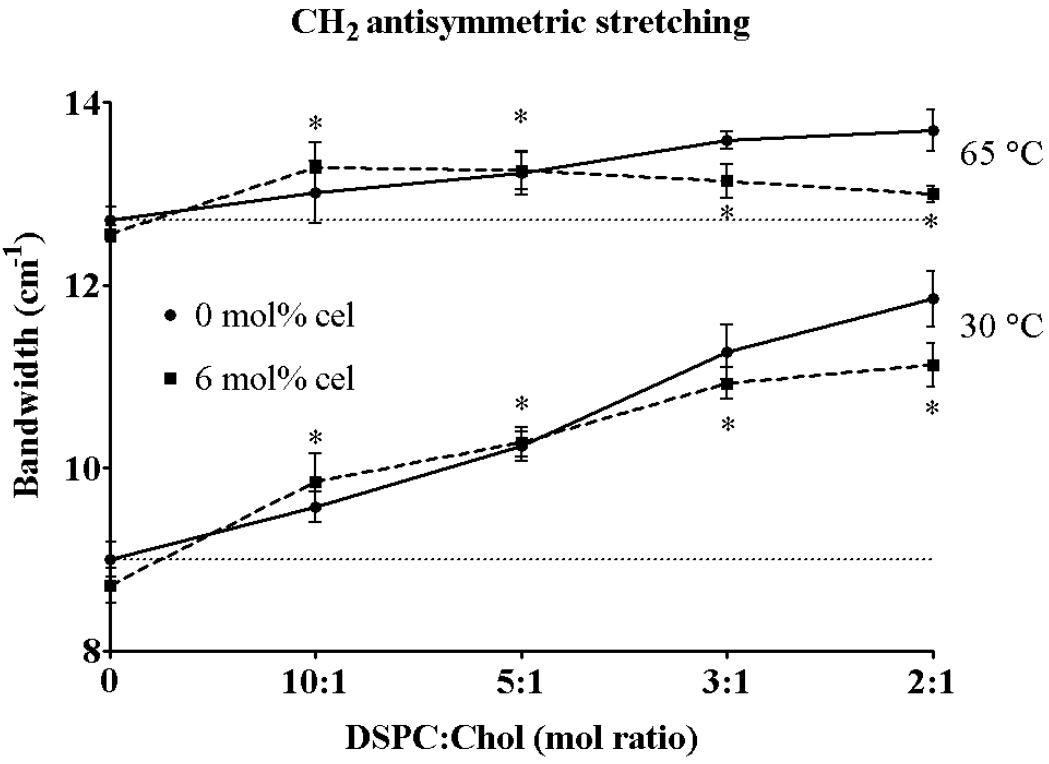

Fig. 3.16 Average bandwidth changes in the CH_2 antisymmetric stretching mode of DSPC MLVs as a function of cholesterol concentration, in the presence and absence of 6 mol% celecoxib at 30 and 65 °C. Each point represents the mean ± SEM (n=5). Significance is shown only for 6 mol% cel for simplicity. *p <0.05 and **p <0.01 compared to controls (0 cholesterol).

Fig. 3.17A and B illustrates the average changes in the frequency of the C=O stretching mode of DSPC MLVs with different concentrations of cholesterol, in the presence and absence of 6 mol% celecoxib, at 30 °C and 65 °C, respectively. At 30 °C, increasing concentrations of cholesterol causes a gradual decrease in the frequency, both in the presence and absence of celecoxib, which indicates hydration around the carbonyl groups. Celecoxib, on the other hand, shows different effects at DSPC:Chol ratios below and over 5:1. Below this cholesterol concentration, the frequency values are lower with respect to both celecoxib and cholesterol, when each is present alone. This indicates an increase in the hydration levels of carbonyl groups. At DSPC:Chol ratios of 5:1 and higher, the frequencies are higher than that of 0 mol% celecoxib, but still below the values of pure DSPC. Similar behavior for both cholesterol and celecoxib is observed at 60 °C.

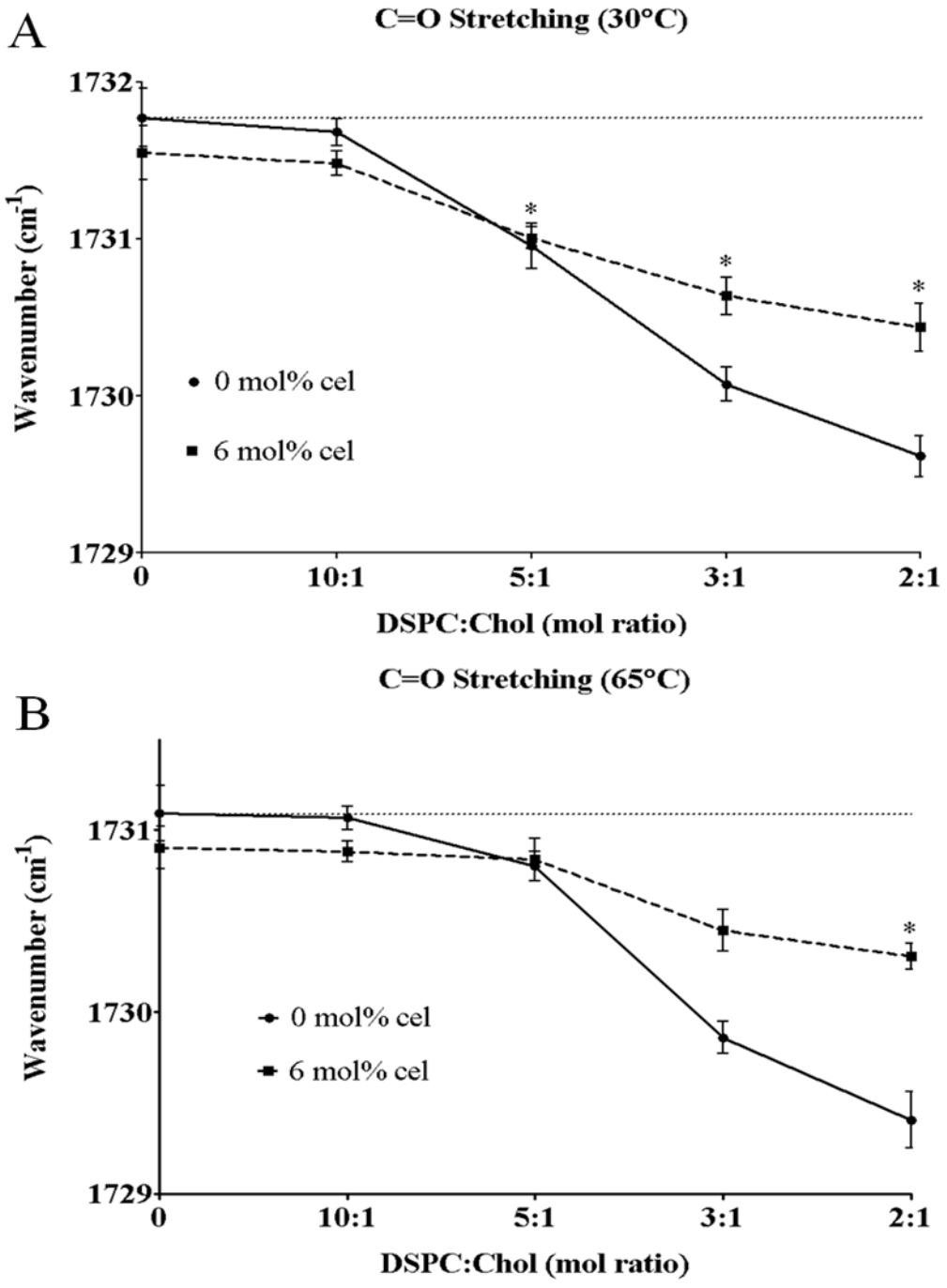

Fig. 3.17 Average frequency changes in the C=O stretching mode of DSPC MLVs as a function of cholesterol concentration, in the presence and absence of 6 mol% celecoxib at 30 **(A)** and 65 °C **(B)**. Each point represents the mean ± SEM (n=5). Significance is shown only for 6 mol% cel for simplicity. *p <0.05 and **p <0.01 compared to controls (0 cholesterol).

The variations in the frequency of the PO_2^- antisymmetric double stretching mode DSPC MLVs for different concentrations of cholesterol, in the presence and absence of 6 mol% celecoxib, at 30 and 65 °C (n=5) are given in Fig. 3.18. In both phases, with the incorporation of cholesterol, a continuous decrease in the frequency is seen, regardless of the presence of celecoxib. This implies an increase in H-bonding around the phosphate groups of phospholipids. When the effect of 6 mol% celecoxib is considered, the frequency values are higher compared to 0 mol% celecoxib, for each concentration of cholesterol. Since celecoxib induces dehydration of the head groups, this is an expected result. However this effect of celecoxib is more profound in the gel phase. In this phase, the frequencies for DSPC:Chol ratios of 10:1 and 5:1 are higher than that of pure DSPC, while in the liquid crystalline phase, the frequencies are all lower compared to pure DSPC.

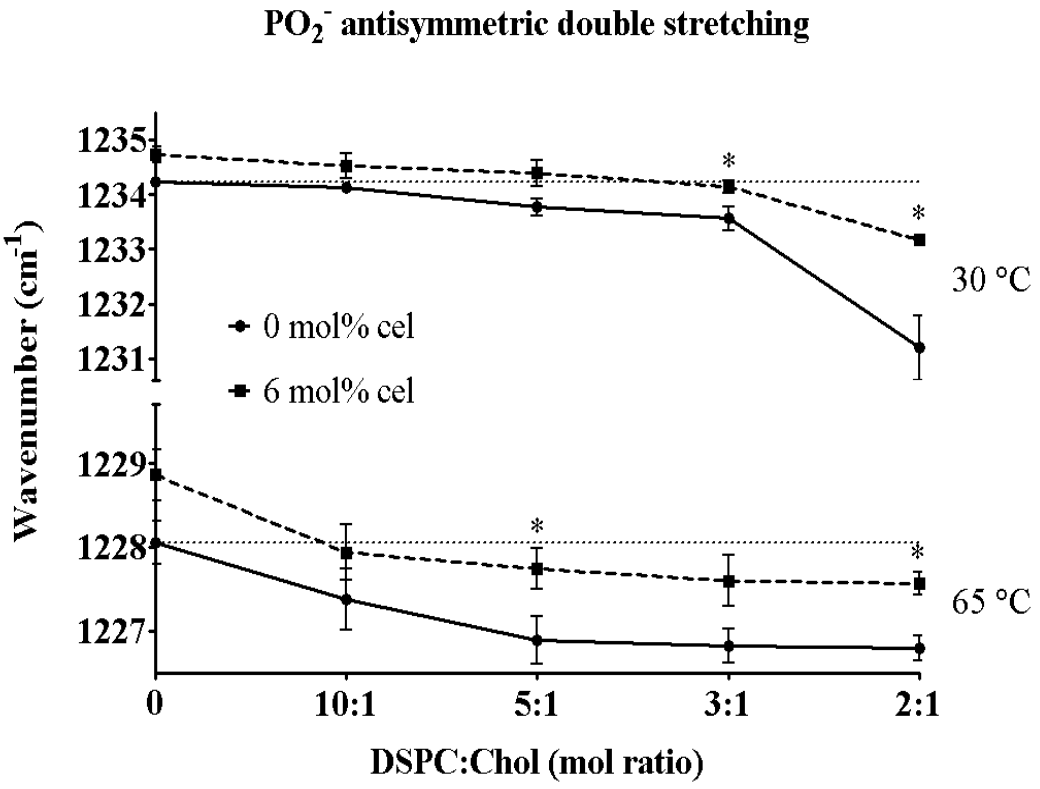

Fig. 3.18 Average bandwidth changes in the PO_2^- antisymmetric double stretching mode of DSPC MLVs as a function of cholesterol concentration, in the presence and absence of 6 mol% celecoxib at 30 and 65 °C. Each point represents the mean ± SEM (n=5). Significance is shown only for 6 mol% cel for simplicity. *p <0.05 and **p <0.01 compared to controls (0 cholesterol).

3.3 Turbidity Studies

Turbidity studies are carried out in order to support the data already obtained by DSC and FTIR for the effects of celecoxib on the dynamic properties of DSPC MLVs.

The visible spectroscopic studies were performed at 440 nm in order to minimize light scattering (Chong and Colbow, 1976; Severcan et al., 2000a). Fig. 3.19 shows the temperature dependent variations in the absorbance values of DSPC MLVs in the

absence and presence of different concentrations of celecoxib. The absorbance was found to decrease as the membrane system went from gel to liquid crystalline phase. The lowering and broadening of phase transition temperature with celecoxib is also evident from the figure which supports our FTIR and DSC data. As seen from the figure, increasing concentrations of celecoxib induces an increase in the absorbance values indicating a decrease in membrane dynamics which is in agreement with our FTIR data.

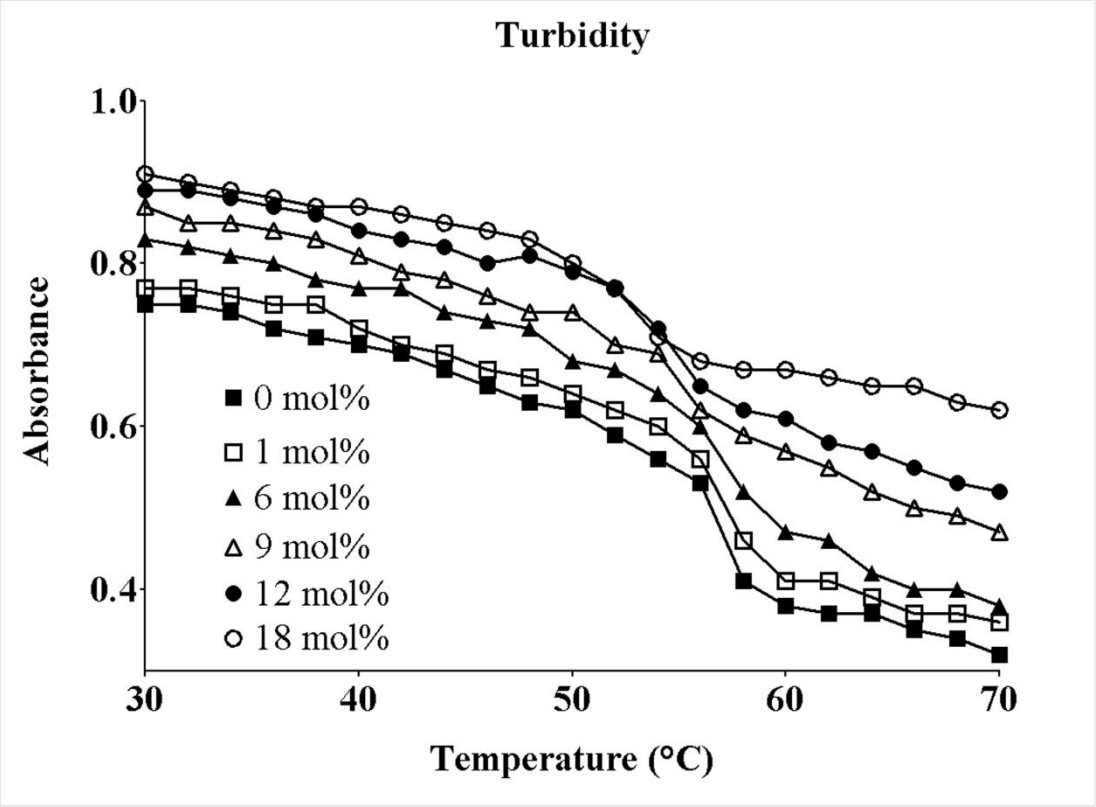

Fig. 3.19 Temperature dependence of the absorbance at 440 nm for DSPC MLVs in the presence of different celecoxib concentrations.

CHAPTER 4

DISCUSSION

In the present study, the interactions of celecoxib with pure and cholesterol containing DSPC membranes were, for the first time, investigated in detail. In addition, the concentration dependent effects of cholesterol on DSPC membranes were studied. We have tried to explain these interactions by examining the changes in the phase transition behavior, acyl chain order, dynamics and the hydration status of the head group and interfacial region of DSPC MLVs using three non-invasive techniques namely FTIR spectroscopy, DSC and turbidity technique at 440 nm.

The DSC and FTIR data reveal that celecoxib eliminates the pre-transition temperature and shifts the main phase transition temperature of DSPC membranes to lower values. The analysis of the frequency of the CH_2 antisymmetric stretching mode showed that low and high concentrations of celecoxib exert opposite effects on the membrane order. At low concentrations celecoxib decreases the acyl chain flexibility, thereby increasing the lipid order, whereas at high concentrations celecoxib increases the acyl chain flexibility and thus disorders the DSPC membranes. This observation is also supported by the changes in the transition enthalpies of the DSC thermograms. Since this parameter reflects the acyl chain packing properties (McElhaney, 1982), higher ΔH_{cal} values for low concentrations of celecoxib indicates a more stabilized membrane and the opposite is valid for high celecoxib concentrations.

Similar to celecoxib, cholesterol also decreases the phase transition temperature of DSPC MLVs but to a smaller extent. The slight increase at DSPC:Chol ratio of 3:1 can be neglected since T_m is considered to be constant after 15 mol% (~5:1 DSPC:Chol) as suggested by Tamai et al. (Tamai et al., 2008). In contrast to celecoxib, the effect of cholesterol on the order-disorder state of DSPC membranes does not depend on concentration, but on the temperature. Cholesterol increases the disorder of the system in the gel phase but it orders the membrane in the liquid crystalline phase. Although there are a few studies with DSPC (Lindblom et al., 1981; McMullen et al., 1994), this is a well known effect of cholesterol shown in numerous studies on other PCs with a variety of techniques (Lindblom et al., 1981; Mannock et al., 2006; McMullen et al., 1994; Severcan et al., 1995; Yeagle, 1985). The decrease in the transition enthalpies with cholesterol incorporation also shows the destabilizing effect of cholesterol in the gel phase.

The phase transition temperatures of ternary mixture of DSPC/Chol/celecoxib in the form of MLVs also decreases with increasing concentrations of cholesterol, as revealed by the DSC data. At DSPC:Chol ratio of 3:1, a remarkable increase is observed, however the presence of a low temperature peak around 39 ˚C shifts the overall T_m to lower values. The analysis of the CH_2 antisymmetric stretching mode of mixed liposomes showed that celecoxib may compete with the disordering effect of cholesterol in the gel phase. This effect is more profound at low cholesterol concentrations (DSPC:Chol ratios of 10:1 and 5:1) in which the system seems more ordered than pure DSPC MLVs. Therefore celecoxib tends to reduce the effects of cholesterol in this phase. In the liquid crystalline phase, cholesterol and celecoxib behave in a synergistic manner at DSPC:Chol ratio of 10:1 and increase the order of the system. At higer concentrations, effect of cholesterol dominates the ternary mixture since the frequency values are closer to that of DSPC/Chol binary system.

The analysis of the bandwidth of the CH_2 antisymmetric stretching mode revealed that celecoxib decreases fluidity of DSPC membranes both at low and high

concentrations. The effect of celecoxib on membrane fluidity was further supported by turbidity measurements. The phase transition from the gel to liquid crystalline phase causes a decrease in turbidity which is mainly due to the change in the refractive index of the lipids, as their density changes during melting (Yi and Macdonal.Rc, 1973). However, a decrease in turbidity can also be due to a decrease in aggregation and fusion among the vesicles, indicating a decrease in particle size (Ohki and Duzgunes, 1979; Severcan et al., 2000a). With the addition of celecoxib into the liposomes, the absorbance values were seen to increase indicating either an increase in aggregation and fusion among the vesicles or most probably a decrease in the lipid mobility due to changes in the refractive index of the medium and thus a decrease in membrane fluidity (Chong and Colbow, 1976; Severcan et al., 2000c; Yi and Macdonal.Rc, 1973). These results are in agreement with previous studies where the effect of celecoxib on both model and biological membranes was investigated using fluorescence spectroscopy (Gamerdinger et al., 2007; Tomisato et al., 2004). Lipid order and fluidity are important parameters for the proper functioning of biological membranes which, in turn, influence cellular processes and disease states (Korkmaz and Severcan, 2005; Maxfield and Tabas, 2005). For instance, membranes of cancerous cells have been found to possess higher fluidity and less ordered acyl chains compared to membranes of non-tumor cells (Sok et al., 2002) which could thus be counteracted by the ability of celecoxib to decrease membrane fluidity. In the past years, several lines of evidence have shown that the modifications of physical characteristics of membrane bilayers lead to altered membrane enzyme activities, membrane bound receptors and the permeability of ion channels (Lee, 2004). Membrane lipid order and fluidity are essential parameters for the correct functioning of ion channels (Awayda et al., 2004). Houslay (1985) has previously reported a reduction in the enzymatic activity of adenylate cyclase with decreased membrane fluidity. This enzyme is responsible for increasing cyclic AMP levels inside the cells, which was shown to activate the MAP kinase pathway, induce cell prolifareation and therefore tumor progression (Abramovitch et al., 2004). As membrane fluidity can be influenced by celecoxib incorporation into the bilayer, it may lead to decreased levels

of cyclic AMP thereby inhibit tumor growth. In a recent study, where cholesterol like effects of celecoxib on cellular membranes were investigated, celecoxib has been shown to inhibit the activity of sarco(endo)plasmic Ca^{2+} -ATPases (SERCA) and it has been proposed that this inhibition is very closely correlated with the decrease in membrane fluidity (Gamerdinger et al., 2007). Inhibition of SERCA activity by the membrane ordering effect of cholesterol is known to induce depletion of ER calcium stores which in turn results in ER stress, activation of unfolded protein response (UPR) pathway and finally apoptosis (Li et al., 2004). Therefore the membrane stabilizing effect of celecoxib could also contribute to its anticancer activity in this manner.

In contrast to celecoxib, a fluidizing effect for cholesterol in DSPC membranes was observed in both phases. This finding is contradictory to the general idea that cholesterol decreases membrane fluidity in the liquid crystalline phase (McMullen et al., 2004). This generalization results from the uncorrect using of fluorescence anisotropy measurements to determine membrane order and fluidity although these two parameters are not related to each other (Ipsen et al., 1987; Lindblom et al., 1981; Vanginkel et al., 1989). Therefore when interpreting the results of the CH_2 stretching vibrations in FTIR spectra, extra care was taken in distinguishing between structural parameters (frequency) describing molecular order and dynamical parameters (bandwidth) describing molecular mobility. In the light of this information, the cholesterol like effects of celecoxib studied by Gamerdinger et al. (Gamerdinger et al., 2007) using fluorescence anisotropy, should be reconsidered. Since the actual parameter measured in this study was order, a similar behavior of celecoxib and cholesterol on SERCA activity should arise from a membrane ordering effect of both molecules, in the liquid crystalline phase. However, in some previous studies in which the bandwidth of the CH_2 stretching modes was investigated by FTIR spectroscopy, cholesterol was found to decrease membrane fluidity of DPPC membranes, in the liquid crystalline phase (Severcan et al., 1995; Umemura et al., 1980). This discrepancy can be explained by the hydrophobic mismatch theory,

mentioned in the introduction. Since the critical chain length was found to be 17C for cholesterol, a different behavior is not unexpected for DPPC (16C) and DSPC (18C) (McIntosh, 1978; McMullen et al., 1993).

For DSPC/Chol/celecoxib liposomes, the fluidity gradually increases with cholesterol incorporation in the gel phase and the values are all close to that of DSPC/Chol liposomes. This indicates that, cholesterol dominates in this phase. However, celecoxib shows an unexpected effect at DSPC:Chol ratio of 10:1. Altough it normally decreases fluidity, the presence of celecoxib at this cholesterol concentration leads to a more fluid bilayer. Thus celecoxib somehow strengthens the effect of cholesterol at DSPC:Chol ratio of 10:1. In the liquid crystalline phase, the same effect of celecoxib is observed for the same cholesterol concentration which cannot be explained with the present knowledge. In addition, a decreasing trend in fluidity is seen at high cholesterol concentrations in the liquid craystalline phase which indicates that the contribution of celecoxib is more profound.

The changes in the frequency and bandwidth of the CH_2 stretching mode are not concerted for high celecoxib concentrations since it induces a decrease in both membrane order and dynamics. This kind of disconcerted behavior in drug – lipid interactions has been previously reported for interactions of model membranes with melatonin (Severcan et al., 2005), progesterone (Korkmaz and Severcan, 2005), vitamin D_2 (Kazanci et al., 2001), vitamin E {Villalain, 1986} and cholesterol (Vanginkel et al., 1989). This controversial effect of high celecoxib concentrations on membrane order and dynamics may reflect the presence of more than one phase in the bilayer (Villalain et al., 1986). In the present study, the celecoxib-induced phase separation was further confirmed by the DSC studies. It is clear from the DSC data that there is an asymmetric broadening of the main phase transition peak, more profoundly at high concentrations of celecoxib which may again indicate the co-existence of more than one domain in the membrane. If these domains are sufficiently large, the exchange of lipids between them cannot be resolved and the

resulting DSC curve will be a superimposition of more than one component (Kazanci et al., 2001). The presence of two components is clearly seen at and above 12 mol% celecoxib concentrations (labeled by arrows in Fig.7). These findings may signify the presence of celecoxib-rich and celecoxib-poor domains whose dynamics are different. Supporting our studies, this kind of domain formation has been previously reported, using FTIR spectroscopy, DSC and other techniques, for several other biomolecules in membranes (Epand, 2008; Kazanci et al., 2001; Korkmaz and Severcan, 2005; Severcan and Cannistraro, 1988; Severcan et al., 2005; Villalain et al., 1986). Furthermore, in agreement with our study, celecoxib has recently been shown to form unstable domains, like a packing mismatch, giving rise to transient large pores on DPPC liposomes, thus increasing membrane permeability (Katsu et al., 2007). This characteristic of celecoxib is noteworthy since an increase in membrane permeability leads to elevated cytoplasmic calcium concentration which in turn decreases mitochondrial membrane potential, induces cytochrome c release and results in apoptosis (Maccarrone et al., 2001). This could be another explanation for the anticarcinogenic activity of celecoxib. It is also essential to note that celecoxib exerts this action while decreasing membrane fluidity as stated by Tomisato et al. (Tomisato et al., 2004).

The same unconcerted behavior is valid for both DSPC/Chol and DSPC/Chol/celecoxib systems which is also supported by DSC results. For DSPC/Chol MLVs, the asymmetric broadening of the DSC thermograms at DSPC:Chol ratios of 10:1 and 5:1 is a well known indication of phase separation. This peak actually consists of two smaller peaks representing cholesterol rich and cholesterol poor domains (McMullen et al., 1993). At higher concentrations of cholesterol the thermograms are rather symmetric which is explained by the disappearance of cholesterol poor domains and presence of a more homogenous bilayer, consisting of smaller cholesterol rich domains. For DSPC/Chol/celecoxib MLVs, the existence of different domains is obvious especially at DSPC:Chol ratios of 5:1 and 3:1. The appearance of the endotherms of these ternary mixtures does not

resemble the ones for either celecoxib or cholesterol. Therefore a totally new phase may have formed by the interactions of both cholesterol and celecoxib with the DSPC membranes.

The carbonyl (C=O stretching) and PO_2^- bands of the FTIR spectrum give information about the interaction of additives with the region near the glycerol backbone and head group, respectively, of the membranes. Celecoxib showed a decrease in hydrogen bonding around the PO_2^- group an increase in dehydration of the head groups. Although the analysis of C=O stretching groups revealed a significant increase in the hydrogen bonding around this functional group in the liquid crystalline phase, opposing effects related to low and high concentrations of celecoxib was observed in the gel phase. The electronegative atom of the celecoxib molecule is the nitrogen of the sulfone amide group. The amido protons (H atoms that are covalently bonded to N) which have a partial positive charge, can make hydrogen bonds with the oxygen atoms in the C=O groups of the phospholipids. The possibility of celecoxib-induced hydrogen bonding between the carbonyl group of DSPC and nearby water molecules should also be considered. In the gel phase, although low concentrations of celecoxib exert the same hydration effect as in the liquid crystalline phase, high concentrations of celecoxib decrease the strength of hydrogen bonding in the interfacial region. This implies that there are free carbonyl groups in the system.

Cholesterol increases hydration, thus H-bonding both around the carbonyl and the phosphate groups. As mentioned in the introduction, the probability of cholesterol to make H-bonds with the phosphate groups is low (Mannock et al., 2008; McIntosh, 1978; Yeagle et al., 1975). In the light of this information, the explanation of these results would be; cholesterol most probably makes H-bonds with the carbonyl groups and increases the distance between the phospholipids so that the phosphate groups make H-bonds with water molecules.

The analysis of the C=O stretching mode for DSPC/Chol/celecoxib liposomes revealed that, in both phases, the population of H-bonded carbonyl groups increases when celecoxib is present, at DSPC:Chol ratio of 10:1. This is an expected result since both molecules are proposed to bond with these groups. However, at higher cholesterol concentrations, the amount of H-bonds decreases with the incorporation of celecoxib, thus the number of free carbonyl groups increases, the possible reason of which will be explained below. The presence of celecoxib in the mixed system also causes dehydration around the phosphate groups. This indicates that, celecoxib reduces the H-bonded population of these groups.

For the DSPC/celecoxib liposomes, the strong hydrogen bonding in the carbonyl region induced by celecoxib at low concentrations and the lack of broadening in the phase transition curve of the CH_2 symmetric band for the same concentrations, suggest that celecoxib does not perturb entirely the cooperativity region (C_2-C_8) of the acyl chains and celecoxib molecules are not located in the hydrophobic interior region of the membranes but most probably at the interfacial region near the head groups (Jain, 1979b; Severcan et al., 2005). These results are in agreement with a previous study where celecoxib has also been found to locate in the interfacial region near the head groups of membranes using small angle X-ray diffraction approaches (Walter et al., 2004). However, in the case of high celecoxib concentrations, the broadening observed in both the phase transition curve of the CH_2 symmetric band and that of the DSC thermograms indicate a decrease in cooperativity and hence penetration of celecoxib molecules more into the cooperativity region (C_2-C_8) of the acyl chains (Jain, 1979b; Korkmaz and Severcan, 2005; Zhao et al., 2007). The reduction in the enthalpy changes at high concentrations of celecoxib also supports this idea since a decrease in ΔH_{cal} is explained by the presence of a molecule in the cooperativity region (Zhao et al., 2007). This implies that packing interactions between the hydrocarbon chains are now less important and results in a decrease in the order of DSPC membranes for high concentrations of celecoxib, observed in the frequency analysis of the CH_2 symmetric mode.

The location of cholesterol in the DSPC membranes is similar to celecoxib as revealed by its strong H-bonding with the carbonyl groups. However cholesterol should also encompass the cooperativity region since a broadening of the DSC endotherms and a decrease in the enthalpy changes are observed. This finding is in aggreement with other studies (Arsov and Quaroni, 2007; McIntosh, 1978; Yeagle et al., 1975).

For DSPC/Chol/celecoxib liposomes, the above suggested locations of celecoxib and cholesterol seems to be valid for low concentrations of cholesterol, since there is an increased level of H-bonding around carbonyl groups with respect to DSPC/Chol membranes. Therefore at low cholesterol concentrations celecoxib and cholesterol molecules are found H-bonded with phospholipids. However at high cholesterol concentrations the amount of hydrogen bonded carbonyls decreases. This may result from the deeper penetration of some celecoxib molecules inside the membrane at high cholesterol concentrations. A similar model has also been suggested for paclitaxel containing DPPC liposomes by Zhao et.al (Zhao et al., 2007). The new phase appeared in the DSC thermograms of ternary mixtures may be composed of these kinds of arrangements; celecoxib confined to the deep interior of the membrane by cholesterol.

CHAPTER 5

CONCLUSIONS

The present study details the interaction of celecoxib with pure and cholesterol containing DSPC MLVs with respect to lipid order and dynamics, phase transition behavior and hydration states of functional groups.

The results reveal that celecoxib exerts opposing effects on membrane order in a concentration dependent manner; ordering and disordering at low and high concentrations respectively and cholesterol disorders and orders the membrane in the gel and liquid crystalline phase, respectively. The liposomes containing ternary mixtures behave similar to cholesterol with a small effect of celecoxib. While celecoxib decrases fluidity of the DSPC membranes, cholesterol shows an opposite effect and in ternary mixtures, a dominant effect of cholesterol is observed. Celecoxib induces hydration around the carbonyl groups, except for high concentrations in the gel phase which show an opposite effect and it causes dehydration around the phosphate groups. Cholesterol induces hydrogen bonding around both the carbonyl and the phosphate groups. A synergistic effect of cholesterol and celecoxib for the ternary mixtures is observed at low cholesterol concentrations; such that the hydration increases markedly around the carbonyl groups but this effect is reversed at high cholesterol concentrations.

An evidence of phase separation has also been observed for all three systems, more obvious in DSPC/Chol/celecoxib membranes. In addition, a possible location of celecoxib in the interfacial region of the membrane has been proposed. Finally,

penetration of celecoxib into the hydrophobic core of the mixed membranes at high cholesterol concentrations and formation of a new phase has also been suggested.

These results clarify, to a certain extent, the molecular interactions of celecoxib and cholesterol with membrane systems and their combined action on these membranes. The results may contribute to a better understanding of COX-2 independent mechanisms of celecoxib action, like its role in different diseases. Furthermore this research may provide useful knowledge for optimizing liposomal formulations of celecoxib for drug delivery systems.

REFERENCES

Abramovitch, R., Tavor, E., Jacob-Hirsch, J., Zeira, E., Amariglio, N., Pappo, O., Rechavi, G., Galun, E., Honigman, A., 2004. A pivotal role of cyclic AMP-responsive element binding protein in tumor progression. Cancer Research 64, 1338-1346.

Arber, N., Eagle, C.J., Spicak, J., Racz, I., Dite, P., Hajer, J., Zavoral, M., Lechuga, M.J., Gerletti, P., Tang, J., Rosenstein, R.B., Macdonald, K., Bhadra, P., Fowler, R., Wittes, J., Zauber, A.G., Solomon, S.D., Levin, B., Pre, S.A.P.T.I., 2006. Celecoxib for the prevention of colorectal adenomatous polyps. New England Journal of Medicine 355, 885-895.

Arrondo, J.L.R., Muga, A., Castresana, J., Goni, F.M., 1993. Quantitative studies of the structure of proteins in solution by fourier-transform infrared-spectroscopy. Progress in Biophysics & Molecular Biology 59, 23-56.

Arsov, Z., Quaroni, L., 2007. Direct interaction between cholesterol and phosphatidylcholines in hydrated membranes revealed by ATR-FTIR spectroscopy. Chemistry and Physics of Lipids 150, 35-48.

Awayda, M.S., Shao, W.J., Guo, F.L., Zeidel, M., Hill, W.G., 2004. ENaC-Membrane interactions: Regulation of channel activity by membrane order. Journal of General Physiology 123, 709-727.

Bangham, A.D., 1972. Model membranes. Chemistry and Physics of Lipids 8, 386-&.

Belton, O., Byrne, D., Kearney, D., Leahy, A., Fitzgerald, D.J., 2000. Cyclooxygenase-1 and-2-dependent prostacyclin formation in patients with atherosclerosis. Circulation 102, 840-845.

Bertagnolli, M.M., Eagle, C.J., Zauber, A.G., Redston, M., Solomon, S.D., Kim, K.M., Tang, J., Rosenstein, R.B., Wittes, J., Corle, D., Hess, T.M., Woloj, G.M., Boisserie, F., Anderson, W.F., Viner, J.L., Bagheri, D., Burn, J., Chung, D.C., Dewar, T., Foley, T.R., Hoffman, N., Macrae, F., Pruitt, R.E., Saltzman, J.R., Salzberg, B., Sylwestrowicz, T., Gordon, G.B., Hawk, E.T., Investigators, A.P.C.S., 2006. Celecoxib for the prevention of sporadic colorectal adenomas. New England Journal of Medicine 355, 873-884.

Biruss, B., Dietl, R., Valenta, C., 2007. The influence of selected steroid hormones on the physicochemical behaviour of DPPC liposomes. Chemistry and Physics of Lipids 148, 84-90.

Campbell, I.D., 1984. Biological Spectroscopy. The Benjamin/Cummings Publishing Company, Inc.

Casal, H.L., Cameron, D.G., Smith, I.C.P., Mantsch, H.H., 1980. Acholeplasma-laidlawii membranes - fourier-transform infrared study of the influence of protein on lipid organization and dynamics. Biochemistry 19, 444-451.

Casal, H.L., Mantsch, H.H., 1984. Polymorphic phase-behavior of phospholipid-membranes studied by infrared-spectroscopy. Biochimica Et Biophysica Acta 779, 381-401.

Chapman, D., Hayward, J.A., 1985. New biophysical techniques and their application to the study of membranes. Biochemical Journal 228, 281-295.

Chen, C.F., Tripp, C.P., 2008. An infrared spectroscopic based method to measure membrane permeance in liposomes. Biochimica Et Biophysica Acta-Biomembranes 1778, 2266-2272.

Chen, S.C., Sturtevant, J.M., Gaffney, B.J., 1980. Scanning calorimetric evidence for a 3rd phase-transition in phosphatidylcholine bilayers. Proceedings of the National Academy of Sciences of the United States of America-Biological Sciences 77, 5060-5063.

Chinery, R., Coffey, R.J., Graves-Deal, R., Kirkland, S.C., Sanchez, S.C., Zackert, W.E., Oates, J.A., Morrow, J.D., 1999. Prostaglandin J(2) and 15-deoxy-Delta(12,14)-prostaglandin J(2) induce proliferation of cyclooxygenase-depleted colorectal cancer cells. Cancer Research 59, 2739-2746.

Chong, C.S., Colbow, K., 1976. Light-scattering and turbidity measurements on lipid vesicles. Biochimica Et Biophysica Acta 436, 260-282.

Coussens, L.M., Werb, Z., 2002. Inflammation and cancer. Nature 420, 860-867.
Demel, R.A., Dekruyff, B., 1976. Function of sterols in membranes. Biochimica Et Biophysica Acta 457, 109-132.

Daniels, R., www.scf-online.com/.../galenik_25_d_dr.htm, last visited on July 2009.

Dogne, J.M., de Leval, X., Hanson, J., Frederich, M., Lambermont, B., Ghuysen, A., Casini, A., Masereel, B., Ruan, K.H., Pirotte, B., Kolh, P., 2004. New developments

on thromboxane and prostacyclin modulators - Part I: Thromboxane modulators. Current Medicinal Chemistry 11, 1223-1241.
Drummond, D.C., Meyer, O., Hong, K.L., Kirpotin, D.B., Papahadjopoulos, D., 1999. Optimizing liposomes for delivery of chemotherapeutic agents to solid tumors. Pharmacological Reviews 51, 691-743.

Edidin, M., 2003. The state of lipid rafts: From model membranes to cells. Annual Review of Biophysics and Biomolecular Structure 32, 257-283.

Eker, F., Durmus, H.O., Akinoglu, B.G., Severcan, F., 1999. Application of turbidity technique on peptide-lipid and drug-lipid interactions. Journal of Molecular Structure 483, 693-697.

Engberts, J., Hoekstra, D., 1995. Vesicle-forming synthetic amphiphiles. Biochimica Et Biophysica Acta-Reviews on Biomembranes 1241, 323-340.
Epand, R.M., 2008. Proteins and cholesterol-rich domains. Biochimica Et Biophysica Acta-Biomembranes 1778, 1576-1582.

FitzGerald, G., 2003. COX-2 and beyond: Approaches to prostaglandin inhibition in human disease. Nature Reviews Drug Discovery 2, 879-890.

Freifelder, D., 1982. Physical biochemistry : applications to biochemistry and molecular biology, San Fransisco.

Funk, C.D., 2001. Prostaglandins and leukotrienes: Advances in eicosanoid biology. Science 294, 1871-1875.

Gamerdinger, M., Clement, A.B., Behl, C., 2007. Cholesterol-like effects of selective cyclooxygenase inhibitors and fibrates on cellular membranes and amyloid-beta production. Molecular Pharmacology 72, 141-151.

Ghosh, R., 1988. P-31 and H-2 NMR-studies of structure and motion in bilayers of phosphatidylcholine and phosphatidylethanolamine. Biochemistry 27, 7750-7758.

Goldenberg, M.M., 1999. Celecoxib, a selective cyclooxygenase-2 inhibitor for the treatment of rheumatoid arthritis and osteoarthritis. Clinical Therapeutics 21, 1497-1513.

Grosch, S., Maier, T.J., Schiffmann, S., Geisslinger, G., 2006. Cyclooxygenase-2 (COX-2)-independent anticarcinogenic effects of selective COX-2 inhibitors. Journal of the National Cancer Institute 98, 736-747.

Gupta, P., Bansal, A.K., 2005. Devitrification of amorphous celecoxib. Aaps Pharmscitech 6.

Harris, R.E., Beebe-Donk, J., Alshafie, G.A., 2006. Reduction in the risk of human breast cancer by selective cyclooxygenase-2 (COX-2) inhibitors. Bmc Cancer 6.

Harris, R.E., Beebe-Donk, J., Alshafie, G.A., 2007. Reduced risk of human lung cancer by selective cyclooxygenase 2 (Cox-2) blockade: Results of a case control study. International Journal of Biological Sciences 3, 328-334.

Hauser, H., Poupart, G., 2004. Lipid Structure, 2 ed. CRC Press.

Houslay, M.D., 1985. Regulation of adenylate-cyclase (ec 4.6.1.1) activity by its lipid environment. Proceedings of the Nutrition Society 44, 157-165.

Hung, W.C., Lee, M.T., Chen, F.Y., Huang, H.W., 2007. The condensing effect of cholesterol in lipid bilayers. Biophysical Journal 92, 3960-3967.

Ipsen, J.H., Karlstrom, G., Mouritsen, O.G., Wennerstrom, H., Zuckermann, M.J., 1987. Phase-equilibria in the phosphatidylcholine-cholesterol system. Biochimica Et Biophysica Acta 905, 162-172.

Jain, M.K., 1979a. Molecular Motions in Biomembranes. Proc. INSA 45A, 558-566.

Jain, M.K., 1979b. possible modes of interaction of small molecules with lipid bilayer in biomembrane. Proc. INSA 45A, 567-577.

Jain, M.K., 1988. Introduction to Biological Membranes, 2 ed. John Wiley & Sons.

Katsu, T., Imamura, T., Komagoe, K., Masuda, K., Mizushima, T., 2007. Simultaneous measurements of K+ and calcein release from liposomes and the determination of pore size formed in a membrane. Analytical Sciences 23, 517-522.

Kazanci, N., Severcan, F., 2007. Concentration dependent different action of tamoxifen on membrane fluidity. Bioscience Reports 27, 247-255.

Kazanci, N., Toyran, N., Haris, P.I., Severcan, F., 2001. Vitamin D-2 at high and low concentrations exert opposing effects on molecular order and dynamics of dipalmitoyl phosphatidylcholine membranes. Spectroscopy-an International Journal 15, 47-55.

Knazek, R.A., Liu, S.C., Dave, J.R., Christy, R.J., Keller, J.A., 1981. Indomethacin causes a simultaneous decrease of both prolactin binding and fluidity of mouse-liver membranes. Prostaglandins and Medicine 6, 403-411.

Korkmaz, F., Severcan, F., 2005. Effect of progesterone on DPPC membrane: Evidence for lateral phase separation and inverse action in lipid dynamics. Archives of Biochemistry and Biophysics 440, 141-147.

Kutchai, H., Chandler, L.H., Zavoico, G.B., 1983. Effects of cholesterol on acyl chain dynamics in multilamellar vesicles of various phosphatidylcholines. Biochimica Et Biophysica Acta 736, 137-149.

Lee, A.G., 2004. How lipids affect the activities of integral membrane proteins. Biochimica Et Biophysica Acta-Biomembranes 1666, 62-87.

Levine, Y.K., Wilkins, M.H.F., 1971. Structure of oriented lipid bilayers. Nature-New Biology 230, 69-&.

Li, G.P., Yang, T., Yan, J., 2002. Cyclooxygenase-2 increased the angiogenic and metastatic potential of tumor cells. Biochemical and Biophysical Research Communications 299, 886-890.

Li, Y.K., Ge, M.T., Ciani, L., Kuriakose, G., Westover, E.J., Dura, M., Covey, D.F., Freed, J.H., Maxfield, F.R., Lytton, J., Tabas, I., 2004. Enrichment of endoplasmic reticulum with cholesterol inhibits sarcoplasmic-endoplasmic reticulum calcium ATPase-2b activity in parallel with increased order of membrane lipids - Implications for depletion of endoplasmic reticulum calcium stores and apoptosis in cholesterol-loaded macrophages. Journal of Biological Chemistry 279, 37030-37039.

Lindblom, G., Johansson, L.B.A., Arvidson, G., 1981. Effect of cholesterol in membranes - pulsed nuclear magnetic-resonance measurements of lipid lateral diffusion. Biochemistry 20, 2204-2207.

Liu, J., Conboy, J.C., 2009. Phase behavior of planar supported lipid membranes composed of cholesterol and 1,2-distearoyl-sn-glycerol-3-phosphocholine examined by sum-frequency vibrational spectroscopy. Vibrational Spectroscopy 50, 106-115.

London, E., 2005. How principles of domain formation in model membranes may explain ambiguities concerning lipid raft formation in cells. Biochimica Et Biophysica Acta-Molecular Cell Research 1746, 203-220.

Lopezgarcia, F., Micol, V., Villalain, J., Gomezfernandez, J.C., 1993. Infrared spectroscopic study of the interaction of diacylglycerol with phosphatidylserine in the presence of calcium. Biochimica Et Biophysica Acta 1169, 264-272.

Lucio, M., Ferreira, H., Lima, J., Matos, C., de Castro, B., Reis, S., 2004. Influence of some anti-inflammatory drugs in membrane fluidity studied by fluorescence anisotropy measurements. Physical Chemistry Chemical Physics 6, 1493-1498.

Mabrey, S., Sturtevant, J.M., 1976. Investigation of phase-transitions of lipids and lipid mixtures by high sensitivity differential scanning calorimetry. Proceedings of the National Academy of Sciences of the United States of America 73, 3862-3866.

Maccarrone, M., Melino, G., Finazzi-Agro, A., 2001. Lipoxygenases and their involvement in programmed cell death. Cell Death and Differentiation 8, 776-784.
Madden, T.D., 1997. Model Membrane Systems. Principles of Medical Biology. JAI Press Inc., pp. 1-17.

Mannock, D.A., Lee, M.Y.T., Lewis, R., McElhaney, R.N., 2008. Comparative calorimetric and spectroscopic studies of the effects of cholesterol and epicholesterol on the thermotropic phase behaviour of dipalmitoylphosphatidylcholine bilayer membranes. Biochimica Et Biophysica Acta-Biomembranes 1778, 2191-2202.

Mannock, D.A., Lewis, R., McElhaney, R.N., 2006. Comparative calorimetric and spectroscopic studies of the effects of lanosterol and cholesterol on the thermotropic phase behavior and organization of dipalmitoylphosphatidylcholine bilayer membranes. Biophysical Journal 91, 3327-3340.

Mantovani, A., Allavena, P., Sica, A., Balkwill, F., 2008. Cancer-related inflammation. Nature 454, 436-444.

Maxfield, F.R., Tabas, I., 2005. Role of cholesterol and lipid organization in disease. Nature 438, 612-621.

McAdam, B.F., Catella-Lawson, F., Mardini, I.A., Kapoor, S., Lawson, J.A., FitzGerald, G.A., 1999. Systemic biosynthesis of prostacyclin by cyclooxygenase (COX)-2: The human pharmacology of a selective inhibitor of COX-2. Proceedings of the National Academy of Sciences of the United States of America 96, 272-277.

McElhaney, R.N., 1982. The use of differential scanning calorimetry and differential thermal-analysis in studies of model and biological-membranes. Chemistry and Physics of Lipids 30, 229-259.

McIntosh, T.J., 1978. Effect of cholesterol on structure of phosphatidylcholine bilayers. Biochimica Et Biophysica Acta 513, 43-58.

McMullen, T.P.W., Lewis, R., McElhaney, R.N., 1993. Differential scanning calorimetric study of the effect of cholesterol on the thermotropic phase-behavior of a homologous series of linear saturated phosphatidylcholines. Biochemistry 32, 516-522.

McMullen, T.P.W., Lewis, R., McElhaney, R.N., 1994. Comparative differential scanning calorimetric and FTIR and P-31-NMR spectroscopic studies of the effects

of cholesterol and androstenol on the thermotropic phase-behavior and organization of phosphatidylcholine bilayers. Biophysical Journal 66, 741-752.

McMullen, T.P.W., Lewis, R., McElhaney, R.N., 2004. Cholesterol-phospholipid interactions, the liquid-ordered phase and lipid rafts in model and biological membranes. Current Opinion in Colloid & Interface Science 8, 459-468.

McMullen, T.P.W., McElhaney, R.N., 1997. Differential scanning calorimetric studies of the interaction of cholesterol with distearoyl and dielaidoyl molecular species of phosphatidylcholine, phosphatidylethanolamine, and phosphatidylserine. Biochemistry 36, 4979-4986.

Melchior, D.L., Steim, J.M., 1976. Thermotropic transitions in biomembranes. Annual Review of Biophysics and Bioengineering 5, 205-238.

Meyerbio1B, meyerbio1b.wikispaces.com/%E2%80%A2Lipids, last visited on July 2009.

Nzeako, U.C., Guicciardi, M.E., Yoon, J.H., Bronk, S.F., Gores, G.Y., 2001. COX-2 inhibits fas-mediated apoptosis in cholangiocarcinoma cells. Digestive Disease Week/102nd Annual Meeting of the American-Gastroenterological-Association, Atlanta, Georgia, pp. 552-559.

Ohki, S., Duzgunes, N., 1979. Divalent cation-induced interaction of phospholipid vesicle and monolayer membranes. Biochimica Et Biophysica Acta 552, 438-449.

Severcan, F., 1997. Vitamin E decreases the order of the phospholipid model membranes in the gel phase: An FTIR study. Bioscience Reports 17, 231-235.

Severcan, F., Cannistraro, S., 1988. Direct electron-spin resonance evidence for alpha-tocopherol-induced phase-separation in model membranes. Chemistry and Physics of Lipids 47, 129-133.

Severcan, F., Durmus, H.O., Eker, F., Akinoglu, B.G., Haris, P.I., 2000a. Vitamin D-2 modulates melittin-membrane interactions. pp. 205-211.

Severcan, F., Durmus, H.O., Eker, F., Akinoglu, B.G., Haris, P.I., 2000b. Vitamin D-2 modulates melittin-membrane interactions. Talanta 53, 205-211.

Severcan, F., Kazanci, N., Baykal, U., Suzer, S., 1995. IR and turbidity studies of vitamin-e-cholesterol-phospholipid MEMBRANE INTERACTIONS. Bioscience Reports 15, 221-229.

Severcan, F., Kazanci, N., Zorlu, F., 2000c. Tamoxifen increases membrane fluidity at high concentrations. Bioscience Reports 20, 177-184.

Severcan, F., Sahin, I., Kazanci, N., 2005. Melatonin strongly interacts with zwitterionic model membranes - evidence from Fourier transform infrared spectroscopy and differential scanning calorimetry. Biochimica Et Biophysica Acta-Biomembranes 1668, 215-222.

Shaikh, S.R., Brzustowicz, M.R., Gustafson, N., Stillwell, W., Wassall, S.R., 2002. Monounsaturated PE does not phase-separate from the lipid raft molecules sphingomyelin and cholesterol: Role for polyunsaturation? Biochemistry 41, 10593-10602.

Sok, M., Sentjurc, M., Schara, M., Stare, J., Rott, T., 2002. Cell membrane fluidity and prognosis of lung cancer. Annals of Thoracic Surgery 73, 1567-1571.

Somerharju, P., Virtanen, J.A., Cheng, K.H., 1999. Lateral organisation of membrane lipids - The superlattice view. Biochimica Et Biophysica Acta-Molecular and Cell Biology of Lipids 1440, 32-48.

Srinivasan, C., Burgess, D.J., 2009. Optimization and characterization of anionic lipoplexes for gene delivery. J Control Release 136, 62-70.

Stuart, B., 1997. Biological Applications of Infrared Spectroscopy. John Wiley & Sons.

Szoka, F., Papahadjopoulos, D., 1980. Comparative properties and methods of preparation of lipid vesicles (liposomes). Annual Review of Biophysics and Bioengineering 9, 467-508.

Tamai, N., Uemura, M., Takeichi, T., Goto, M., Matsuki, H., Kaneshina, S., 2008. A new interpretation of eutectic behavior for distearoylphosphatidylcholine-cholesterol binary bilayer membrane. Biophysical Chemistry 135, 95-101.

Tomisato, W., Tanaka, K., Katsu, T., Kakuta, H., Sasaki, K., Tsutsumi, S., Hoshino, T., Aburaya, M., Li, D.W., Tsuchiya, T., Suzuki, K., Yokomizo, K., Mizushima, T., 2004. Membrane permeabilization by non-steroidal anti-inflammatory drugs. Biochemical and Biophysical Research Communications 323, 1032-1039.

Toyran, N., Severcan, F., 2003. Competitive effect of vitamin D-2 and Ca2+ on phospholipid model membranes: an FTIR study. Chemistry and Physics of Lipids 123, 165-176.

Umemura, J., Cameron, D.G., Mantsch, H.H., 1980. A Fourier-transform infrared spectroscopic study of the molecular interaction of cholesterol with 1,2-dipalmitoyl-sn-glycero-3-phosphocholine. Biochimica Et Biophysica Acta 602, 32-44.
Vane, J.R., 1971. Inhibition of prostaglandin synthesis as a mechanism of action for aspirin-like drugs. Nature-New Biology 231, 232-&.

Vane, J.R., Bakhle, Y.S., Botting, R.M., 1998. Cyclooxygenases 1 and 2. Annual Review of Pharmacology and Toxicology 38, 97-120.

Vanginkel, G., Vanlangen, H., Levine, Y.K., 1989. The membrane fluidity concept revisited by polarized fluorescence spectroscopy on different model membranes containing unsaturated lipids and sterols. Biochimie 71, 23-32.

Villalain, J., Aranda, F.J., Gomezfernandez, J.C., 1986. Calorimetric and infrared spectroscopic studies of the interaction of alpha-tocopherol and alpha-tocopheryl acetate with phospholipid-vesicles. European Journal of Biochemistry 158, 141-147.

Vist, M.R., Davis, J.H., 1990. Phase-equilibria of cholesterol dipalmitoylphosphatidylcholine mixtures - h-2 nuclear magnetic-resonance and differential scanning calorimetry. Biochemistry 29, 451-464.

Walter, M.F., Jacob, R.F., Day, C.A., Dahlborg, R., Weng, Y.J., Mason, R.P., 2004. Sulfone COX-2 inhibitors increase susceptibility of human LDL and plasma to oxidative modification: comparison to sulfonamide COX-2 inhibitors and NSAIDs. Atherosclerosis 177, 235-243.

Yeagle, P.L., 1985. Cholesterol and the cell-membrane. Biochimica Et Biophysica Acta 822, 267-287.

Yeagle, P.L., Hutton, W.C., Huang, C.H., Martin, R.B., 1975. Headgroup conformation and lipid-cholesterol association in phosphatidylcholine vesicles - p-31(h-1) nuclear overhauser effect study. Proceedings of the National Academy of Sciences of the United States of America 72, 3477-3481.

Yi, P.N., Macdonal.Rc, 1973. Temperature-dependence of optical properties of aqueous dispersions of phosphatidylcholine. Chemistry and Physics of Lipids 11, 114-134.

Zhao, L.Y., Feng, S.S., Kocherginsky, N., Kostetski, I., 2007. DSC and EPR investigations on effects of cholesterol component on molecular interactions between paclitaxel and phospholipid within lipid bilayer membrane. International Journal of Pharmaceutics 338, 258-266.